Organotrifluoroborate Hydrolysis: Boronic Acid Release Mechanism and an Acid-Base Paradox in Cross-Coupling

Alastair J. J. Lennox and Guy C. Lloyd-Jones*

* *Guy.lloyd-jones@bristol.ac.uk*

Supporting Information

Contents:

General experimental details

Techniques

Manipulations involving air and moisture sensitive materials were conducted employing standard Schlenk-line techniques, using vacuum lines attached to a double manifold with greaseless J. Youngs valves equipped with an oil pump (0.1 mmHg) under an atmosphere of dry nitrogen. Where air/moisture sensitive reactions were conducted, glassware and needles were placed in an oven (200 °C) prior to use and allowed to cool under an atmosphere of dry nitrogen or under vacuum at 0.1 mmHg (oil pump). Liquid reagents, solutions or solvents were added *via* syringe through rubber septa; solid reagents were added *via* Schlenk type adapters. The removal of solvents *in vacuo* was achieved using a Büchi rotary evaporator (bath temperatures up to 40 °C) at a pressure of 15 mmHg (diaphragm pump), or at 0.1 mmHg (oil pump) on a vacuum line at room temperature.

Solvents

Dry solvents were obtained by passing solvent through a column of anhydrous alumina using equipment from *Anhydrous Engineering* situated in the University of Bristol chemistry department. Strauss flasks fitted with a greaseless J. Youngs valve were used to collect anhydrous solvents, they were dispensed using gas-tight syringes balanced by a nitrogen inlet. Solvents that required degassing were subjected to three cycles of freeze-pump-thaw with the exception of THF and water. THF was distilled under N_2, sodium and benzophenone, and water was saturated with N_2 *via* bubbling for at least 30 min. Anhydrous, degassed solvents were withdrawn from Strauss flask through rubber septa using gas-tight syringes balanced by a nitrogen inlet. Commercial grade solvents were used for chromatography and extraction. Deuterated solvents for NMR analysis were purchased from *Cambridge Isotopes Limited.*

Analysis

NMR spectra were recorded on *Varian 400, Varian 500, JEOL GX 300* or *Eclipse 300* spectrometers. All chemical shifts were quoted in parts per million (ppm); ^{1}H and ^{13}C NMR spectra were referenced to TMS as an internal standard, ^{19}F to $CFCl_3$ and ^{11}B to $BF_3.OEt_2$ with a deuterated solvent unless otherwise stated. Coupling constants, *J*, were calculated using *ACDLabs* to the nearest 0.1 Hz. The following abbreviations (and their combinations) were used to label the multiplicities: s (singlet), d (doublet), t (triplet), q (quartet), m (multiplet) and br (broad). Mass spectra were determined by the University of Bristol mass spectrometry service using a *Fisons VG Analytical Autospec* spectrometer in electron impact (EI) ionisation mode.

Chromatography

TLC analysis was performed on Merck Silica gel $60F_{254}$ glass backed plates. Visualisation was achieved by UV fluorescence (254 nm). Flash column chromatography was conducted using Fluorochem 60 silica: 230-400 mesh (40-63 μm).

Reagents

Reagents and materials purchased from commercial suppliers were used without further purification unless stated. 1,3-Bis(trifluoromethyl)-5-bromobenzene, potassium cyclopropyltrifluoroborate (**1d**), potassium benzyltrifluoroborate (**1h**), potassium 2-furyltrifluoroborate (**1b**), potassium vinyltrifluoroborate (**1c**), potassium phenylethynyltrifluoroborate (**1e**), potassium 4-trifluoromethylphenyltrifluoroborate (**1q**), potassium 3,5-bistrifluoromethylphenyltrifluoroborate (**1s**), potassium 4-methylphenyltrifluoroborate (**1m**), potassium phenyltrifluoroborate (**1n**), potassium 2-naphthyltrifluoroborate (**1p**), [$^{2}H_{5}$]-bromobenzene, diisopropylethylamine, triethylamine, 3-(*N*-morpholino)propanesulfonic acid (MOPS) and boric acid (99% ^{10}B) were purchased from *Sigma Aldrich.* Potassium 4-fluorophenyltrifluoroborate (**1a**), benzotrifluoride, 1,8-diazabicycloundec-7-ene (DBU), di-*n*-butylamine, 4-bromobenzonitrile, potassium 3-nitrophenyltrifluoroborate (**1r**), copper(I)iodide were purchased from *Alfa Aesar.* Trimethylsilylacetylene, cesium carbonate, sodium sulphate and potassium carbonate were purchased from *Fisher Scientific.* 4-Fluorophenylboronic acid (**2a**) was purchased from *Maybridge.* Tris(hydroxymethyl)aminomethane (TRIS) was purchased from *Melford*. Bis(triphenylphosphine)palladium(II) chloride $[PdCl_2(PPh_3)_2]$[S1], dichloro-[1,1'-bis(diphenylphosphino)ferrocene]palladium(II) $[PdCl_2(dppf)]$[S2], potassium cyclobutyltrifluoroborate[S3] and [$^{2}H_{4}$]-4-fluorophenylboronic acid[S4] were prepared by known methods. Potassium 1-naphthyltrifluoroborate (**1o**), potassium 4-

methoxyphenyltrifluoroborate (**1l**), potassium cyclohexyltrifluoroborate (**1j**) and potassium phenylethenyltrifluoroborate (**1k**) were prepared via an unpublished route; material identical (^{1}H, ^{13}C, ^{19}F and ^{11}B NMR) to that previously published.[S5] Potassium isopropyltrifluoroborate (**1g**) and 1,3-diphenylpropyl (**1i**) were kindly donated by Prof. V. K. Aggarwal and Dr. T. G. Elford (University of Bristol).

Accurate masses of these reagents and products were measured on a calibrated Sartorius BP 211 balance.

^{10}B labeling experiments

Synthesis of [^{10}B]-potassium 4-fluorophenyltrifluoroborate, [^{10}B]-1a

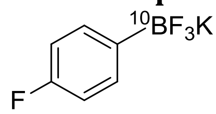

[^{10}B]-**1a**

*Preparation of [^{10}B]-B(O*i*-Pr)$_3$*

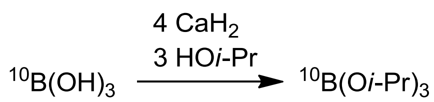

To an oven dried round-bottomed flask was charged [^{10}B] – boric acid (0.03 mol, 1.83 g) and calcium hydride (0.12 mol, 5.04 g) and then purged with nitrogen. Anhydrous isopropanol (0.09 mol, 5.4 g) was added dropwise with stirring down a condenser and over a stream of N_2. After bubbling had ceased the reaction mixture was heated to 90 °C for 12 hours, after which the volatile compounds were pumped off *in vacuo* and trapped at -78 °C. The contents of the trap were then purified by reduced pressure distillation (47-50 °C at 30 mm Hg) to give the title compound as a clear colourless oil (3.62g, 64.5 %) **^{1}H NMR** (300 MHz, $CDCl_3$) δ = 4.34 (sept. ^{3}J = 6 Hz 3H), 1.13 (d, ^{3}J = 6 Hz 18H). ^{10}B incorporation was not determined for this material, but analysis of the **1a** derived from it, *vide infra*, confirmed high abundance.

Data is consistent with that expected based on published data for the same compound with natural abundance $^{10}B/^{11}B$ (20/80)[S6]

Preparation of [^{10}B]-potassium 4-fluorophenyltrifluoroborate, [^{10}B]-1a [S7]

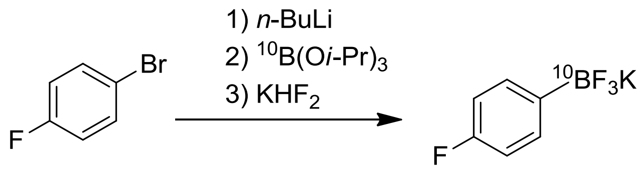

[^{10}B]-**1a**

To a two necked round bottomed-flask, purged with nitrogen and a magnetic stirrer bar, was added 4-fluorobromobenzene (0.023 mol, 4.067 g) and dry diethylether (23 mL). A solution of *n*-butyllithium (10.4 mL of a 2.22 M solution in THF) was added dropwise at -78 °C and stirred for 30 mins before being allowed to warm to room temperature and stirred for a further 15 mins. This solution was then cannulated into a flask charged with [^{10}B]-triisopropylborate (0.019 mol, 3.623 g) in dry diethylether (76 mL) under an N_2 atmosphere at -78 °C and was stirred for one further hour. The reaction mixture was again allowed to warm to room temperature before a saturated aqueous solution of KHF_2 (0.087 mol, 6.8 g) was added dropwise and solvent was removed *in vacuo*. The solids were extracted with acetone (2 x room temperature, 2 x boiling), combined and filtered. The solvent was evaporated before being taken up in the minimal volume of hot acetone, filtered and cooled before diethylether was added. The white solid was filtered off, washed with diethylether and dried *in vacuo,* to give the title compound (3.45 g, 88%) **^{1}H NMR** (300 MHz, d_6-acetone) δ = 7.45 (t ^{3}J = 6.97 Hz 2H), 6.81 (t ^{3}J = 8.62 Hz 2H). **^{19}F NMR** (282 MHz, d_6-acetone) δ = -120.45 (1F), 142.3 (3H). MS (EI) analysis of the boronic acid [^{10}B]-**2a** derived by hydrolysis indicated 94.8% ^{10}B incorporation. Isotope cluster *m/z* (%) calc.: (for 94.5% ^{10}B) 139.1 (100); 140.1 (12.4); 141.1 (0.96), observed: 139.1 (100); 140.1 (12.5); 141.1 (8).

Data is consistent with that expected based on published data for the same compound with natural abundance ^{10}B/^{11}B (20/80).[S5]

Exchange study

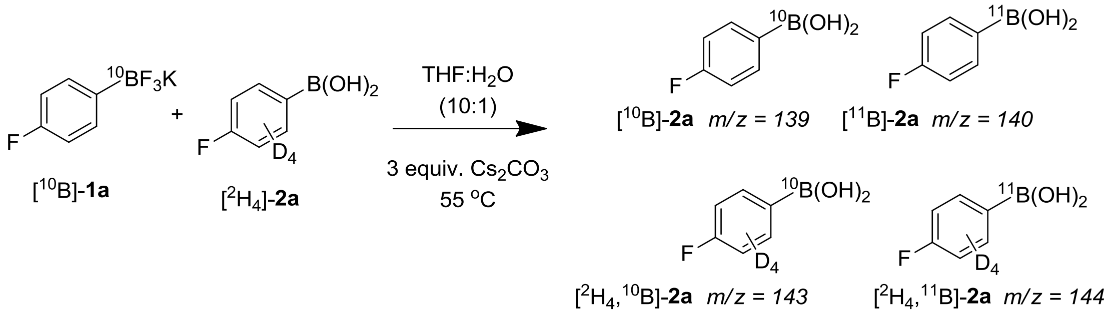

[^{10}B] Potassium 4-fluorophenyltrifluoroborate ([^{10}B]-**1a**) (1.76 x 10^{-5} mol, 3.5 mg) and [$^{2}H_4$] 4-fluorophenylboronic acid ([$^{2}H_4$]-**2a**) (1.76 x 10^{-5} mol, 2.5 mg) were added as solids to a Schlenk tube. To this was added THF (2 mL) and cesium carbonate (1.06 x 10^{-4} mol, 34 mg) in water (0.2 mL). This stirring solution was then heated at 55 °C for five hours after ^{19}F NMR confirmed complete conversion to the 4-fluorophenylboronic acid had occurred. A sample was removed and immediately analysed by MS (EI). **MS(EI)** *m/z* (%): 139 (93.7), 140 (8.9), 141 (4.8), 142 (2.2), 143 (30.1), 144 (100), 145 (18.8).

B(OH)F$_3$K study

Conditions were used that had previously been found to produce detectable levels of B(OH)F_3K, with a substrate stable to protodeboronation on the relevant time scales.

[^{10}B] Potassium 4-fluorophenyltrifluoroborate [^{10}B]-**1a** (6.00 x 10^{-5} mol, 12.1 mg) was added as a solid to a PTFE lined NMR tube. To this was added D_2O (0.3 mL) followed by Cs_2CO_3 (0.5 equiv., 3.00 x 10^{-5}, 9.78 mg) in D_2O (0.06 mL). The tube was shaken for approximately 10 min before being analysed by ^{19}F NMR (128 scans, 25 °C).

This procedure was repeated (2 x scale) but stirred in a glass test tube for 10 min before a sample was removed and placed in a NMR tube *without* a PTFE liner.

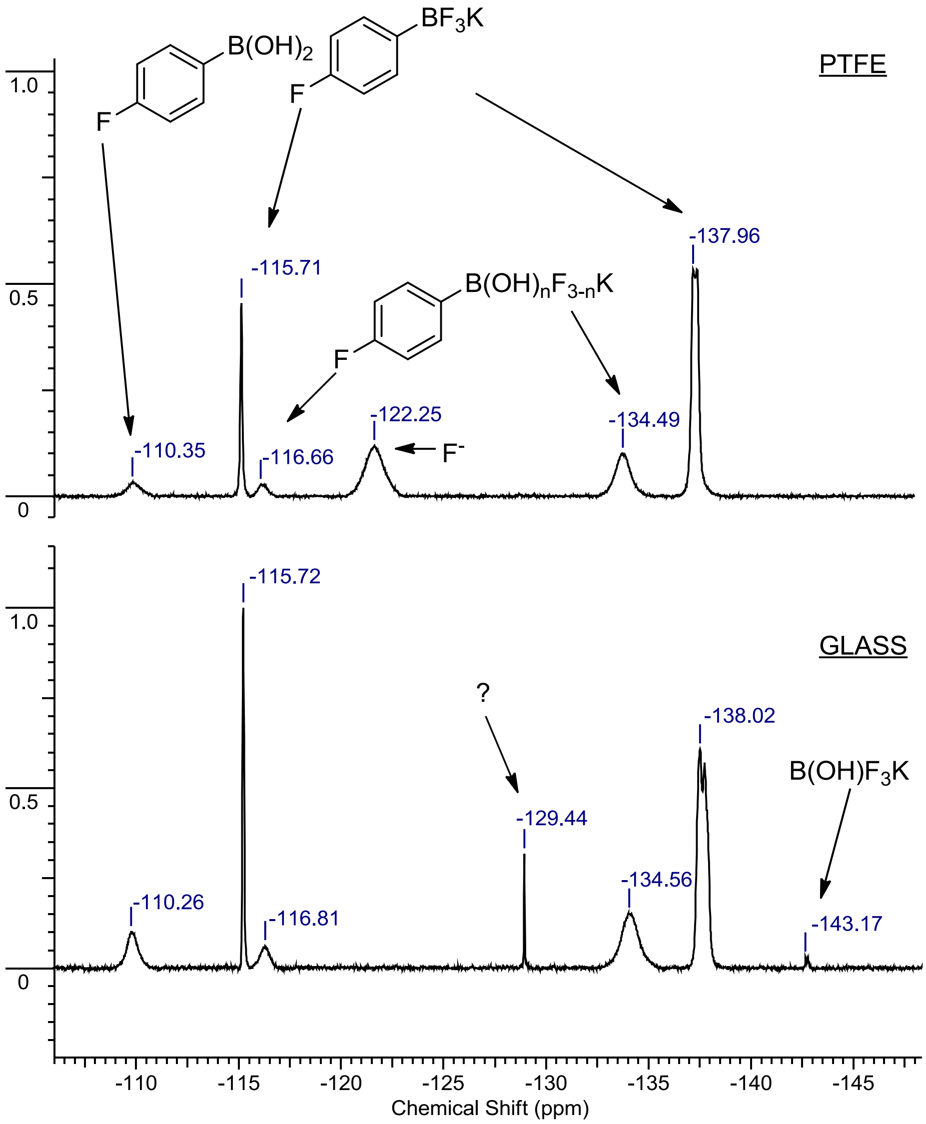

Figure S1. ^{19}**F NMR spectra of 1a in basic (0.5 eq.** Cs_2CO_3**)** D_2O **in a PTFE vessel (upper spectrum) and a glass vessel (lower spectrum). Two extra peaks are clearly shown in the lower spectrum.**

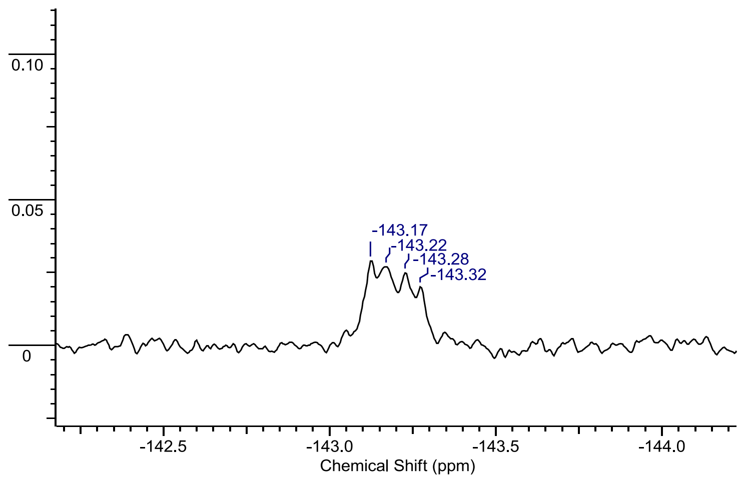

Figure S2. An expansion of ^{19}**F NMR Figure S1 showing the superimposed septet and quartet couplings arising from natural abundance material (**^{11}**B 80%, spin = 3/2, and** ^{10}**B 20%, spin = 3).**

Hydrolysis of 1a under *basic* conditions

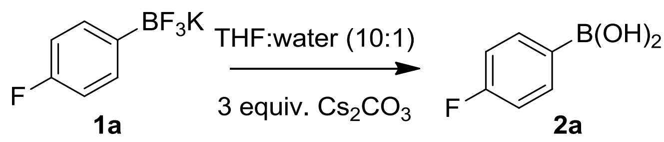

Large volume reactions

The reaction vessel (50 mL rbf, 15 mm wide conical-shaped base Schlenk tube, 15 mL wide round shaped base Schlenk tube, 15 mm wide PTFE test tube and 15 mm wide PTFE test tube with added glass powder (20 mg grade 3)) was charged with potassium 4-fluorophenyltrifluoroborate (**1a**) (4.36×10^{-5} mol, 8.8 mg), cesium carbonate (1.3×10^{-4} mol, 43 mg) and an appropriate magnetic stirring bar for the vessel. A preheated (55 °C) solution of THF:water (10:1, 5 mL: 0.5 mL) was added and samples (ca. 10 over a 2/3 hour period) were removed with a plastic syringe and placed immediately in PTFE lined NMR tubes, pre-cooled to 0 °C. The samples were kept at that temperature until they were placed directly into the *Eclipse 300* NMR probe. Each sample was analysed by ^{19}F NMR and subject to 128 pulses (4 min 17 s) at 25 °C.

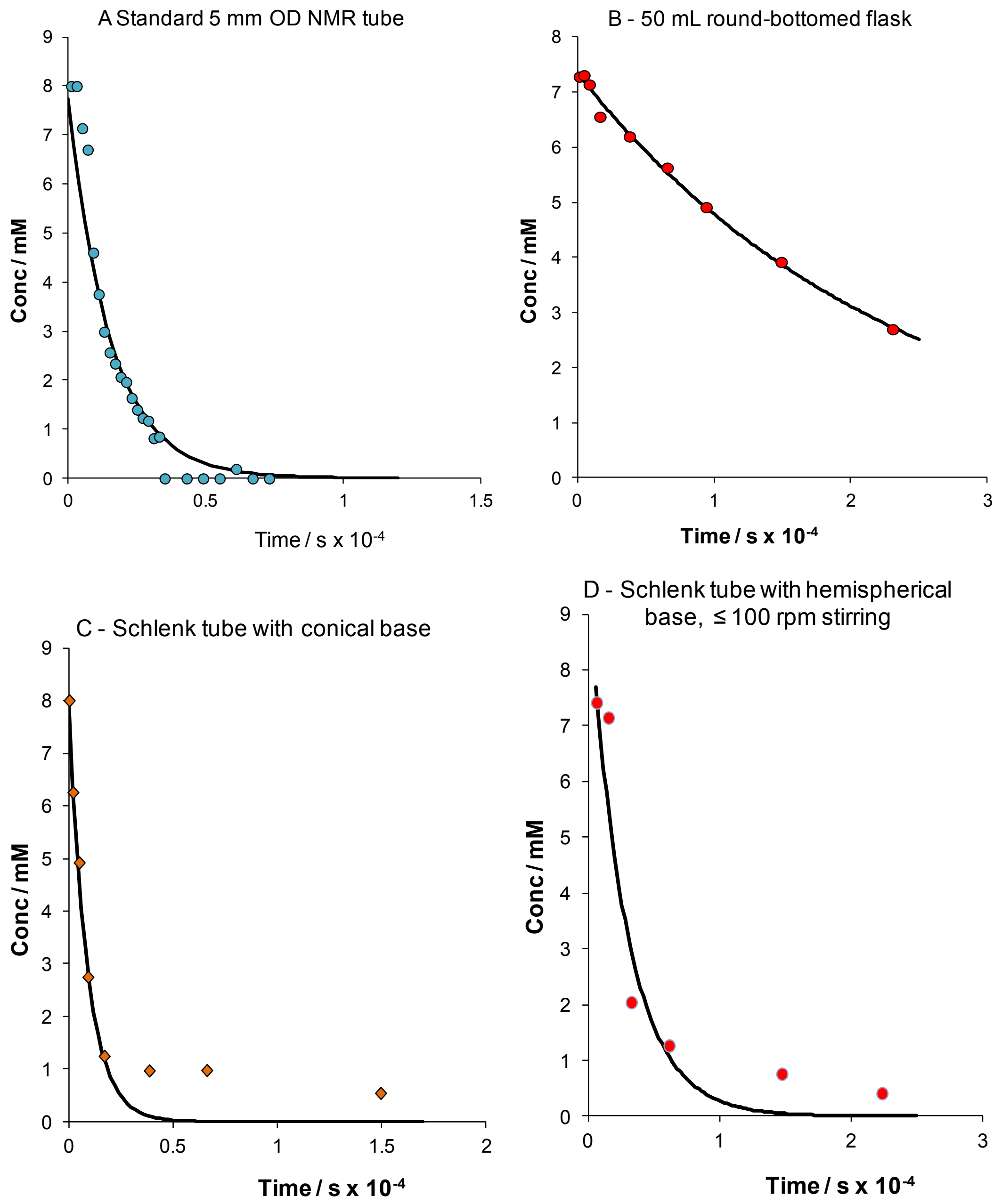
A Standard 5 mm OD NMR tube
Conc / mM
Time / s x 10-4
B - 50 mL round-bottomed flask
Conc / mM
Time / s x 10-4
C - Schlenk tube with conical base
Conc / mM
Time / s x 10-4
D - Schlenk tube with hemispherical base, ≤ 100 rpm stirring
Conc / mM
Time / s x 10-4

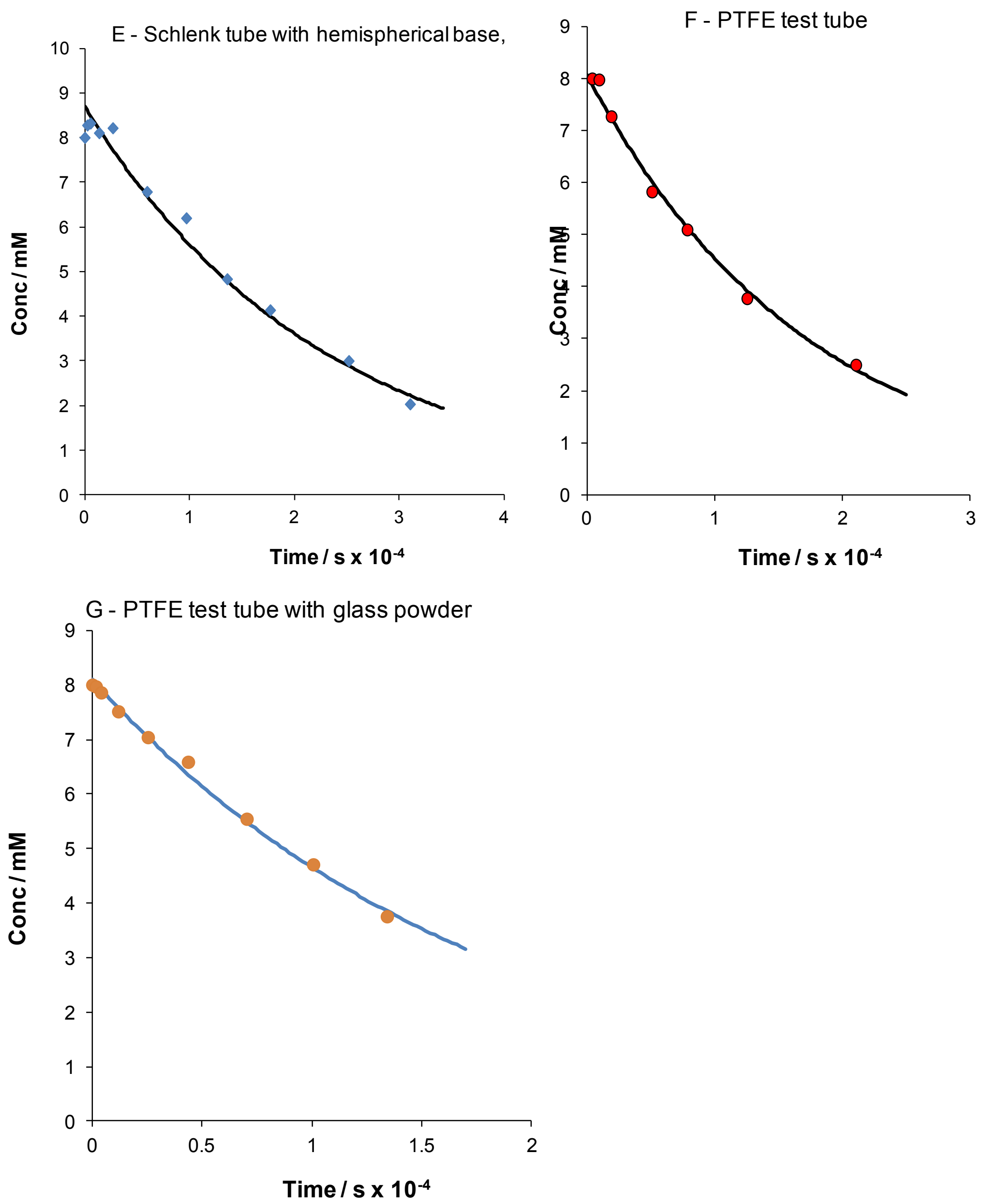

Figure S3. Hydrolysis of 1a (8 mM) to 2a in THF:water (10:1) with 3 equiv. of Cs_2CO_3 at 55 °C in reaction vessels A-G, see Figure 1 in main text.

NMR tube reactions

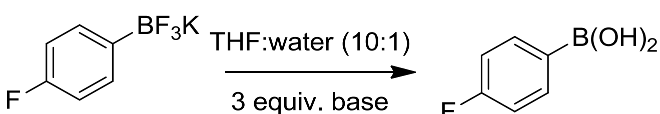

1a **2a**

The following experiments were undertaken in a Norell S502 NMR tube in a *Varian 500* spectrometer probe.

Cs_2CO_3

Potassium 4-fluorophenyltrifluoroborate (**1a**) (5.28×10^{-6} mol) in dry THF (0.1 mL) was added to a Norell 502 NMR tube containing dry THF (0.5 mL). To this was added Cs_2CO_3 (1.58×10^{-5} mol) in D_2O (0.06 mL), bringing the total THF:water ratio to 10:1, the volume to 0.66 mL, the Cs_2CO_3 concentration to 24 mM and the **1a** concentration to 8 mM. The tube was briefly shaken then immediately placed into the *Varian 500* probe which was preheated to 55 °C. The reaction was monitored by ^{19}F NMR using a time delayed array to separate the acquisitions. These acquisitions were roughly every 300 seconds for the first 1.5 hours of reaction then every 900 seconds for the remaining hour.

DBU

1,8-Diazabicycloundec-7-ene (DBU) (1.584×10^{-5} mol) in dry THF (0.3 mL) was added to the Norell 502 NMR tube containing D_2O (0.06 mL). This was followed by the addition of **1a** (5.28×10^{-6} mol) in dry THF (0.3 mL), bringing the total THF:water ratio to 10:1 and volume to 0.66 mL, the DBU concentration to 24 mM and the **1a** concentration to 8 mM. The tube was briefly shaken then immediately placed into the *Varian 500* probe which was preheated to 55 °C. The reaction was monitored by ^{19}F NMR using a time delayed array to separate the acquisitions. These acquisitions were roughly every 300 seconds for the first 1.5 hours of reaction then every 900 seconds for the remaining hour.

NEt_3

Triethylamine (1.584×10^{-5} mol) in dry THF (0.5 mL) was added to the Norell 502 NMR tube containing D_2O (0.06 mL). This was followed by the addition of **1a** (5.28×10^{-6} mol) in dry THF (0.1 mL), bringing the total THF:water ratio to 10:1 and volume to 0.66 mL, the DBU concentration to 24 mM and the **1a** concentration to 8 mM. The tube was briefly shaken then immediately placed into the *Varian 500* probe which was preheated to 55 °C. The reaction was monitored by ^{19}F NMR using a time delayed array to separate the acquisitions. These acquisitions were roughly every 300 seconds for the first 1.5 hours of reaction then every 900 seconds for the remaining hour.

N,N-Diisopropylethylamine (Hünig's base)

Hünig's base (1.584 x 10^{-5} mol) in dry THF (0.5 mL) was added to the Norell 502 NMR tube containing D_2O (0.06 mL). This was followed by the addition of **1a** (5.28 x 10^{-6} mol) in dry THF (0.1 mL), bringing the total THF:water ratio to 10:1 and volume to 0.66 mL, the DBU concentration to 24 mM and the **1a** concentration to 8 mM. The tube was briefly shaken then immediately placed into the *Varian 500* probe which was preheated to 55 °C. The reaction was monitored by ^{19}F NMR using a time delayed array to separate the acquisitions. These acquisitions were roughly every 300 seconds for the first 1.5 hours of reaction then every 900 seconds for the remaining hour.

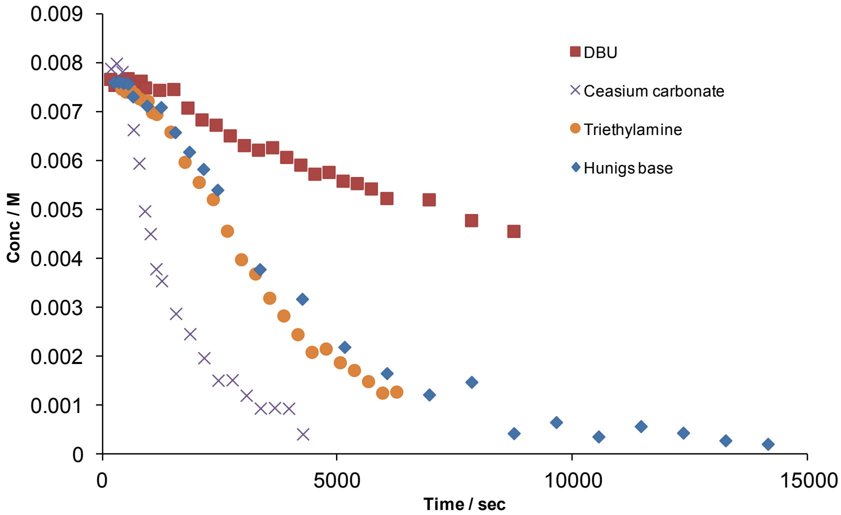

Figure S4. Hydrolysis of 1a (8 mM) to 2a in THF:water (10:1) with 3 equiv. of base (see above) at 55 °C in a Norell S502 NMR tube.

Sonication

Cesium carbonate (1.58 x 10^{-5} mol) in D_2O (0.06 mL) was added to the Norell 502 NMR tube containing THF (0.54 mL) and then sonicated for 20 seconds. Potassium 4-fluorophenyltrifluoroborate (**1a**) (5.28 x 10^{-6} mol) in dry THF (0.06 mL) was added to the pre-sonicated solution in the NMR tube, bringing the total THF:water ratio to 10:1 and volume to 0.66 mL, the cesium carbonate concentration to 24 mM and the **1a** concentration to 8 mM). The solution was then sonicated for a further 20 seconds before being placed directly into the preheated (55 °C) *Varian 500* probe. The reaction was monitored by ^{19}F NMR using a time delayed array to separate the acquisitions. These acquisitions were every 180 seconds for the first 30 mins then every 5 mins for the following 50 mins then every 15 min for the remaining two hours.

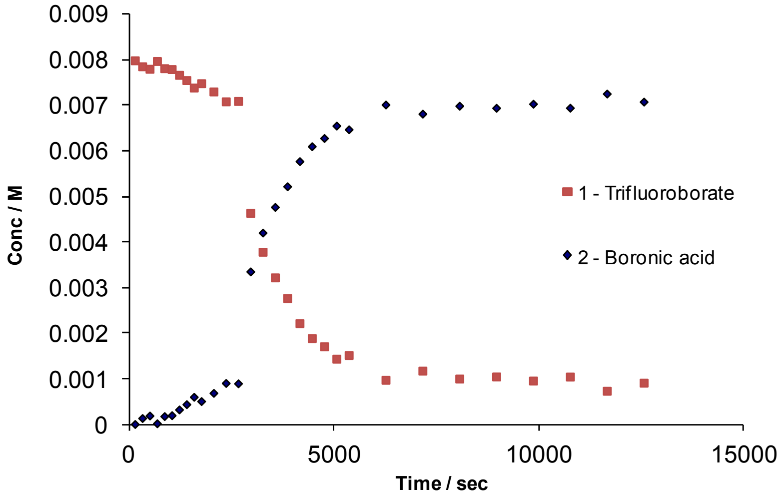

Figure S5. Hydrolysis of 1a (8 mM) to 2a with 3 equiv. Cs_2CO_3 in THF:water (10:1) at 55 °C, after 20 seconds sonication, in an NMR tube. After approximately 5000 seconds hydrolysis proceeds predominantly by the *direct* rather than *acid catalysed* pathway, due to the increase in pH caused by the reduced rate of hydrolysis.

pH monitoring

A pre-heated (55 °C) solution of THF:water (10:1, 6.6 mL) was added to a solid mixture of potassium 4-fluorophenyltrifluoroborate (**1a**) (5.28×10^{-5} mol, 10.6 mg) and Cs_2CO_3 (3 equiv., 1.58×10^{-4} mol, 51.6 mg) in a 15 mm diameter Schlenk tube. The stirring (100 rpm) solution was heated at 55 °C and the pH was read from an uncalibrated Hanna HI 98103 pH probe every 10 seconds for the first 10 min and every 30 seconds for the following 2 hours. Samples (0.3 mL) were removed throughout the reaction using a plastic syringe and placed in pre-cooled PTFE lined NMR tubes at 0° C. The samples were kept at that temperature until they were placed directly into the *Eclipse 300* NMR probe. Each sample was analysed by ^{19}F NMR and subject to 128 pulses (4 min 17 s) at 25 °C.

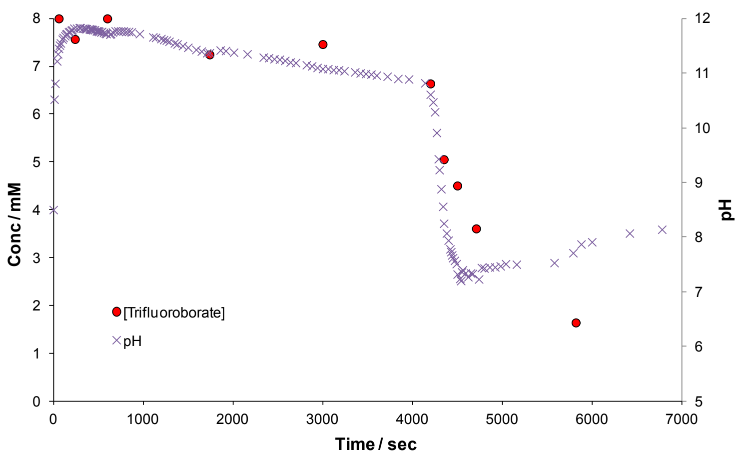

Figure S6. Hydrolysis of 1a (8 mM) to 2a with 3 equiv. Cs_2CO_3 in THF:water (10:1) at 55 °C.

Hydrolysis of 1a under *buffered* conditions

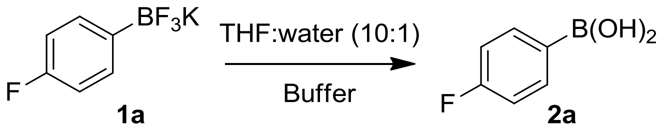

Tris buffer

Tris(hydroxymethyl)aminomethane (Tris) (6.6×10^{-5} mol, 8 mg) was added as a solid to the Norell 502 NMR tube containing THF:water (0.5 mL:0.06 mL). Potassium 4-fluorophenyltrifluoroborate (**1a**) (5.28×10^{-6} mol) in dry THF (0.1 mL) was then added, bringing the total THF:water ratio to 10:1 and volume to 0.66 mL, the Tris concentration to 100 mM and the **1a** concentration to 8 mM. The tube was briefly shaken then immediately placed into the *Varian 500* probe which was preheated to 55 °C. The reaction was monitored by ^{19}F NMR using a time delayed array to separate the acquisitions. These acquisitions were roughly every 300 seconds for the first 1.5 hours of reaction then every 900 seconds for the remaining hour.

MOPS buffer

3-(*N*-morpholino)propanesulfonic acid (MOPS) (6.6×10^{-5} mol, 13.7 mg) was added as a solid to the Norell 502 NMR tube containing THF:water (0.5 mL:0.06 mL). **1a** (5.28×10^{-6} mol) in dry THF (0.1 mL) was then added, bringing the total THF:water ratio to 10:1 and volume to 0.66 mL, the MOPS concentration to 100 mM and the **1a** concentration to 8 mM. The tube was briefly shaken then immediately placed into the

Varian 500 probe which was preheated to 55 °C. The reaction was monitored by ^{19}F NMR using a time delayed array to separate the acquisitions. These acquisitions were roughly every 300 seconds for the first 1.5 hours of reaction then every 900 seconds for the remaining hour.

This experiment was repeated with half the concentration of MOPS (3.3 x 10^{-5} mol, 6.85 mg, 50 mM overall)

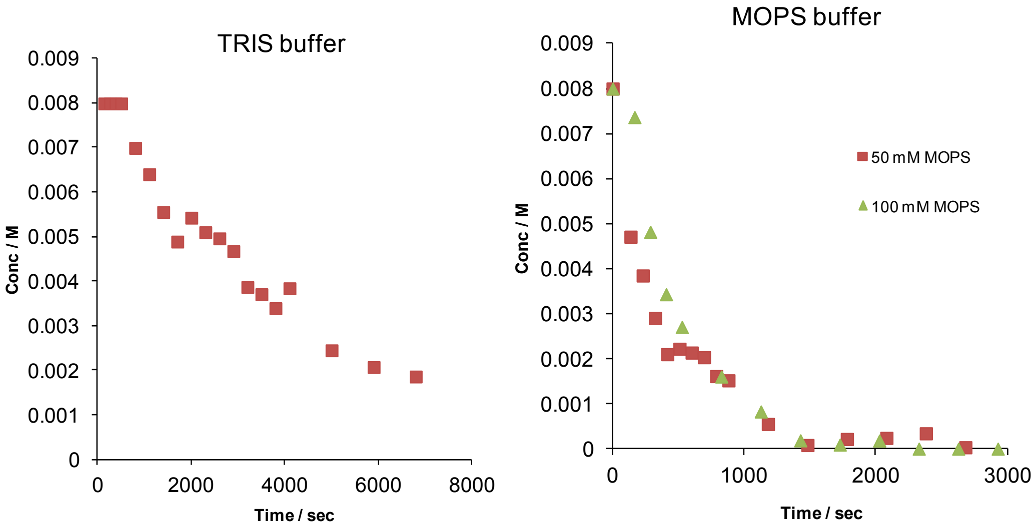

Figure S7. Hydrolysis of 1a (8 mM) to 2a under buffered (Tris - 100mM right graph, MOPS - 50 and 100 mM, left graph) THF:water (10:1). An unidentified signal in the ^{19}F NMR accompanied 2a formation in the TRIS buffered solution that is possibly the boronic ester of TRIS.

Phosphazene base P_4-*t*-Bu

Phosphazene base P_4 *t*-Bu (6.6 x 10^{-5} mol, 66 µL 1 M solution in hexane) in dry THF (0.3 mL) was added to the Norell 502 NMR tube containing potassium 4-fluorophenyltrifluoroborate (**1a**) (5.28 x 10^{-6} mol) in dry THF (0.3 mL). This was followed by the addition of D_2O (0.06 mL), bringing the total THF:water ratio to 10:1, the P_4 base concentration to 100 mM and the **1a** concentration to 8 mM. The tube was briefly shaken then immediately placed into the *Varian 500* probe which was preheated to 55 °C. The reaction was monitored by ^{19}F NMR using a time delayed array to separate the acquisitions. These acquisitions were roughly every 600 seconds for the first 2.5 hours of reaction then every 1800 seconds for the remaining 4 hours.

DBU

DBU (6.6 x 10^{-5} mol, 9.9 µL) in dry THF (0.3 mL) was added to the Norell 502 NMR tube containing potassium 4-fluorophenyltrifluoroborate (**1a**) (5.28 x 10^{-6} mol) in dry THF (0.3 mL). This was followed by the addition of D_2O (0.06 mL), bringing the total THF:water ratio to 10:1, the DBU concentration to 100 mM and the **1a** concentration to 8 mM. The tube was briefly shaken then immediately placed into the *Varian 500* probe which was preheated to 55 °C. The reaction was monitored by ^{19}F NMR using a time delayed array to separate the acquisitions. These acquisitions were roughly every 600 seconds for the first 2.5 hours of reaction then every 1800 seconds for the remaining 2.5 hours.

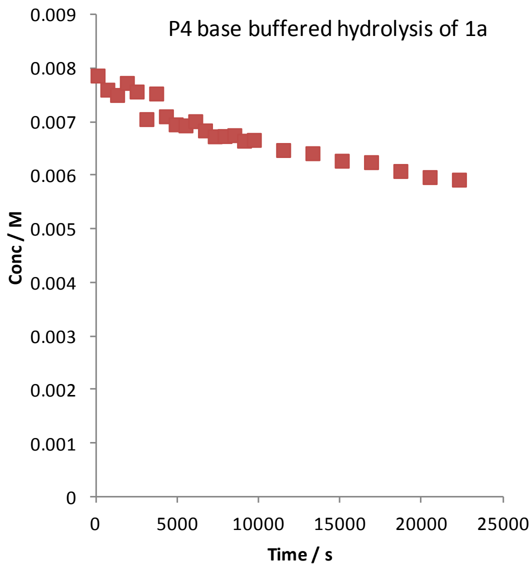

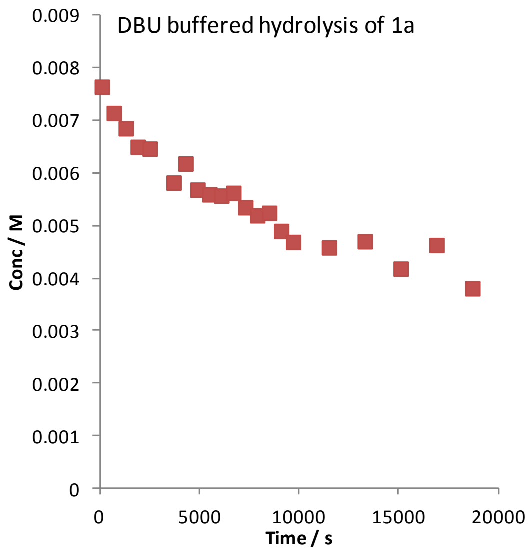

Figure S8 Hydrolysis of 1a to 2a under buffered conditions (left plot is P_4 *t*-Bu base (100 mM), right plot is DBU (100 mM)).

pH measurement

The pH of each buffer, MOPS (100 mM) and TRIS (100 mM), no buffer and base, Et_3N (24 and 100 mM), Hunigs base (24 and 100 mM), DBU (100 mM) and P_4-*t*-Bu (100 mM) were measured in THF:water (10:1) using a Hanna HI 98103 pH probe calibrated only to pH 7 (phosphate buffer) and pH 4 (phthalate buffer). The probe was given five aqueous washes in between measurements followed by a single wash of THF:water (10:1). The pH of each solution was measured twice and normalized to “no buffer” at pH 7.

Table S1. pH of each buffer and base used for homogeneous rate measurements of the hydrolysis of **1a** to **2a**.

Buffer (100 mM)	**pH** $_1$	**pH** $_2$	**pH** $_{av.}$
MOPS[a]	4.50	4.05	4.28
None	7.00	7.00	7.00
TRIS	8.90	8.30	8.60
Et_3N	8.00	7.75	7.86
Hünigs base	7.70	7.65	7.68
DBU	11.05	10.80	10.93
P_4 *t*-Bu	13.70	13.35	13.53

[a] MOPS solution was not completely homogeneous.

Buffer (24 mM)	**pH**
Et_3N	7.9
Hünigs base	7.65

Hydrolysis of 1a under *base-free* conditions

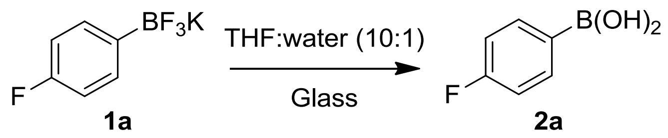

Addition of glass powder to pre-equilibrated system

Potassium 4-fluorophenyltrifluoroborate (**1a**) (4.4×10^{-5} mol, 8.8 mg) was heated at 55 °C in a stirring solution of THF:water (10:1, 5.5 mL) in a PTFE lined test tube. After 280 min, glass powder (20 mg grade 3) was added. Samples (0.5 mL) were removed throughout the reaction with a plastic syringe and placed immediately in pre-cooled (0 °C) PTFE lined NMR tubes. The samples were kept at that temperature until they were placed directly into the *Eclipse 300* NMR probe. Each sample was analysed by ^{19}F NMR and subject to 128 pulses (4 min 17 s) at 25 °C.

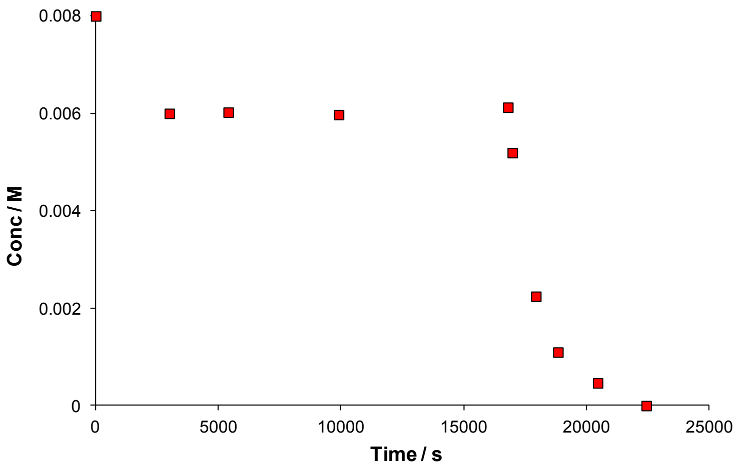

Figure S9. Equilibration of 1a with 2a at 55 °C in THF:water (10:1) in a PTFE lined test tube. After 16800 seconds glass powder (20 mg) was added.

Effect of glass surface area[S8]

Glass powder (Grades 1, 2 and 3, 2.00×10^{-2} g) was added to a PTFE lined test tube loaded with a stirrer bar and sealed with a rubber septum under a N_2 atmosphere. Degassed THF:H_2O (10:1, 8.25 mL) was then added and the test tube was placed into a preheated oil bath at 55 °C. After 10 minutes of stirring, potassium 4-fluorophenyltrifluoroborate (**1a**) (6.6×10^{-5} mol, 1.33×10^{-2} g) was added and samples (0.3 mL) were removed into pre-cooled (0 °C) PTFE lined NMR tubes at regular time intervals using a plastic syringe. These were stored at 0 °C prior to ^{19}F NMR analysis where they were subject to a maximum of 5 min at room temperature. Spectra were acquired by accumulating 128 scans at 25 °C.

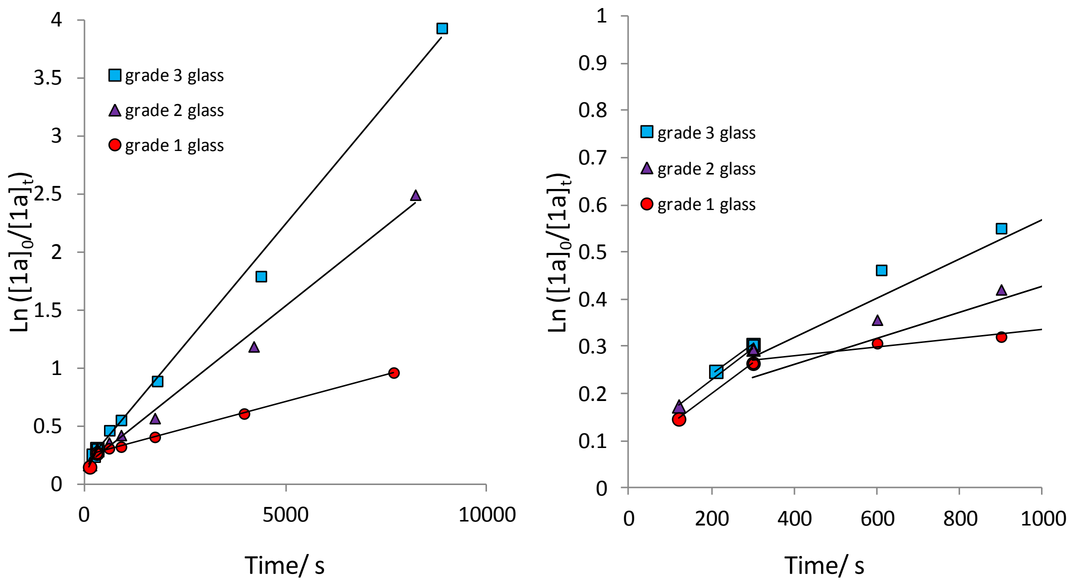

Figure S10. First order log plots of the hydrolysis of 1a (8 mM) to 2a in THF:water (10:1) at 55 °C with the addition of three different grades of glass powder. The right hand graph is an expansion of the initial period of the left graph showing the rapid pre-equilibrium.

Hydrolytic equilibration of 1a with 2a under *base and glass free* conditions

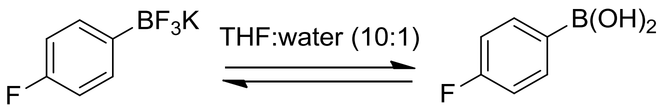

1a **2a**

Rate of equilibration of 1a with 2a

Potassium 4-fluorophenyltrifluoroborate (**1a**) (4.36×10^{-6} mol) was added as a solid to a PTFE lined NMR tube. To this was added firstly dry THF (0.5 mL) and lastly D_2O (0.05 mL) before being briefly shaken and placed immediately into the preheated (55 °C) *Varian 500* NMR probe. The reaction was monitored by ^{19}F NMR using a time delayed array to separate the acquisitions. Each acquisition was 64 scans (93 s) long with a time delay between separate acquisitions of 0 seconds. To ensure accuracy this experiment was repeated a further two times.

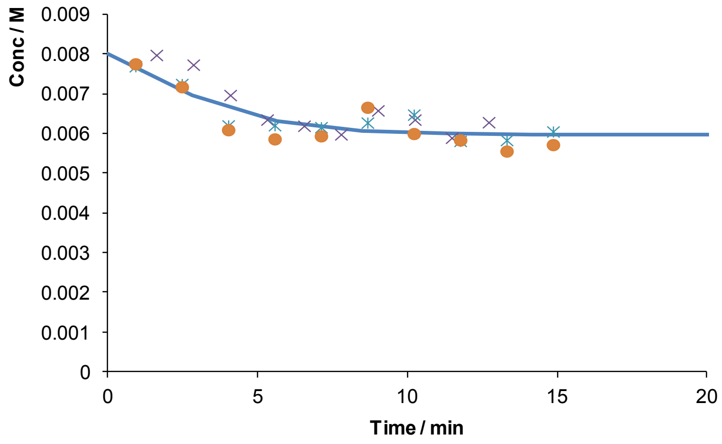

Figure S11 The equilibration between 1a and 2a for the three separate runs performed in THF:water (10:1) at 55 °C in PTFE lined NMR tubes. The fit is derived from the equilibration model outlined below, Scheme 1.

Equilibration Model

Concentration data, Figure S11, were analysed using the model shown below, Scheme 1:

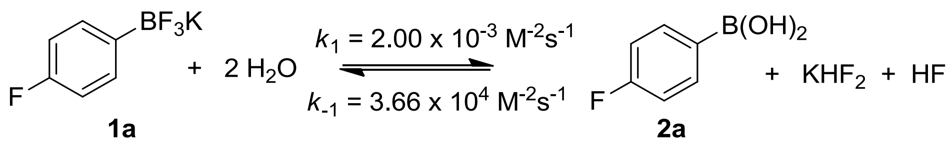

Scheme 1. Model used for equilibration between 1a and 2a.

Rate constants (k_1 and k_{-1}) were derived from parallel iterations of five data sets.[S9] The calculated equilibrium constant ($K_1 = k_1/k_{-1} = 5.46 \times 10^{-8}$) has then been used to model the effect of [**1a**] and [H_2O] on the equilibrium between **1a** and **2a**, Scheme 2.

Effect of [1a] on equilibrium

Potassium 4-fluorophenyltrifluoroborate (**1a**) (5.5×10^{-7}, 2.75×10^{-6}, 4.4×10^{-6}, 8.25×10^{-6} and 1.1×10^{-5} mol) was added as a stock solution in dry THF (0.5 mL) to a PTFE lined NMR tube. To this was added D_2O (0.05 mL), bringing the total THF:water ratio to 10:1, the volume to 0.55 mL and [**1a**] to 1, 5, 8, 10, 15 and 20 mM respectively. The tube was briefly shaken and placed immediately into the preheated (55 °C) *Varian 500* NMR probe. Each sample was given 15 mins of heating before being analysed by ^{19}F NMR (2000 – 200 scans depending on the concentration, 55 °C)

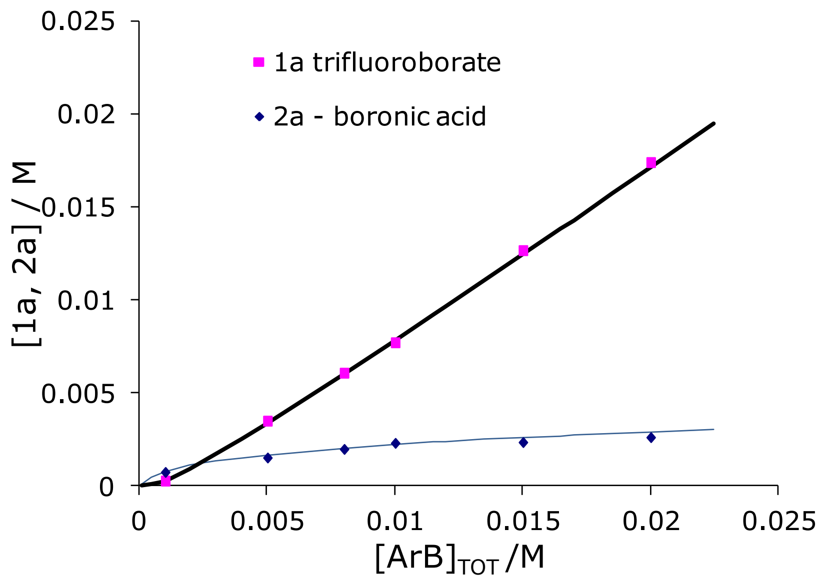

Figure S12. Equilibrium concentrations of 1a and 2a as a function of different initial 1a concentrations in THF:water (10:1) in PTFE NMR tubes. Solid lines come from the same model (1a + $2H_2O$ <-> 2a + KHF_2 + HF) as that shown in Figure S11 and Scheme 2, where k_1 = 2.00 x 10^{-3} $M^{-2}s^{-1}$, k_{-1} = 3.66 x 10^{-4} $M^{-2}s^{-1}$ therefore K_1 = 5.46 x 10^{-8}.

Effect of [H_2O] on equilibrium

Potassium 4-fluorophenyltrifluoroborate (**1a**) (3.9 x 10^{-6} mol, 0.8 mg) was added to a PTFE lined NMR tube in THF:water (20:1, 10:1, 7:1, 3:1, 1.66:1, 1:1, 1:1.66, 1:3, 1:7, 0:1) (0.5 mL). The tube was heated at 55 °C in a water bath for 20 min before being placed into a preheated (55 °C) *Eclipse 300* NMR probe where it was analysed by ^{19}F NMR (200 scans, 55 °C). This procedure was repeated at with one hour equilibration time at 25 °C before being analysed by ^{19}F NMR (200 scans, 25 °C).

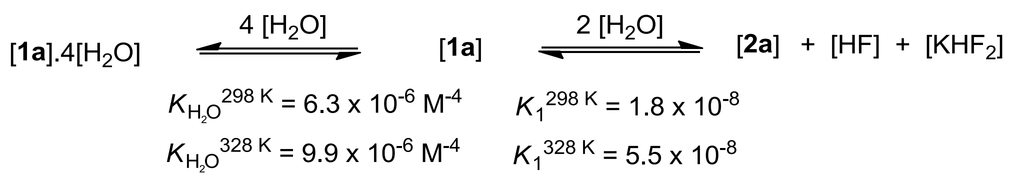

Scheme 2. Model used for simulating data for the effect of [1a] concentration and [H_2O] on the equilibrium between 1a and 2a. It was found that 1a undergoes a stabilising solvation at high [H_2O]. The experimental data was best fit, at the two temperatures (273 K and 326 K), by using 4 H_2O molecules.

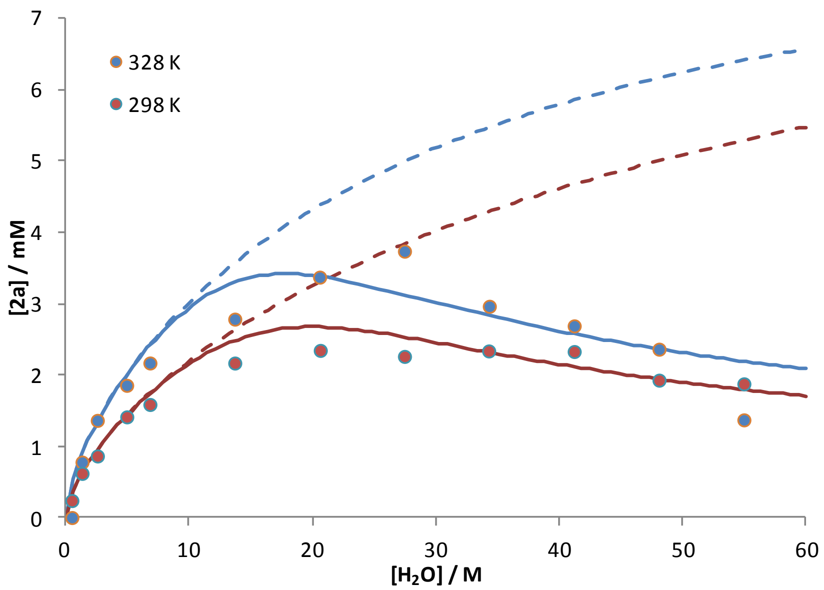

Figure S13. The effect of [H_2O] on concentration of 2a at hydrolytic equilibrium at 298 K and 328 K. Solid lines are concentration data from the model shown in Scheme 2. Dashed lines are how the model predicts the system without any solvation of 1a.

Van't Hoff analysis

Potassium 4-fluorophenyltrifluoroborate (**1a**) (3.20×10^{-6} mol) in dry THF (0.4 mL) was added to a PTFE lined NMR tube containing a D_2O (0.04 mL), bringing the total ratio to 10:1, the volume to 0.44 mL and [**1a**] to 8 mM. The tube was immediately placed into the *Varian 500* probe at 25 °C. It was analysed by ^{19}F NMR at four different temperatures (25°C, 35°C, 45°C and 55°C). The reaction was subjected to 15 min equilibration time at each temperature before the acquisition (120 scans) began. Measurements were performed twice at each temperature and equilibrium analysed as follows K_{app} = [**2a**][HF][KHF_2]/[**1a**][H_2O]^2 = [**2a**]^3/25*[**1a**]. Van't Hoff analysis (Figure S14) indicates that ΔH = 0.4 kJmol^{-1}, ΔS = -0.5 Jmol^{-1}K^{-1}. *However, we emphasize that this analysis will be highly dependent on the accuracy of the initial concentrations (**1a** and H_2O) and should be interpreted accordingly.*

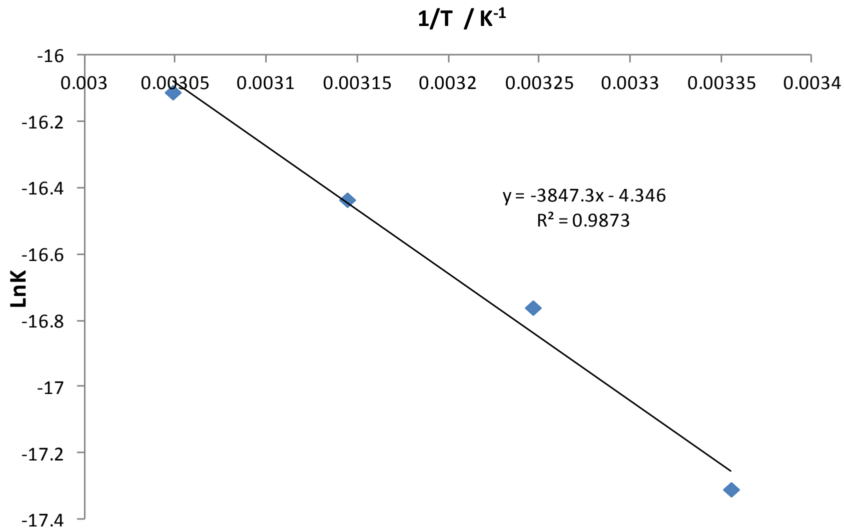

Figure S14. Van't Hoff plot of equilibrium between 1a (Initial conc. = 8 mM) and 2a at four temperatures (25, 35, 45 and 55 °C) in THF:water (10:1). K = K_{app} = $[2a]^3/25*[1a]$.

Equilibration of R-BF_3K (1a-i) with boronic acids (2a-i).

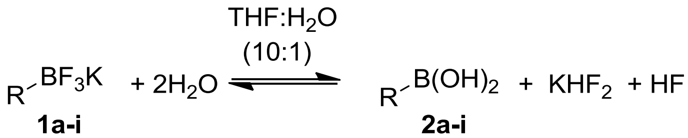

The potassium organotrifluoroborate (**1a-i**) (4.4 x 10^{-6} mol) was added to a PTFE lined Quartz NMR tube. THF:water (10:1, 0.55 mL) was added after which the tube was shaken and placed immediately into the preheated (55 °C) *Eclipse 300* probe. The sample was heated at 55 °C for 15 min before being analysed by ^{11}B NMR (2500 scans) and ^{19}F NMR (200 scans) at 55 °C.

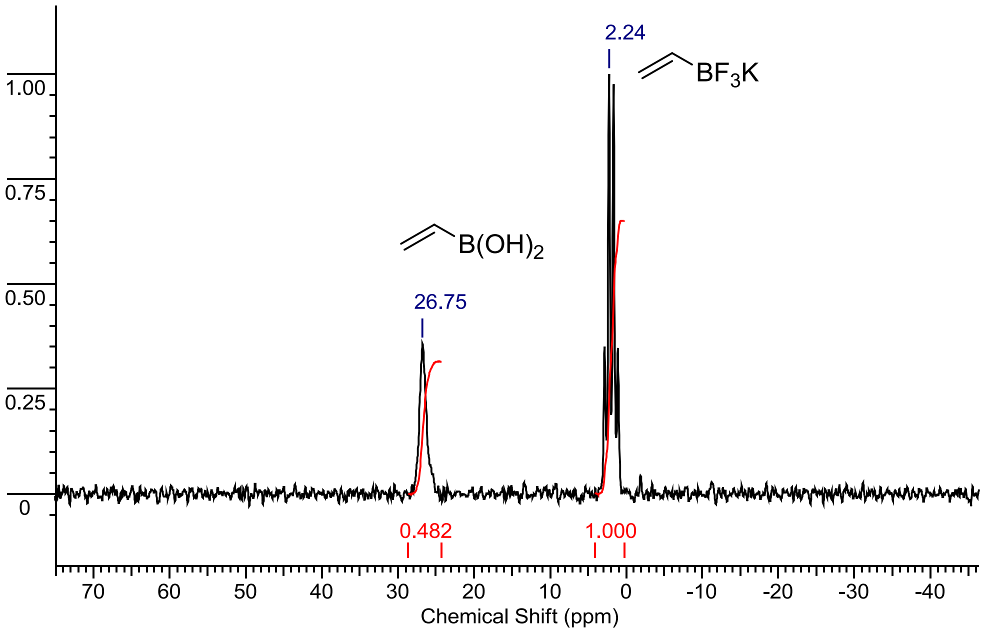

Figure S15. An example [11]B NMR spectrum showing substrate 1c at equilibrium in THF:H_2O (10:1) at 55 °C.

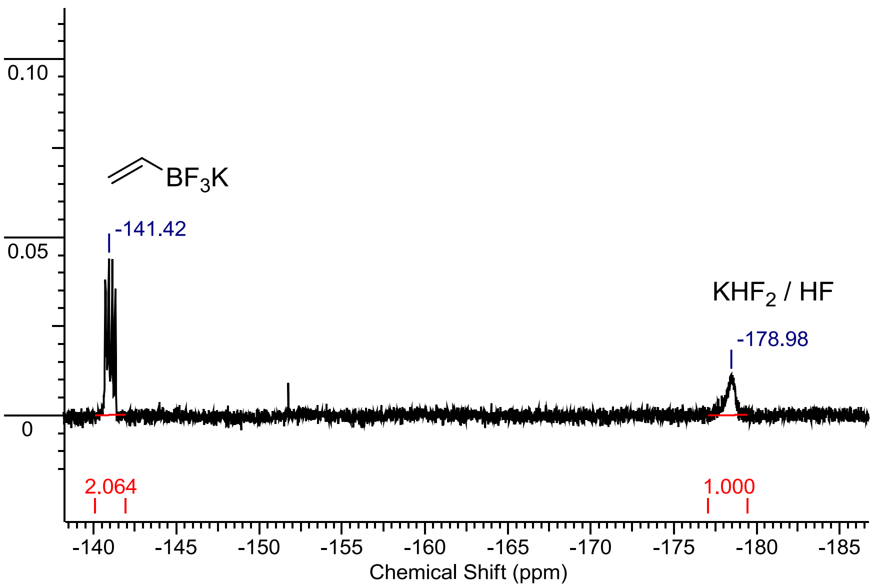

Figure S16. An example [19]F NMR spectrum showing substrate 1c at equilibrium in THF:H_2O (10:1) at 55 °C.

Table S2. Equilibrium populations of substrates **1a-1i** in THF:H_2O (10:1) at 55 °C at 8 mM

Substrate (8 mM)	x_1[a]	x_2[b]	K_{app}[c]
Aryl (**a**)	0.75	0.25	5.3E-08
Furanyl (**b**)	0.81	0.19	2.2E-08
Vinyl (**c**)	0.67	0.33	1.4E-07
Cyclopropyl (**d**)	0.39	0.61	1.5E-06
Alkynyl (**e**)	1.00	0.00	0.00
Cyclobutyl (**f**)	0.61	0.39	2.5E-07
Isopropyl (**g**)	0.71	0.29	8.8E-08
Benzyl (**h**)	0.83	0.17	1.5E-08
1,3-Diphenylpropyl (**i**)	0.79	0.21	3.0E-08

[a] Where $x_1 = [\mathbf{1}]_{eq.} / ([\mathbf{1} + \mathbf{2}]_{eq.})$ – rounded up to 2 d.p.
[b]Where $x_2 = [\mathbf{2}]_{eq.} / ([\mathbf{1} + \mathbf{2}]_{eq.})$ – rounded up to 2 d.p.
[c] Where $K_{app} = [\mathbf{2}]^3/(25*[\mathbf{1}])$

Table S3. Equilibrium populations of substrates **1a-1i** in THF:H_2O (10:1) at 55 °C at 100 mM

Substrate (100 mM)	x_1[a]	x_2[b]	K_{app}[c]
Aryl (**a**)	0.97	0.03	7.1E-11
Furanyl (**b**)	0.97	0.03	7.1E-11
Vinyl (**c**)	0.96	0.04	1.7E-10
Cyclopropyl (**d**)	0.89	0.11	3.8E-09
Alkynyl (**e**)	1.00	0.00	0.00
Cyclobutyl (**f**)	0.95	0.05	3.4E-10
Isopropyl (**g**)	0.97	0.03	7.1E-11
Benzyl (**h**)	0.93	0.07	9.4E-10
1,3-Diphenylpropyl (**i**)	0.92	0.08	1.4E-09

[a] Where $x_1 = [\mathbf{1}]_{eq.} / ([\mathbf{1} + \mathbf{2}]_{eq.})$ – rounded up to 2 d.p
[b] Where $x_2 = [\mathbf{2}]_{eq.} / ([\mathbf{1} + \mathbf{2}]_{eq.})$ – rounded up to 2 d.p
[c] Where $K_{app} = [\mathbf{2}]^3/(25*[\mathbf{1}])$

Degenerate exchange between 1a and 2a

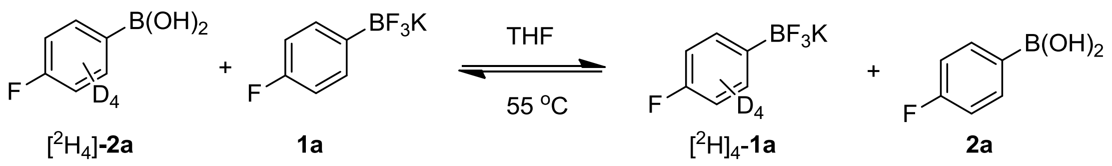

Potassium 4-fluorophenyltrifluoroborate (**1a**) (2.2 x 10^{-5} mol, 4.4 mg) and [$^2H_4$] – 4-fluorophenylboronic acid ([$^2H_4$] **-2a**) (2.2 x 10^{-5} mol, 3.16 mg) were added as solids to dry THF (5 mL) in a PTFE lined test tube. The solution was heated at 55 °C for two hours under an atmosphere of dry N_2. A sample was removed with a plastic syringe and placed immediately into a PTFE lined NMR tube, which was analysed by ^{19}F NMR (128 scans, 25 °C)

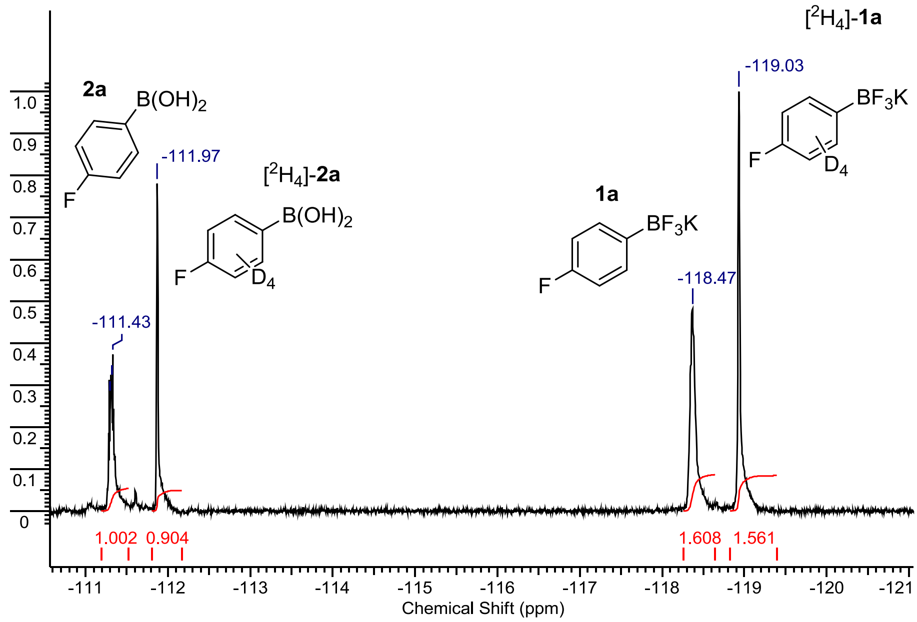

Figure S17. ^{19}F NMR spectrum showing the degenerate exchange between 1a and 2a at 55 °C in THF in PTFE, as indicated by deuterium labelling of 2a and then the isotope shift (Δδ = 0.4 - 0.5 ppm) observed in the ^{19}F NMR.

pH monitoring

A pre-heated (55 °C) solution of THF:water (10:1, 6.6 mL) was added to a solid mixture of potassium 4-fluorophenyltrifluoroborate (**1a**) (5.28 x 10^{-5} mol, 10.6 mg) and Cs_2CO_3 (3 equiv., 1.58 x 10^{-4} mol, 51.6 mg) in a 15 mm diameter PTFE lined test tube. This stirring (100 rpm) solution was heated at 55 °C and the pH was read from an uncalibrated Hanna HI 98103 pH probe every 10 seconds for the first 10 min and every 30 seconds for the following 2 hours. Samples (0.3 mL) were removed throughout the reaction using a plastic syringe and placed in pre-cooled (0° C) PTFE lined NMR tubes. The samples were kept at that temperature until they were placed directly into the *Eclipse 300* NMR probe. Each sample was analysed by ^{19}F NMR and subject to 128 pulses (4 min 17 s) at 25 °C.

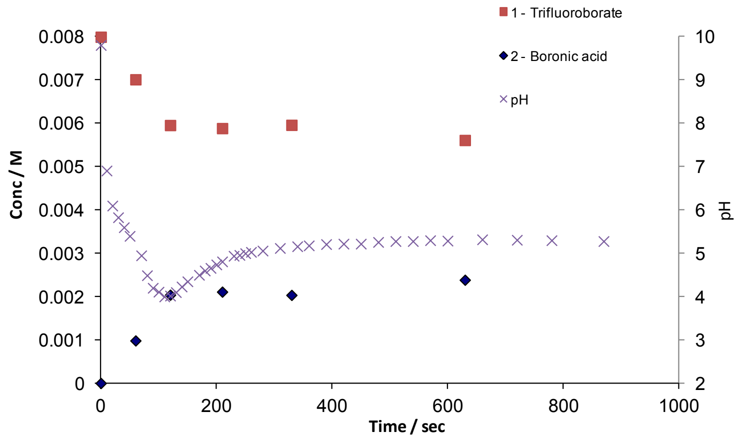

Figure S18. Equilibration of 1a (8 mM) with 2a in THF:water (10:1) in a PTFE lined test tube at 55 °C

Effect of Cs_2CO_3 on THF/H_2O phase splitting

Cs_2CO_3 titration

A 2 mL graduated pipette was filled with THF:water (10:1, 2 mL) until the solvent was above the top graduation mark. The outlet was then occluded with a small piece of molten plastic and the solvent removed until the meniscus was level with the top graduation mark. Cs_2CO_3 was then added in aliquots (1.59×10^{-5} – 1.38×10^{-4} mol), and the apparatus gently agitated to ensure dissolution of the base and mixing of the phases before allowing it to settle for about a minute. The level of the phase boundary was then noted after each addition.

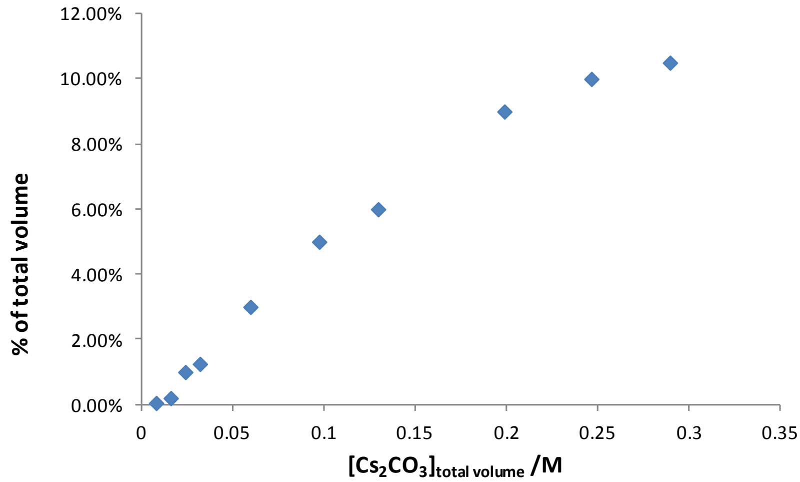

Figure S19. Volume (%) of minor biphase as a function of $[Cs_2CO_3]_{NET}$ in THF:water (10:1) at 25 °C.

Sonication of a basic biphasic solution of 4-fluorophenylboronic acid (2a) in THF:water

A NMR tube containing THF (0.8 mL) was charged with Cs_2CO_3 (2.64 x 10^{-5} mol,) in H_2O (0.1 mL). To this was added 4-fluorophenylboronic acid (**2a**) (8.8 x 10^{-6} mol 1.23 mg) in THF (0.2 mL). This sample was analysed by ^{19}F NMR at 55 °C before and immediately after one minute sonication. A time averaged ^{19}F NMR signal is indicative of Ar-B(OH)$_2$ (**2a**) <-> Ar-B(OH)$_3^-$ (**5a**, n = 3) equilibrium position, where δ = -111.5 ppm : ≥ 95 % **2a** and δ = -118 ppm : ≥ 95 % **5a**.[S4]

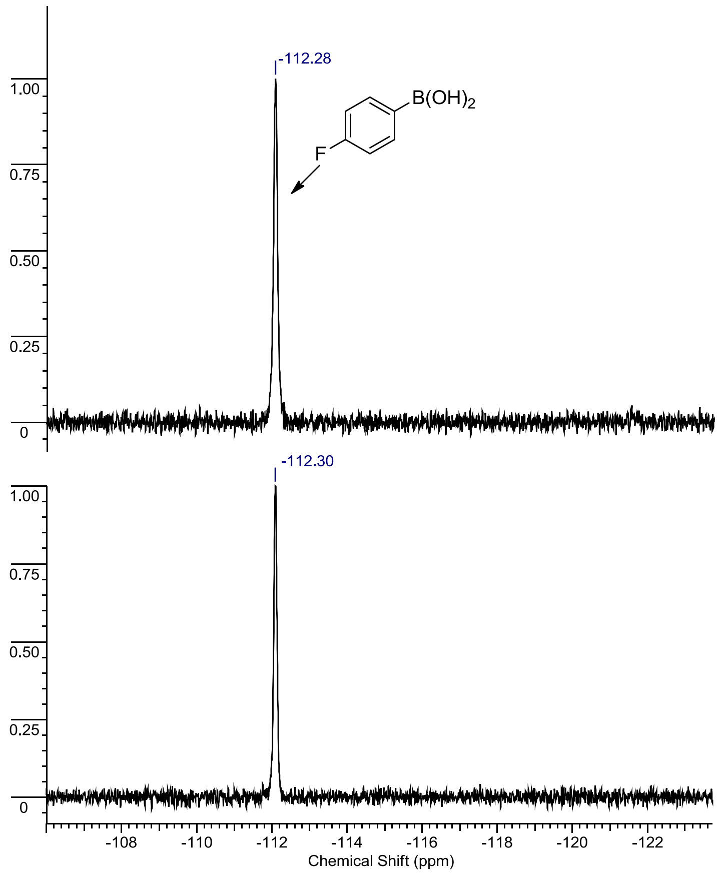

Figure S20. **^{19}F NMR spectra of 2a before (upper spectrum) and after (lower spectrum) one minute sonication in basic (3 equiv. Cs_2CO_3) and biphasic THF:water (10:1)**

Suzuki Miyaura couplings

Suzuki -Miyaura coupling in different reaction vessels

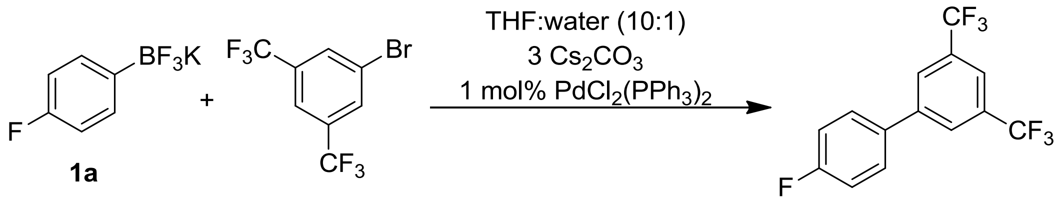

To a 15 mm wide Schlenk tube with a hemispherical base, under a N_2 atmosphere, was charged Cs_2CO_3 (3 equiv., 1.32 x 10^{-4} mol), degassed water (0.5 mL) and degassed THF (3 mL). To this was added 1,3-bis(trifluoromethyl)-5-bromobenzene (4.4 x 10^{-5} mol) in dry degassed THF (0.5 mL), potassium 4-fluorophenyltrifluoroborate (**1a**) (4.4 x 10^{-5} mol) in dry degassed THF (0.5 mL) and finally bis(triphenylphosphine)palladium(II) chloride (4.4 x 10^{-7} mol) in dry degassed

THF (1 mL), bringing the total THF:water ratio to 10:1 and volume to 5.5 mL and **1a** concentration to 8 mM. The same procedure was repeated in parallel but in a 15 mm wide Schlenk tube with a conical shaped base.

In both cases ≥ 85 % of the reaction volume was within the cylindrical section of the tube. The top of the Schlenk tube was left open to the air, to keep the concentration of O_2 constant. The solution was stirred at a rate in which no vortex was produced and heated at 55 °C for six hours, before being analysed by ^{19}F NMR (200 scans, 25 °C).

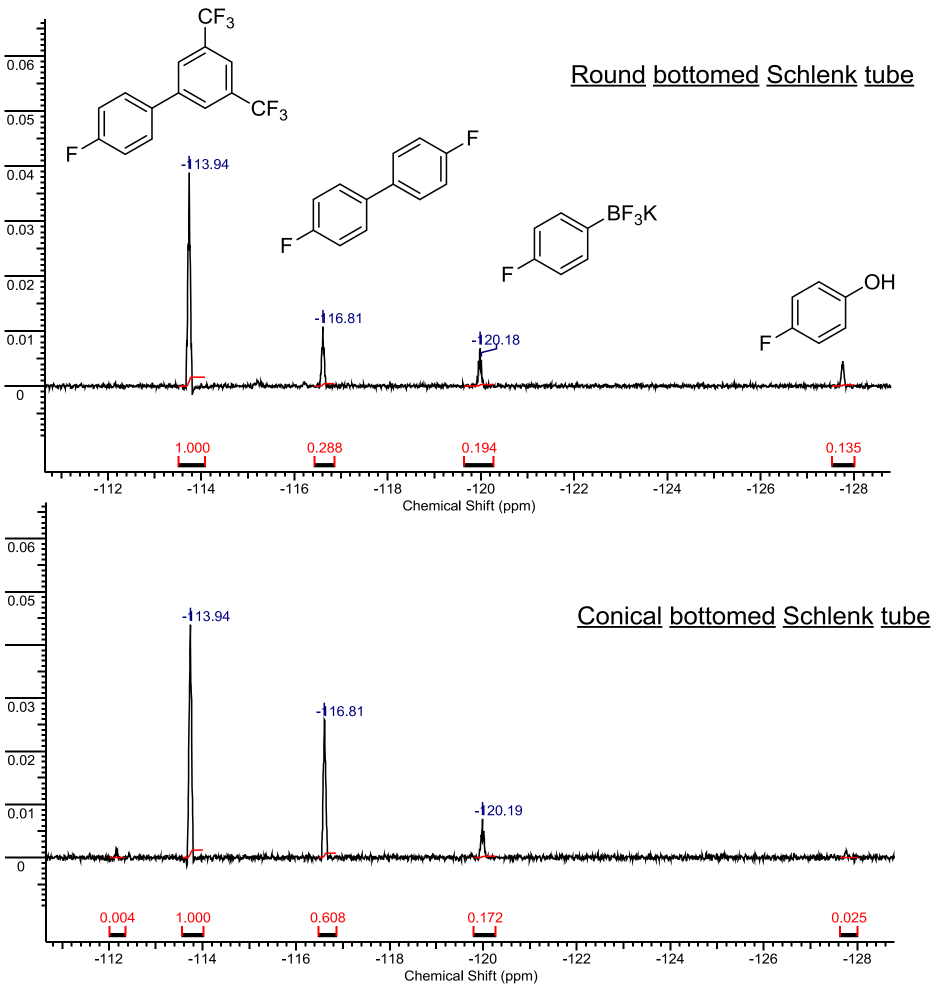

Figure S21 SM coupling of 1a with ArBr indicating how the ratio of side products to cross-coupled product varies under identical conditions other than the reaction vessel shape. We note that under fast release conditions (conical bottomed Schlenk tube) the relative stoichiometries of the 4-fluorophenol and 4,4'-difluorobiphenyl are not consistent with that expected based on the literature mechanism.[S10] We have noticed this on other occasions when there are high concentrations of fluoride. In contrast, the relative stoichiometries are correct under slow release conditions in the round bottomed Schlenk tube.

Chemoselective coupling

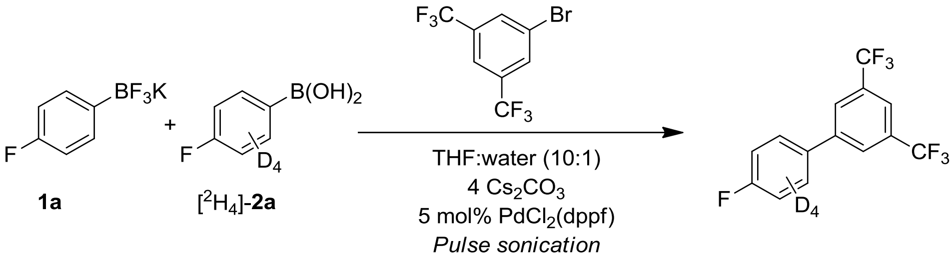

To a pre-sonicated mixture of Cs_2CO_3 (1.23 x 10^{-4} mol, 4 equiv.), 1,3-bis(trifluoromethyl)-5-bromobenzene (3.08 x 10^{-5} mol, 1 equiv.), [$^2H_4$]-4-fluorophenylboronic acid ([$^2H_4$]-**2a**) (3.08 x 10^{-5} mol, 1 equiv.) and degassed THF (6.3 mL) and water (0.7 mL) was added potassium 4-fluorophenyltrifluoroborate (**1a**) (3.08 x 10^{-5} mol, 1 equiv.) in THF (0.5 mL) dropwise and sonicated for a further 20 seconds. Dichloro-[1,l'-bis(diphenylphosphino)ferrocene]palladium(II) [$PdCl_2$(dppf)] (1.54 x 10^{-6} mol, 5 mol% in THF (0.2 mL)) was added dropwise to this vigorously stirring solution at 55 °C. The solution was subjected to 10 second sonication pulses every 10 min. A sample was removed after 40 min and placed into a pre-cooled (0 °C) PTFE lined NMR tube and analysed by ^{19}F NMR (128 scans at 25 °C).

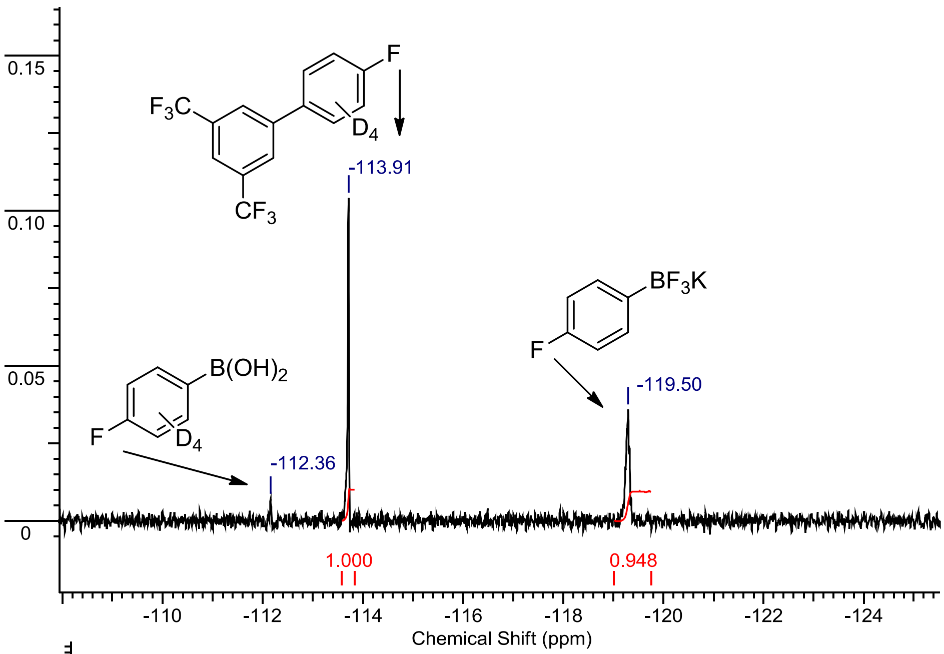

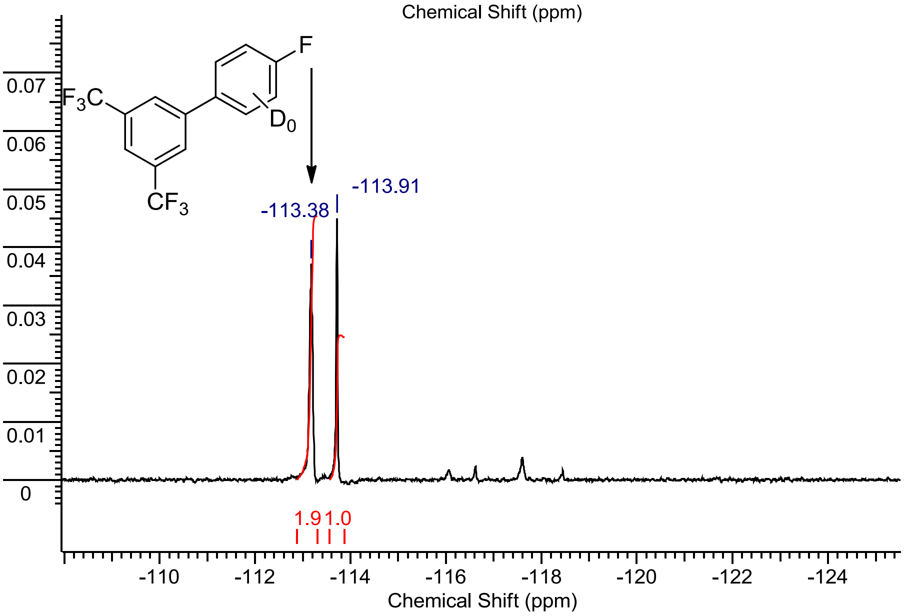

Figure S22. Upper spectrum - ^{19}F NMR spectrum after 40 min of reaction, showing clean generation of solely the [$^{2}H_4$] cross-coupled product. Lower spectrum – reference ^{19}F NMR spectrum of a mixture of D_0/D_4 cross coupled product where initial 1a: [$^{2}H_4$]-2a ratio = 60:40 [S4]

Cyclobutyl SM coupling[S3]

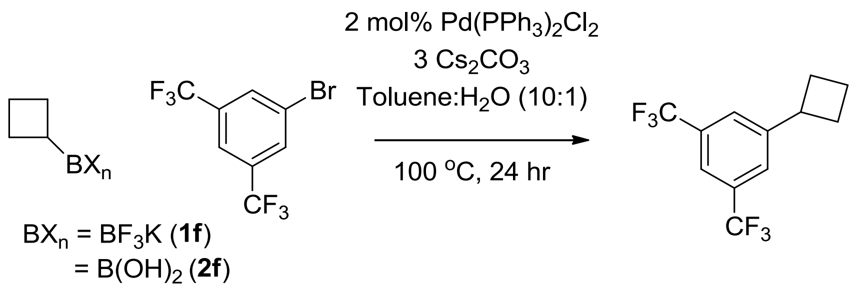

Dry and degassed toluene (3 mL) was added to a Schlenk tube, under an atmosphere of N_2, charged with a solid mixture of potassium cyclobutyltrifluoroborate (**1f**) (1.65 x 10^{-4} mol, 26.7 mg), bis(triphenylphosphine)palladium(II) chloride (3.3 x 10^{-6} mol, 2.3 mg) and Cs_2CO_3 (3 equiv. 4.95 x 10^{-4} mol, 161 mg). To this was added 1,3-bis(trifluoromethyl)-5-bromobenzene (1.65 x 10^{-4} mol, 48.3 mg) and water (0.03 mL). The stirring solution was heated 100 °C for 24 hours. A sample was removed after one hour and after 24 hours and analysed by ^{19}F NMR (128 scans, 25 °C).

A parallel reaction was run in which the above procedure was repeated with the replacement of potassium cyclobutyltrifluoroborate (**1f**) with cyclobutylboronic acid (**2f**) (1.65 x 10^{-4} mol, 16.5 mg).

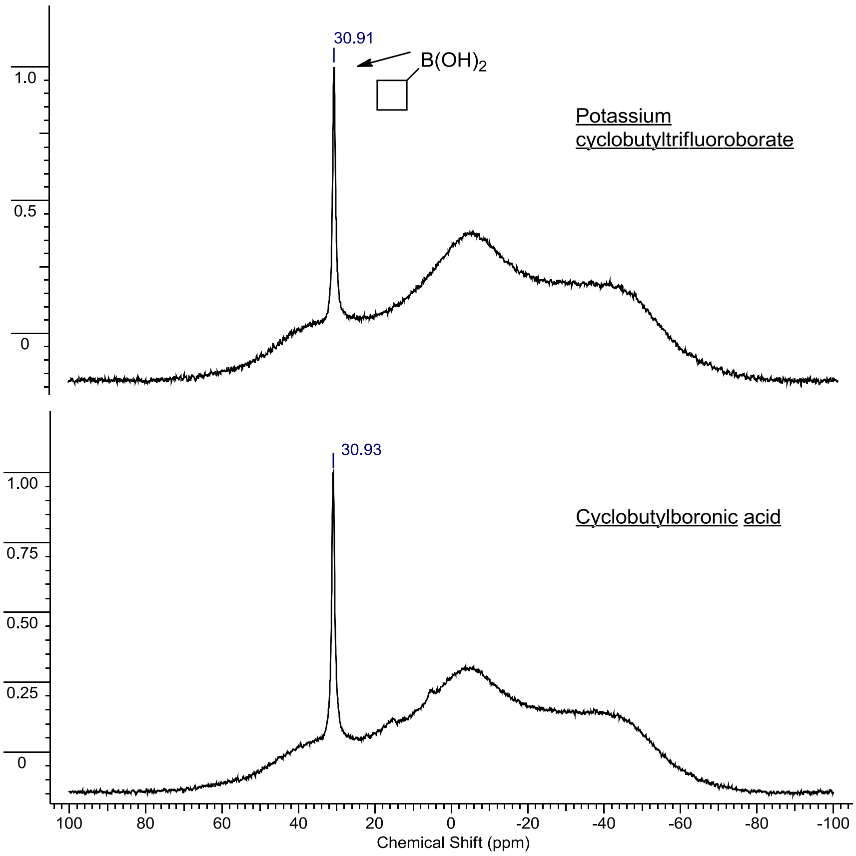

Figure S23. ^{11}B NMR spectra of a SM coupling reaction between potassium cyclobutyltrifluoroborate (1f) (upper spectrum) and cyclobutylboronic acid (lower spectrum) with ArBr, after 1 hour of heating at 100 °C. ^{11}B NMR shift of (1f) at 5 ppm.

Hydrolysis of R-BF$_3$K reagents (1a-1s)

Hydrolysis mediated by glass

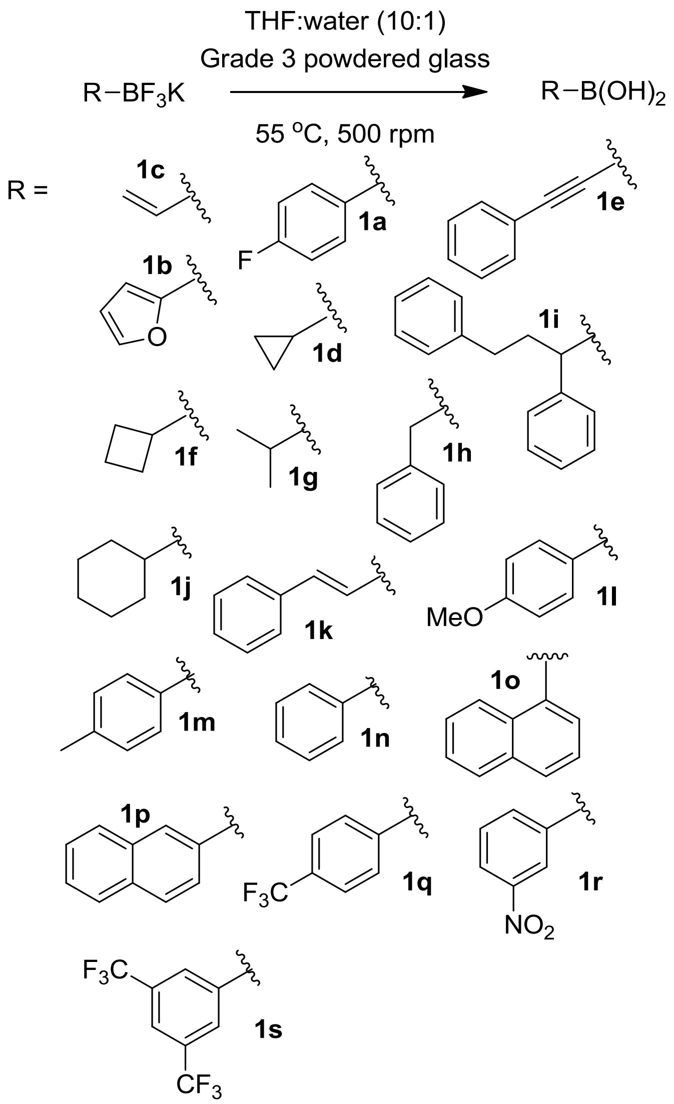

A preheated (55 °C) solution of THF:water (10:1, 6.6 mL) plus benzotrifluoride (10 μL) was added to the potassium organotrifluoroborate (5.28×10^{-5} mol) and glass powder (Grade 3, 20 mg) in a 15 mm diameter PTFE flat-bottomed test tube. A sample (0.3 mL) was immediately removed with a plastic syringe and placed in a pre-cooled (0 °C) PTFE lined NMR tube. The solution was then stirred at 500 rpm and heated at 55 °C for 2 - 24 hours, depending on the substrate. Samples were removed at regular time intervals into pre-cooled (0 °C) PTFE lined NMR tubes. Each sample was analysed by ^{19}F NMR spectroscopy and was subjected to 128 scans at 25 °C. The integration of R-BF_3K peak was normalised against the standard and concentrations calculated by comparison to the "0 seconds" time point assumed to be the known initial concentration. ^{11}B NMR was used to confirm conversion to the appropriate boronic acid had occurred. The protodeboronated product (**6**) was observed from substrate **1e**.

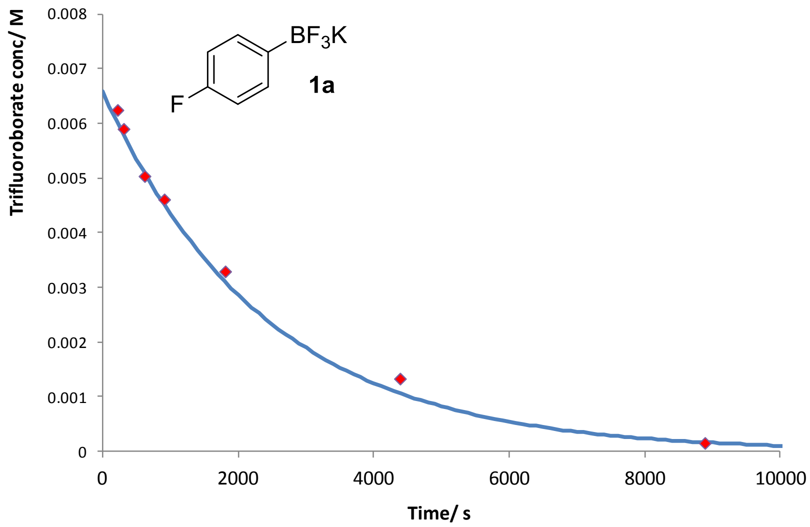

Figure S24. Pseudo first order hydrolysis of potassium 4-fluorophenyltrifluoroborate (1a), with added glass powder.

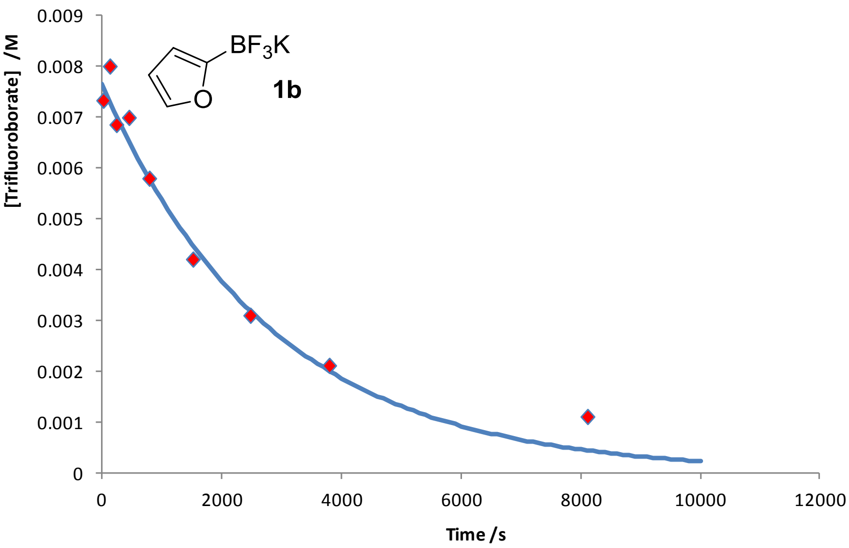

Figure S25 Pseudo first order hydrolysis of potassium 2-furyltrifluoroborate (1b), with added glass powder.

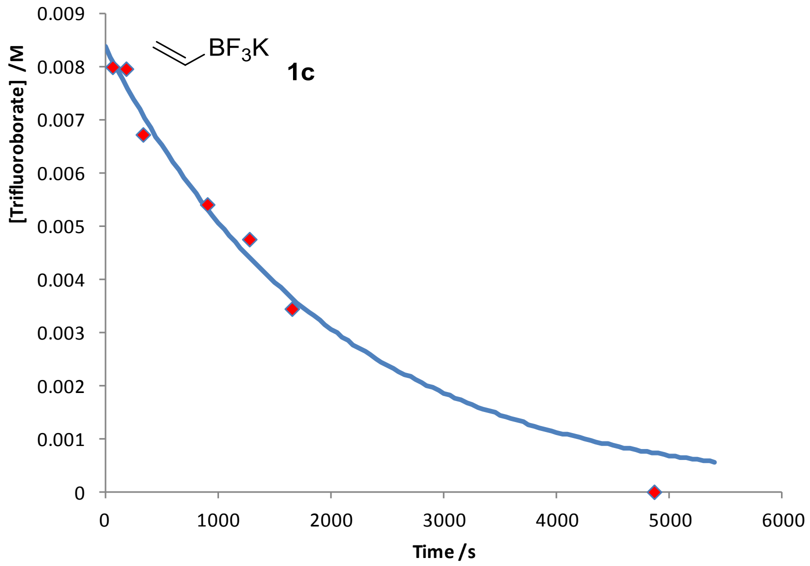

Figure S26 Pseudo first order hydrolysis of potassium vinyltrifluoroborate (1c), with added glass powder.

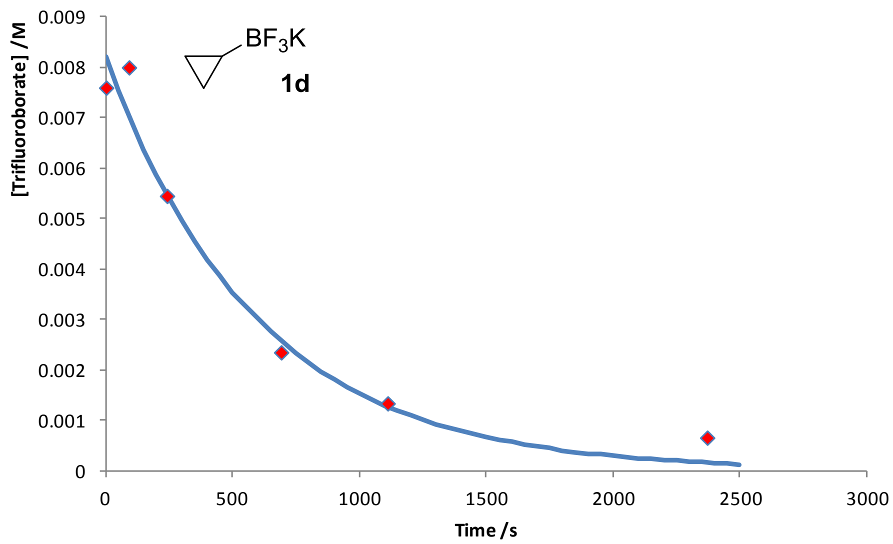

Figure S27 Pseudo first order hydrolysis of potassium cyclopropyltrifluoroborate (1d), with added glass powder.

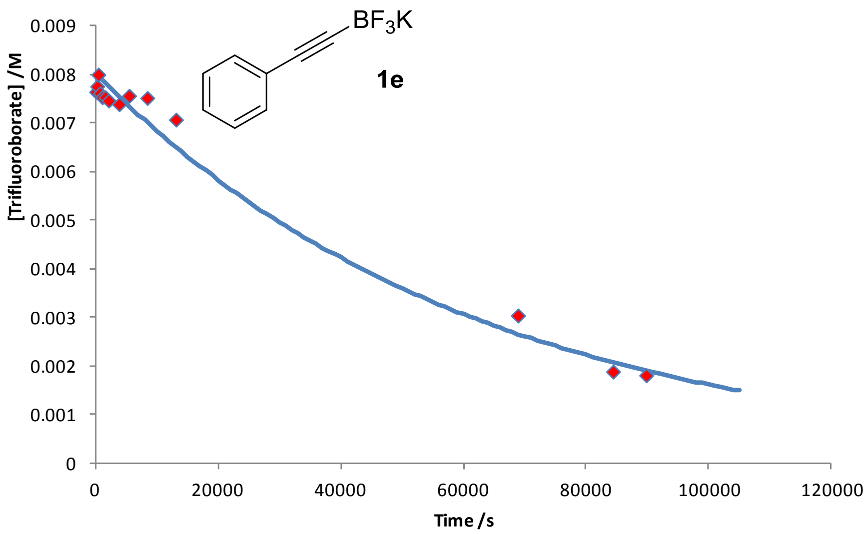

Figure S28 Pseudo first order hydrolysis of potassium phenylethynyltrifluoroborate (1e), with added glass powder.

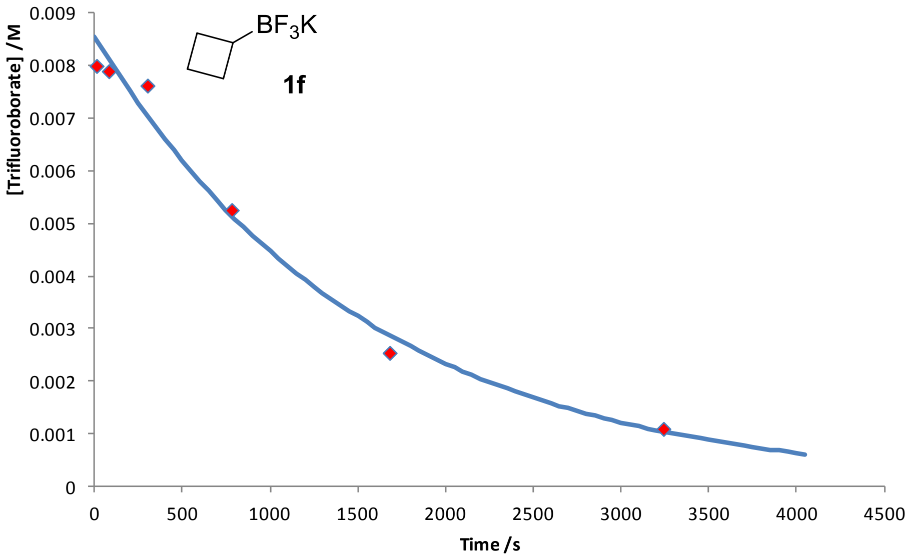

Figure S29 Pseudo first order hydrolysis of potassium cyclobutyltrifluoroborate (1f), with added glass powder.

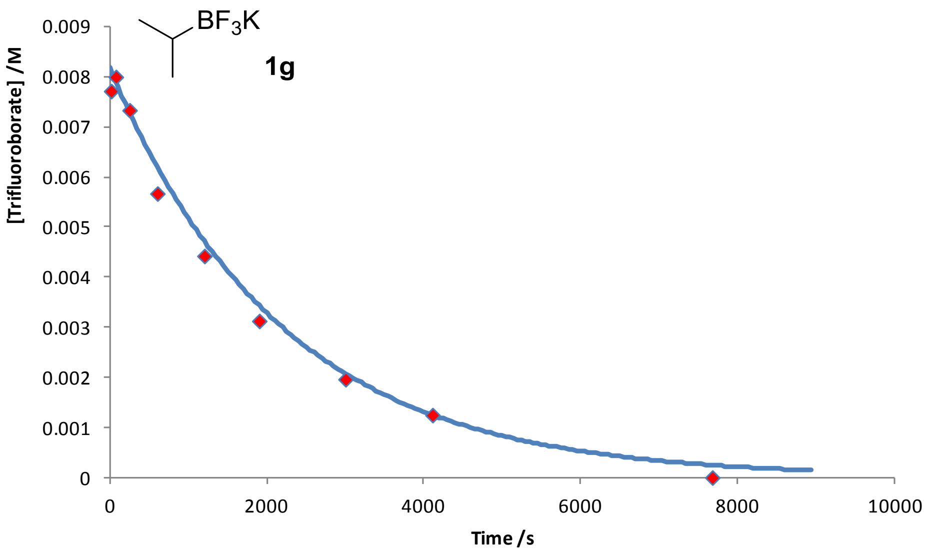

Figure S30 Pseudo first order hydrolysis of potassium isopropyltrifluoroborate (1g), with added glass powder.

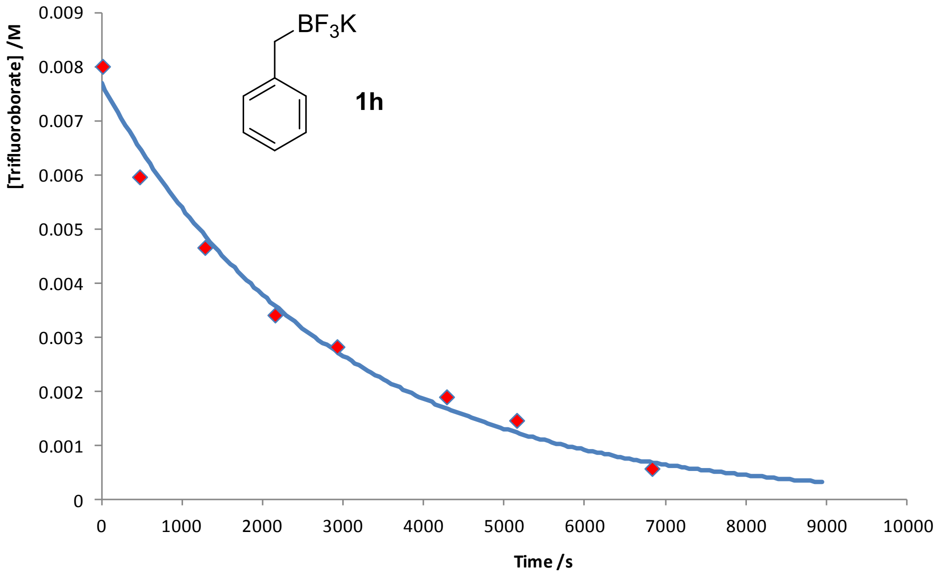

Figure S31 Pseudo first order hydrolysis of potassium benzyltrifluoroborate (1h), with added glass powder.

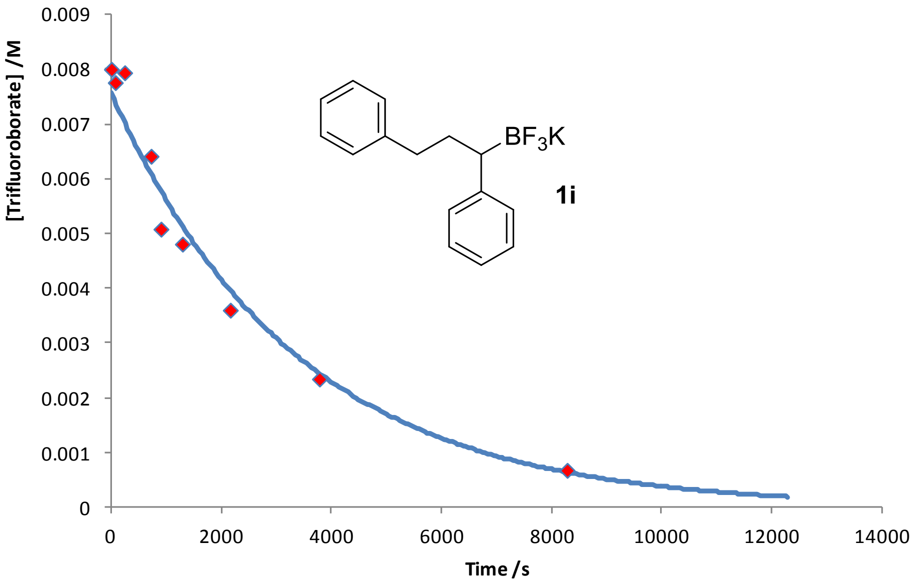

Figure S32 . Pseudo first order hydrolysis of potassium 1,3 diphenylpropyltrifluoroborate (1i), with added glass powder.

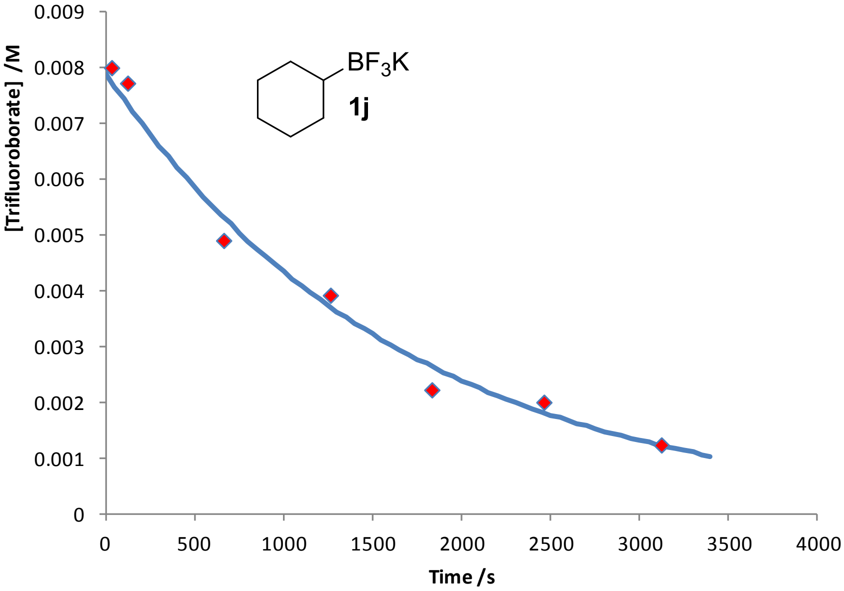

Figure S33 Pseudo first order hydrolysis of potassium cyclohexyltrifluoroborate (1j), with added glass powder.

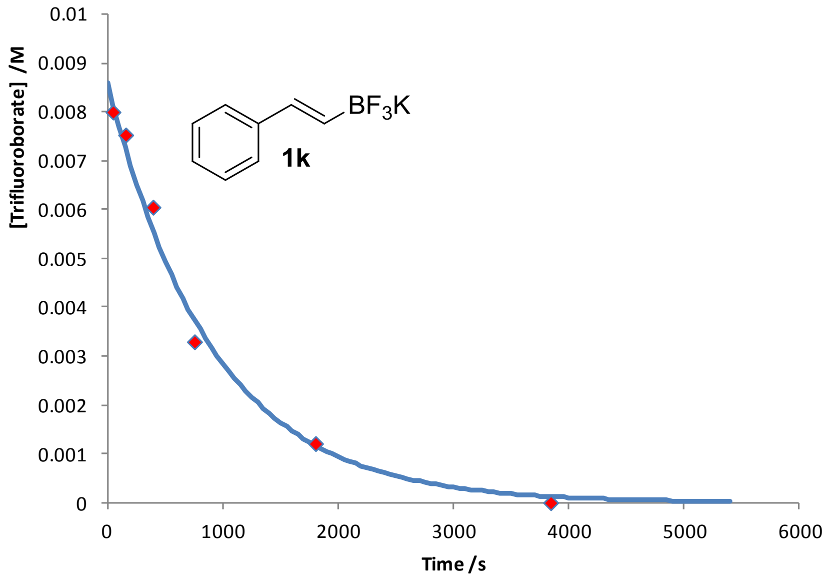

Figure S34. Pseudo first order hydrolysis of potassium phenylethenyltrifluoroborate (1k), with added glass powder.

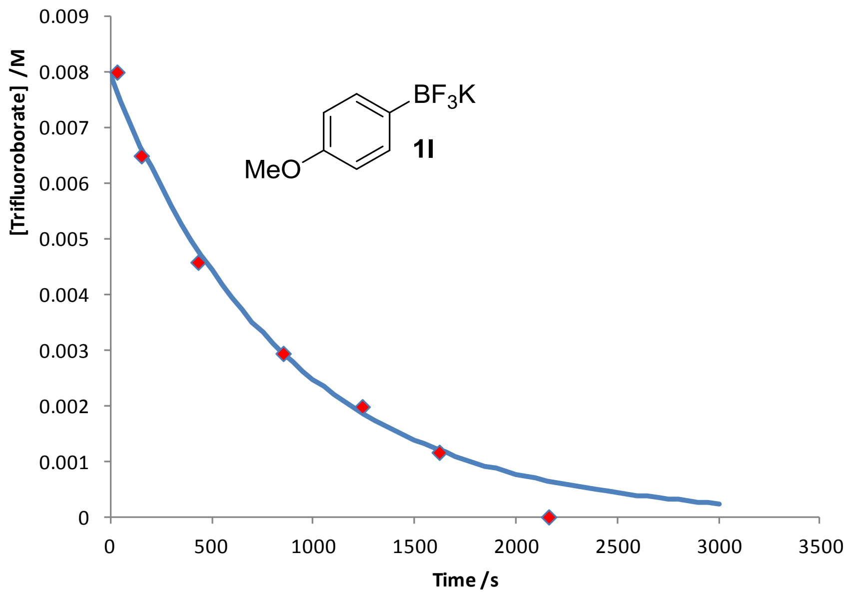

Figure S35. Pseudo first order hydrolysis of potassium 4-methoxyphenyltrifluoroborate (1l), with added glass powder.

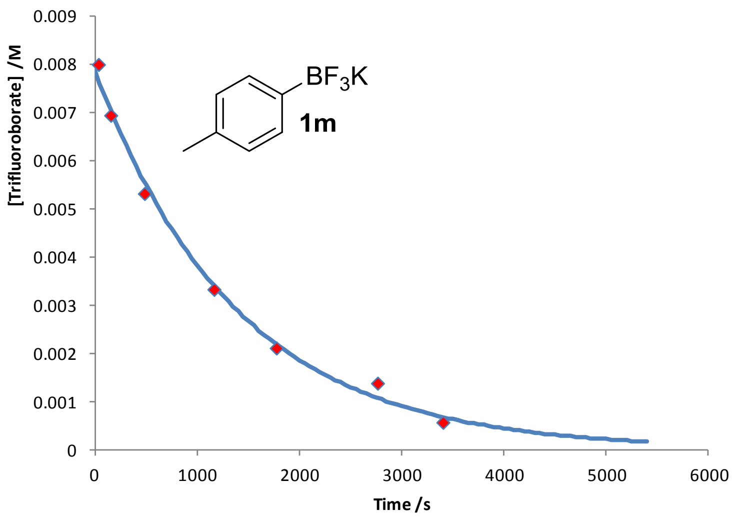

Figure S36. Pseudo first order hydrolysis of potassium 4-methylphenyltrifluoroborate (1m), with added glass powder.

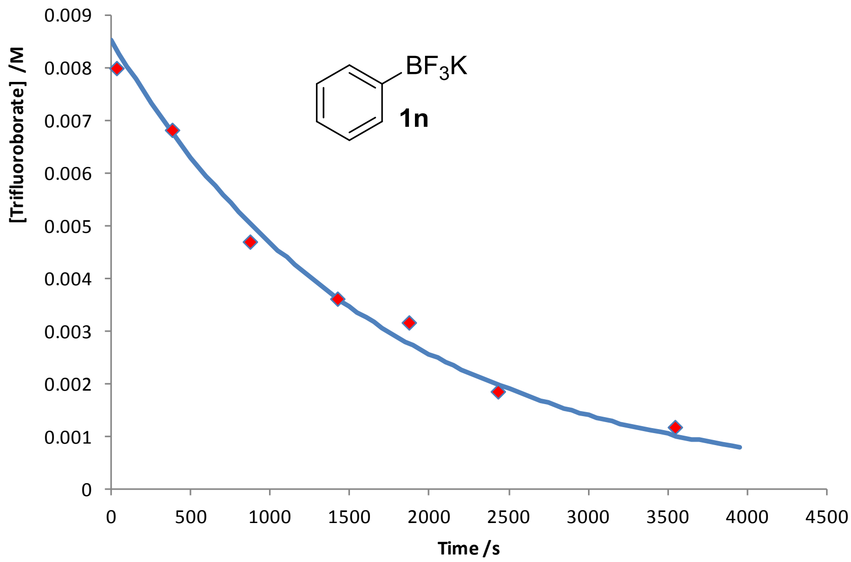

Figure S37. Pseudo first order hydrolysis of potassium phenyltrifluoroborate (1n), with added glass powder.

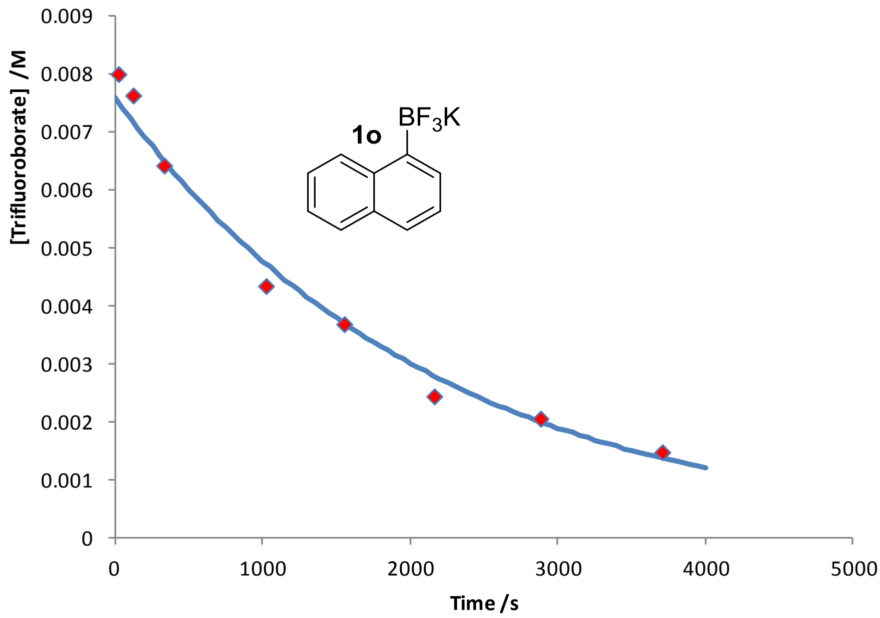

Figure S38. Pseudo first order hydrolysis of potassium 1-naphthyltrifluoroborate (1o), with added glass powder.

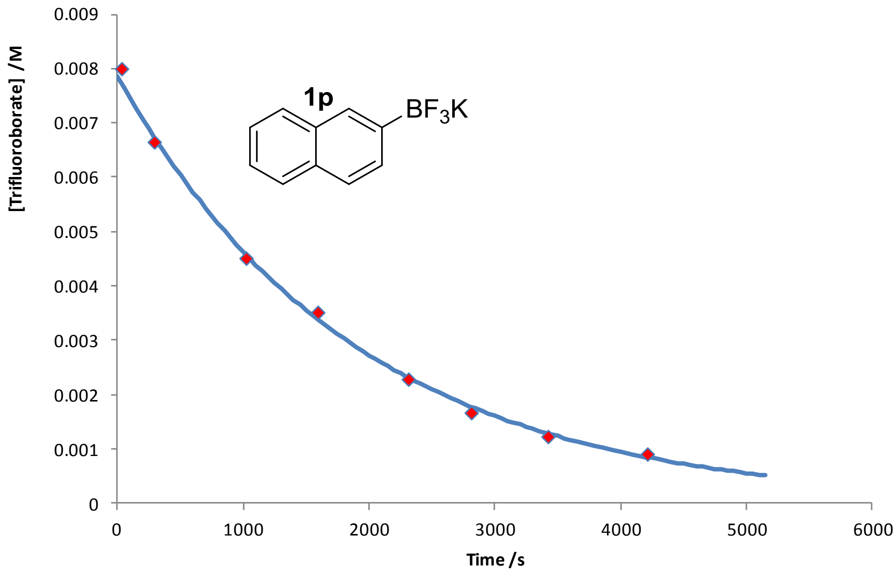

Figure S39. Pseudo first order hydrolysis of potassium 2-naphthyltrifluoroborate (1p), with added glass powder.

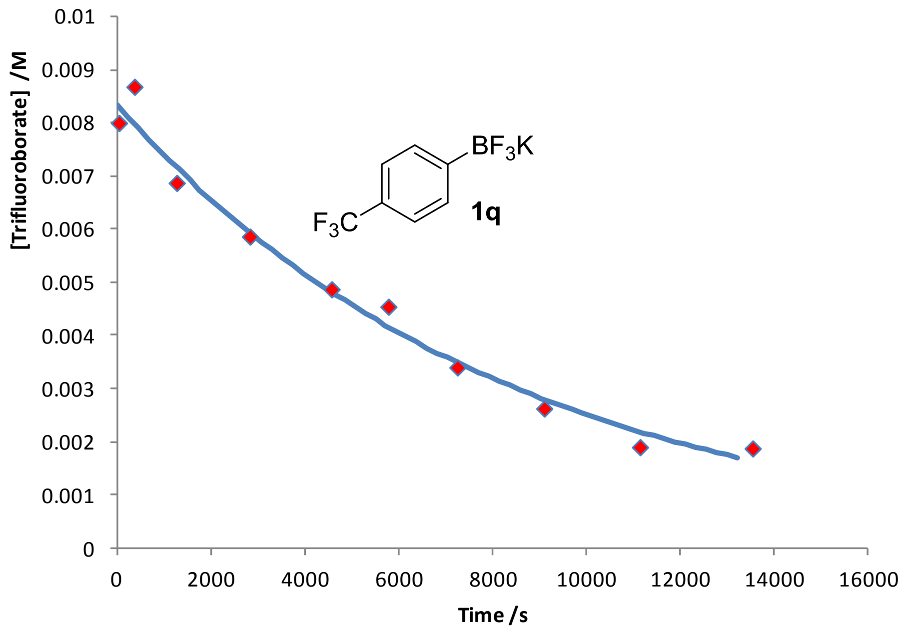

Figure S40. Pseudo first order hydrolysis of potassium 4-trifluoromethyltrifluoroborate (1q), with added glass powder.

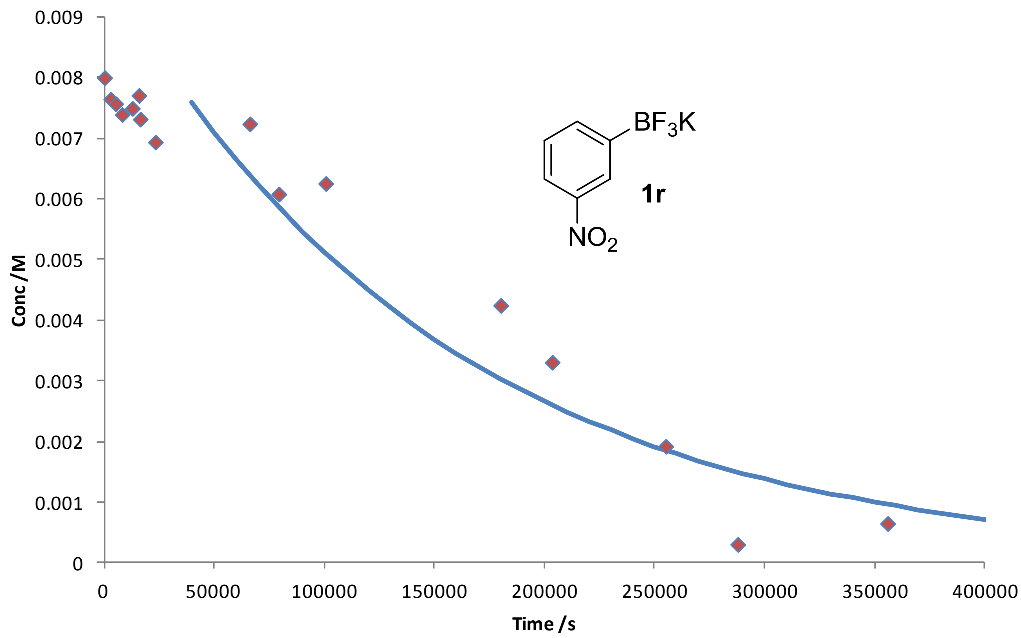

Figure S41. Pseudo first order hydrolysis of potassium 3-nitrophenyltrifluoroborate (1r), with added glass powder. Progressive rate acceleration, leading to deviation from first order decay, may arise from milling of glass powder over the extended reaction period, leading to a larger glass surface area and fluorophilic capacity.

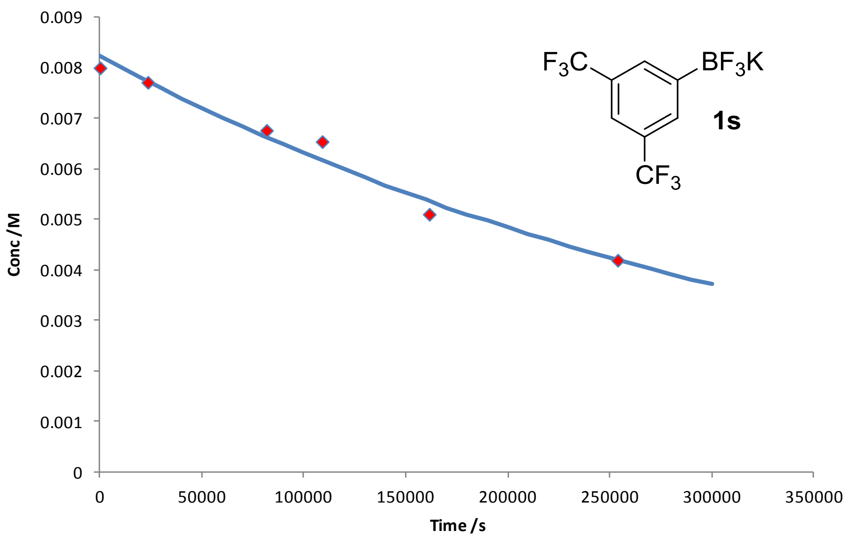

Figure S42. Pseudo first order hydrolysis of potassium 3-nitrophenyltrifluoroborate (1r), with added glass powder.

Hydrolysis under basic conditions

Cs_2CO_3

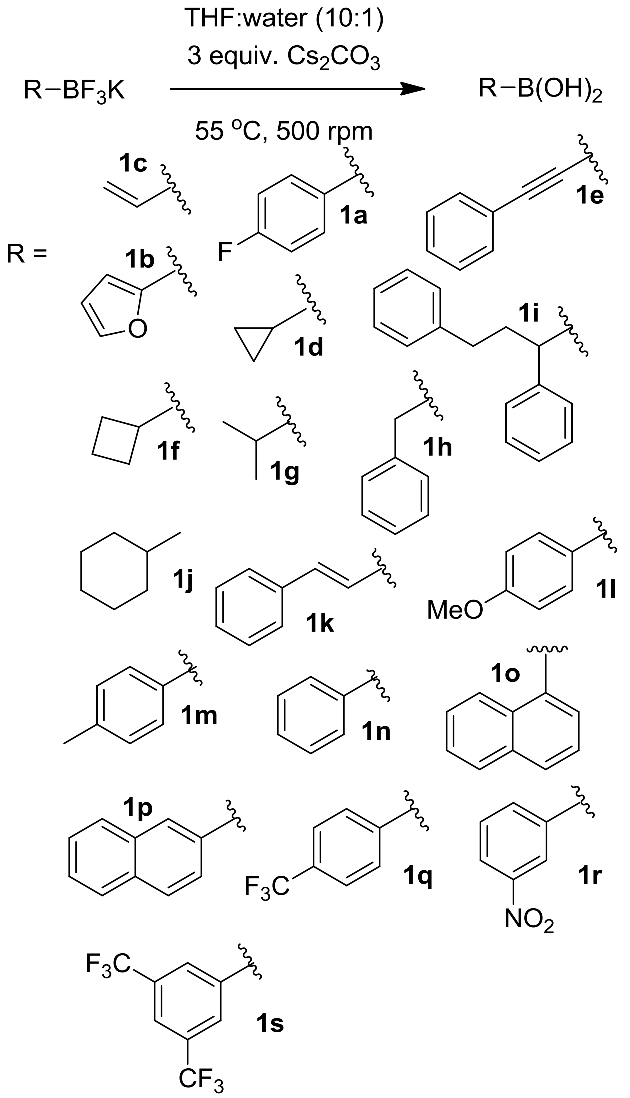

A preheated (55 °C) solution of THF (6 mL) plus benzotrifluoride (10 µL) was added to the potassium organotrifluoroborate (5.28×10^{-5} mol) and glass powder (Grade 3, 20 mg) in a 15 mm diameter PTFE flat-bottomed test tube. A solution of Cs_2CO_3 (1.58×10^{-4} mol) in water (0.6 mL) was added before immediately removing a sample (0.3 mL) into a pre-cooled (0 °C) PTFE lined NMR tube. The reaction was stirred at 500 rpm at 55 °C for 6 - 168 hours depending on the substrate. Samples were removed at regular time intervals into pre-cooled (0 °C) PTFE lined NMR tubes. Each sample was analysed by ^{19}F NMR spectroscopy and was subjected to 128 scans at 25 °C. The integration of R-BF_3K peak was normalised against the standard and concentrations calculated by comparison to the "0 seconds" time point assumed to be the known initial concentration. ^{11}B NMR was used to confirm conversion to the appropriate boronic acid had occurred. Conversion to the protodeboronated product (**6**) was observed from substrate **1e** and **1s.**

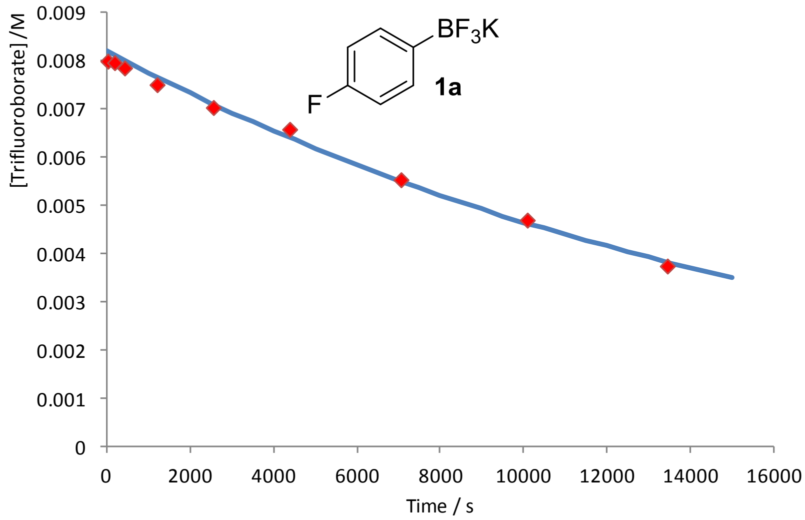

Figure S43 Pseudo first order hydrolysis of potassium 4-fluorophenyltrifluoroborate (1a), under basic (Cs_2CO_3) conditions.

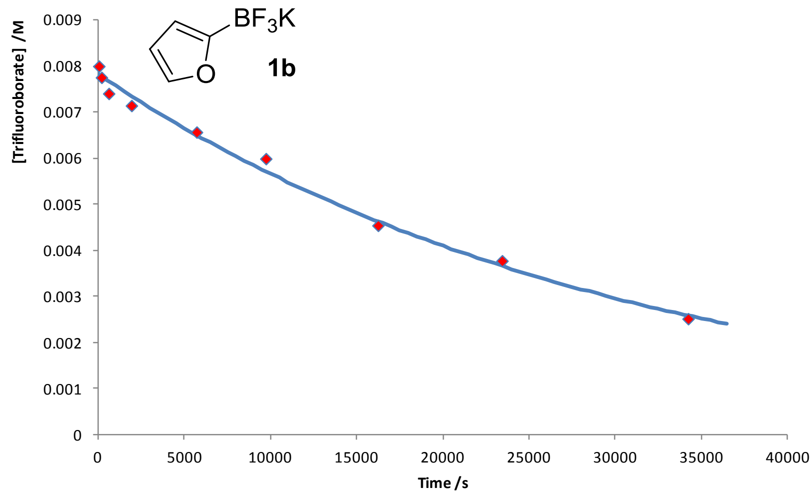

Figure S44 Pseudo first order hydrolysis of potassium 2-furyltrifluoroborate (1b), under basic (Cs_2CO_3) conditions.

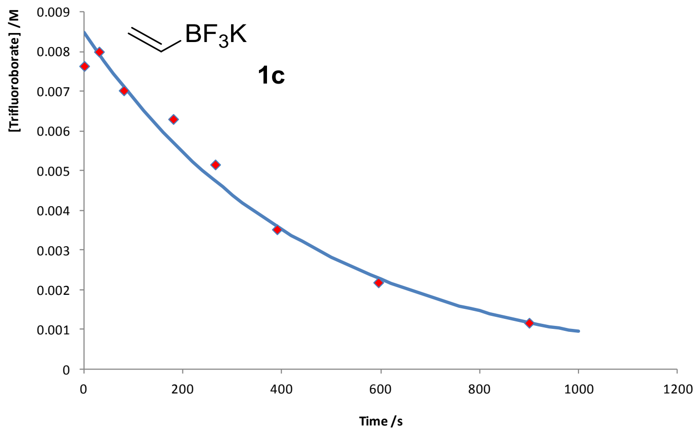

Figure S45 Pseudo first order hydrolysis of potassium vinyltrifluoroborate (1c), under basic (Cs_2CO_3) conditions.

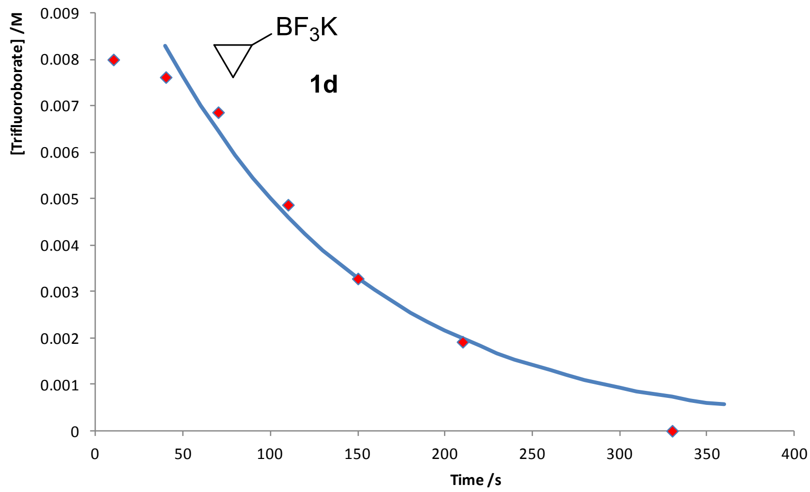

Figure S46 Pseudo first order hydrolysis of potassium cyclopropyltrifluoroborate (1d), under basic (Cs_2CO_3) conditions. The apparent induction period is possibly due to the time taken for 1d to dissolve. Accordingly, the concentration (y-axis) maybe relative rather than absolute. However this should not corrupt the value determined for the pseudo first order rate constant for hydrolysis.

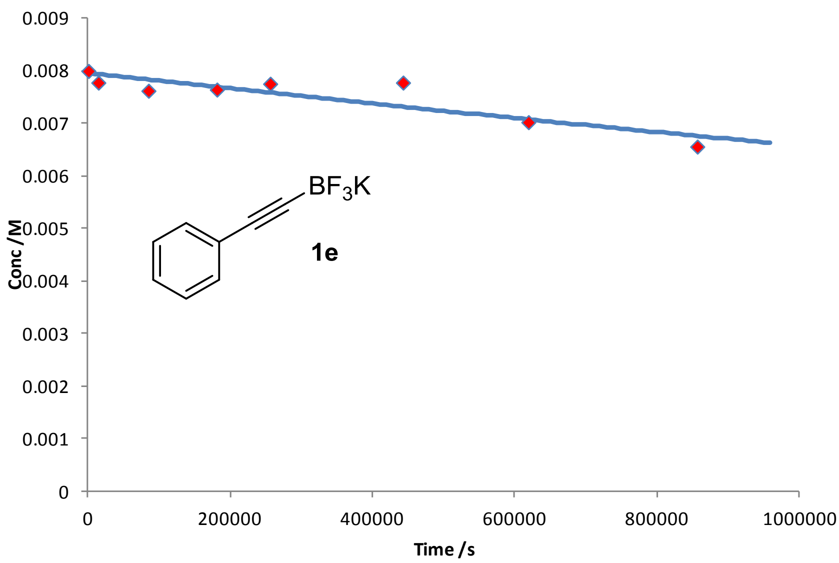

Figure S47 Pseudo first order hydrolysis of potassium phenylethynyltrifluoroborate (1e), under basic (Cs_2CO_3) conditions. In contrast to all of the other substrates studied (1a-d, 1f-r) the alkynyl (1e) system does not liberate detectable quantities of the boronic acid (2e). The pseudo first order rate constant may therefore be over estimated

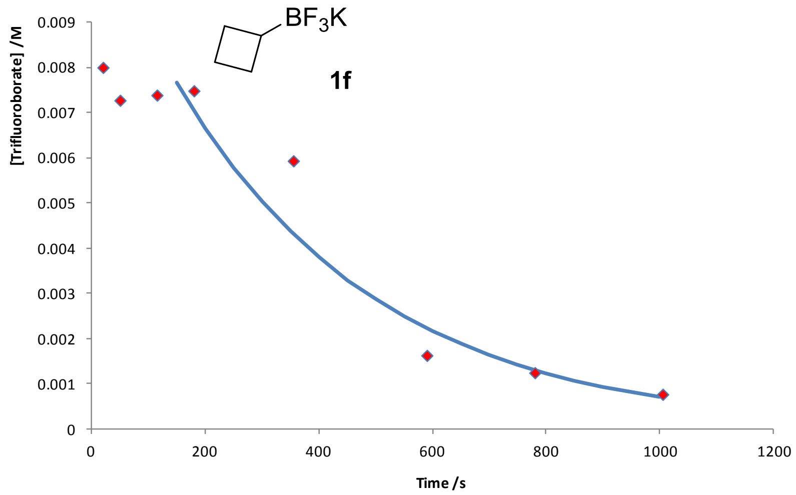

Figure S48. Pseudo first order hydrolysis of potassium cyclobutyltrifluoroborate (1f), under basic (Cs_2CO_3) conditions. The apparent induction period is possibly due to the time taken for 1f to dissolve. Accordingly, the concentration (y-axis) maybe relative rather than absolute. However this should not corrupt the value determined for the pseudo first order rate constant for hydrolysis.

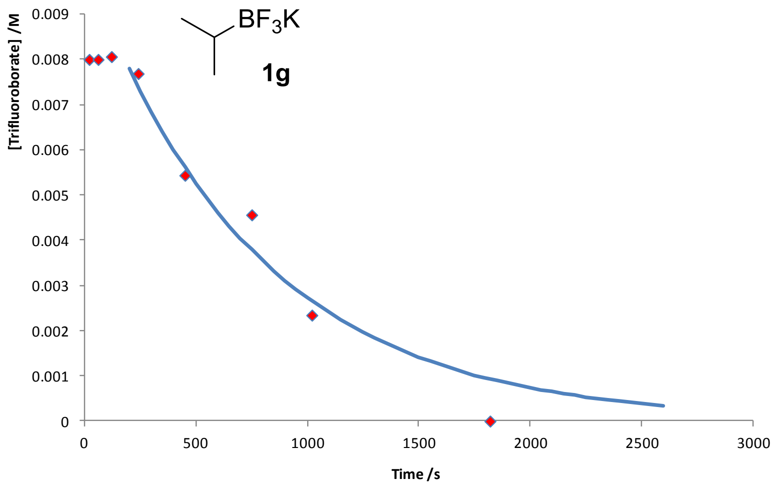

Figure S49 Pseudo first order hydrolysis of potassium isopropyltrifluoroborate (1g), under basic (Cs_2CO_3) conditions. The apparent induction period is possibly due to the time taken for 1g to dissolve. Accordingly, the concentration (y-axis) maybe relative rather than absolute. However this should not corrupt the value determined for the pseudo first order rate constant for hydrolysis.

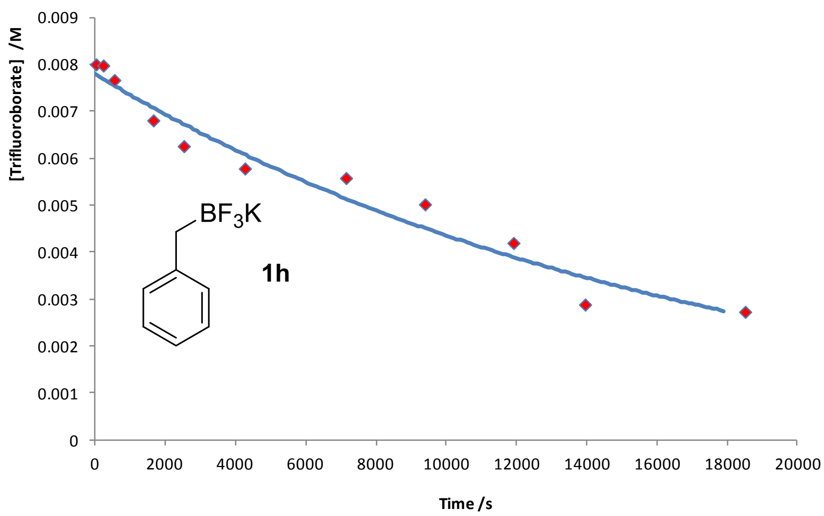

Figure S50 Pseudo first order hydrolysis of potassium benzyltrifluoroborate (1h), under basic (Cs_2CO_3) conditions.

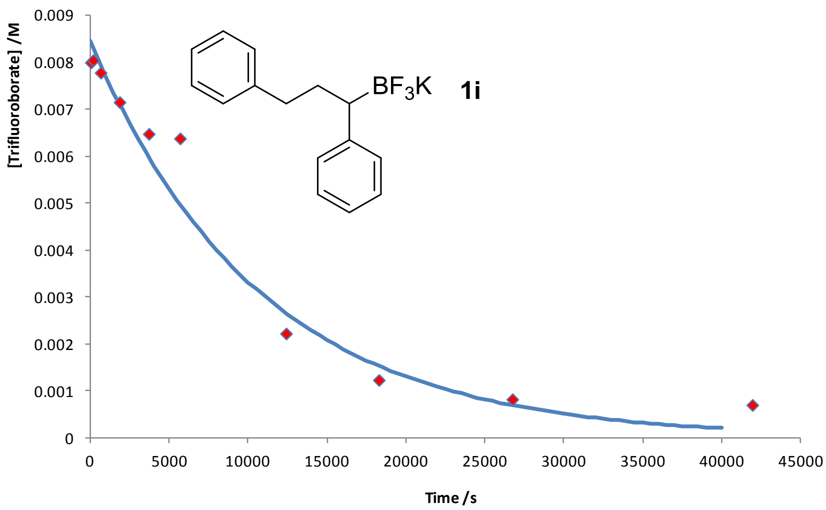

Figure S51 Pseudo first order hydrolysis of potassium 1,3 diphenylpropyltrifluoroborate (1i), under basic (Cs_2CO_3) conditions.

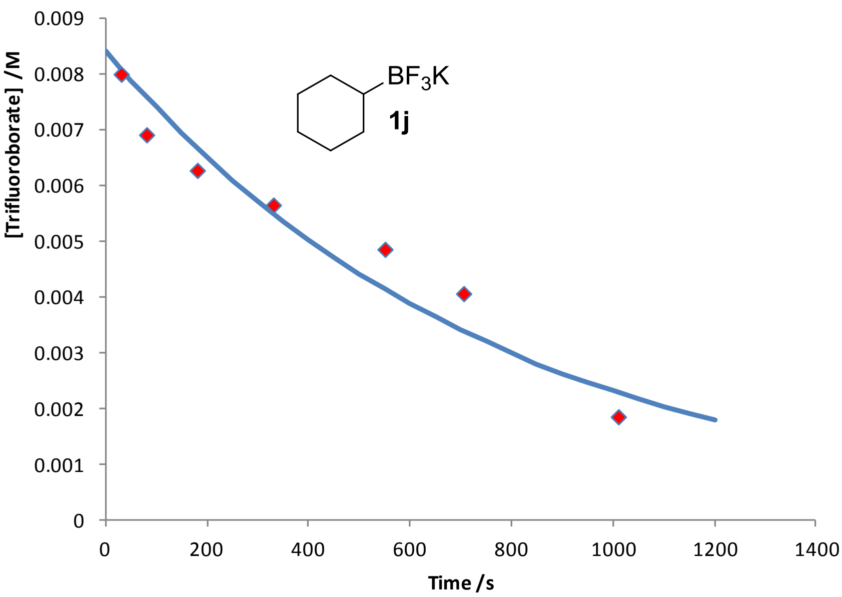

Figure S52 Pseudo first order hydrolysis of potassium cyclohexyltrifluoroborate (1j), under basic (Cs_2CO_3) conditions. The sensitivity of 1j to acid catalysed hydrolysis is high, which renders the measurement of reliable and reproducible kinetic data difficult. This causes a typical reaction profile to consist of both the acid catalysed and direct dissociation pathways, which may account for the imperfect first order decay characteristics of this plot.

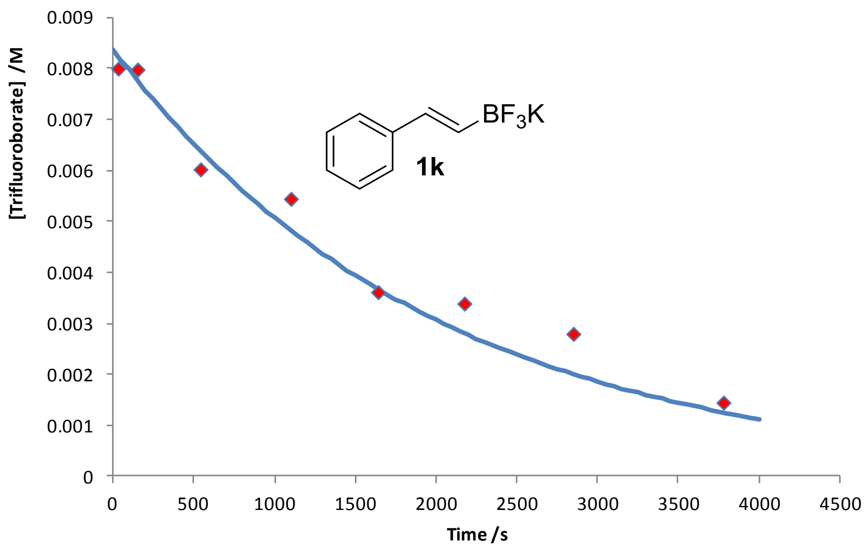

Figure S53. Pseudo first order hydrolysis of potassium phenylethenyltrifluoroborate (1k), under basic (Cs_2CO_3) conditions.

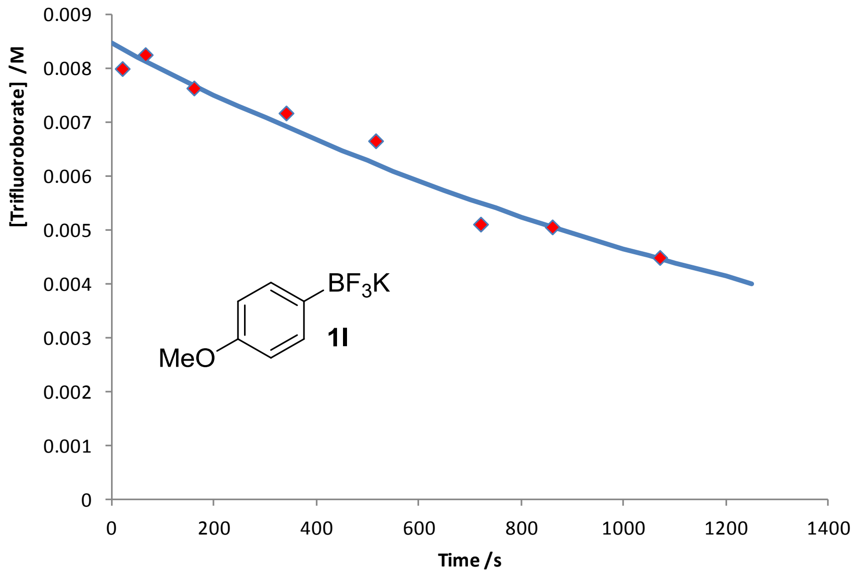

Figure S54. Pseudo first order hydrolysis of potassium 4-methoxyphenyltrifluoroborate (1l), under basic (Cs_2CO_3) conditions.

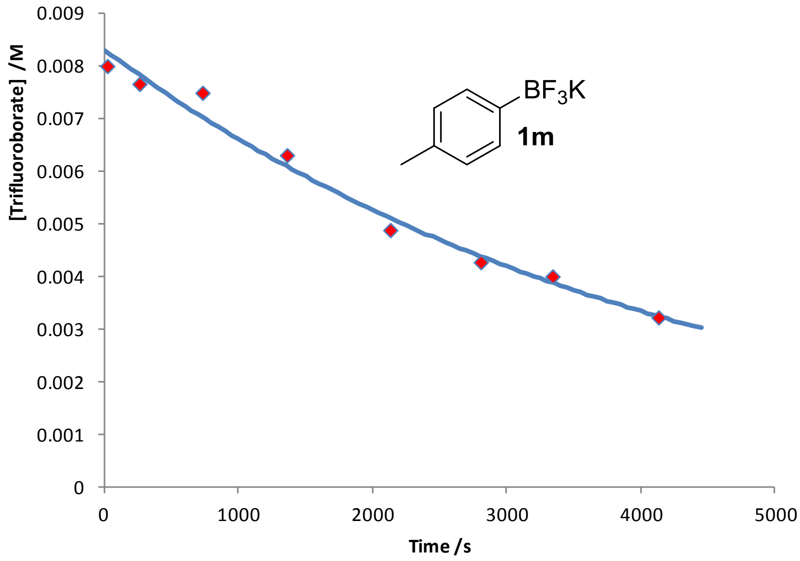

Figure S55. Pseudo first order hydrolysis of potassium 4-methylphenyltrifluoroborate (1m), under basic (Cs_2CO_3) conditions.

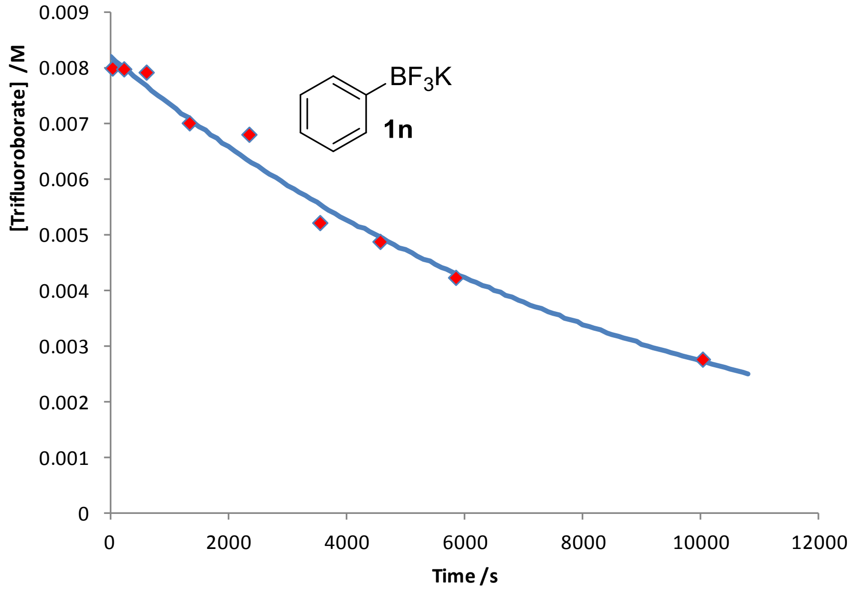

Figure S56 Pseudo first order hydrolysis of potassium phenyltrifluoroborate (1n), under basic (Cs_2CO_3) conditions.

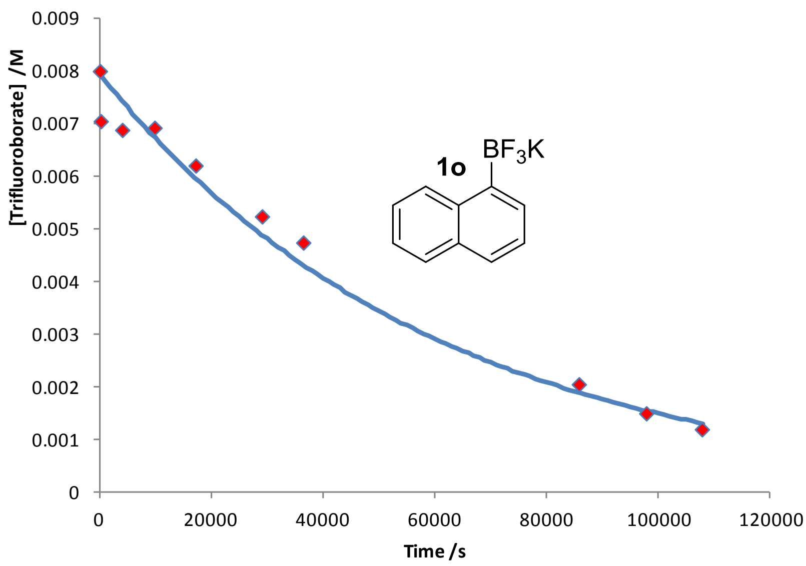

Figure S57. Pseudo first order hydrolysis of potassium 1-naphthyltrifluoroborate (1o), under basic (Cs_2CO_3) conditions.

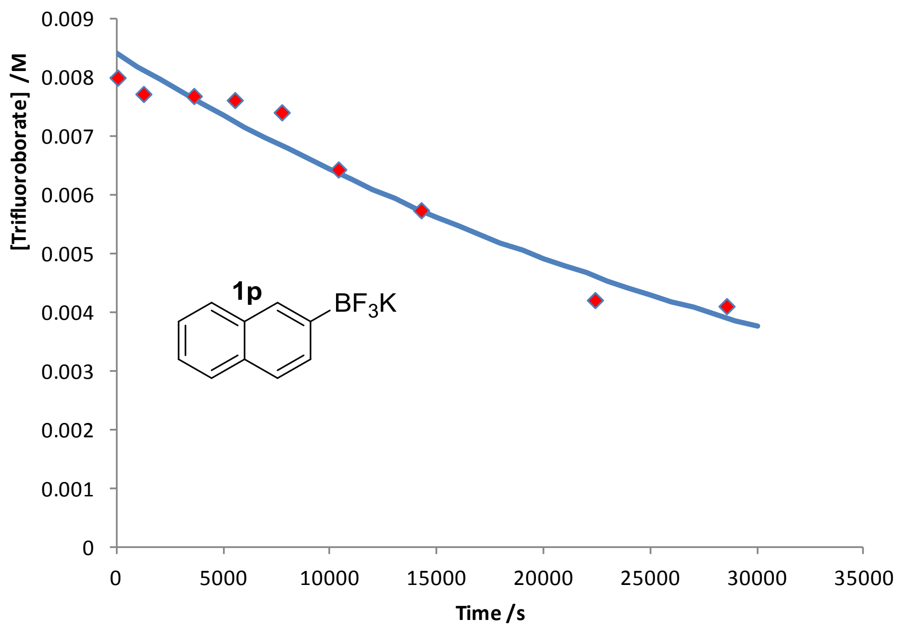

Figure S58. Pseudo first order hydrolysis of potassium 2-naphthyltrifluoroborate (1p), under basic (Cs_2CO_3) conditions.

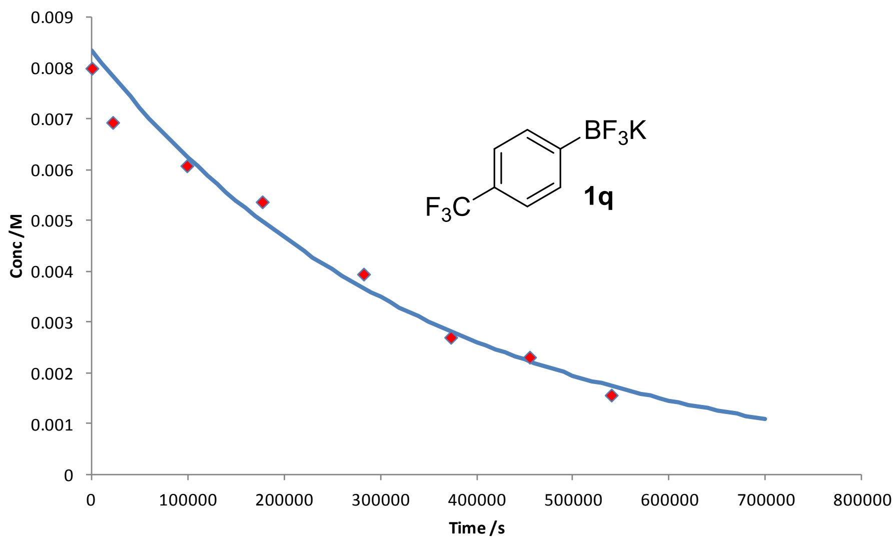

Figure S59. Pseudo first order hydrolysis of potassium 4-trifluoromethyltrifluoroborate (1q), under basic (Cs_2CO_3) conditions.

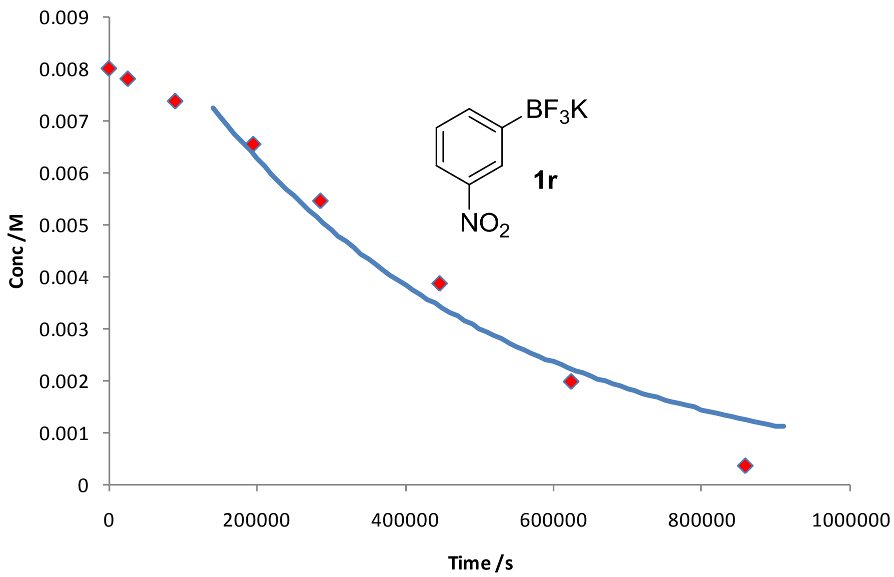

Figure S60. Pseudo first order hydrolysis of potassium 3-nitrophenyltrifluoroborate (1r), under basic (Cs_2CO_3) conditions. Progressive rate acceleration, leading to deviation from first order decay towards a zero order decay rate profile, may arise from competing hydrolysis pathway iii, see main text for full details.

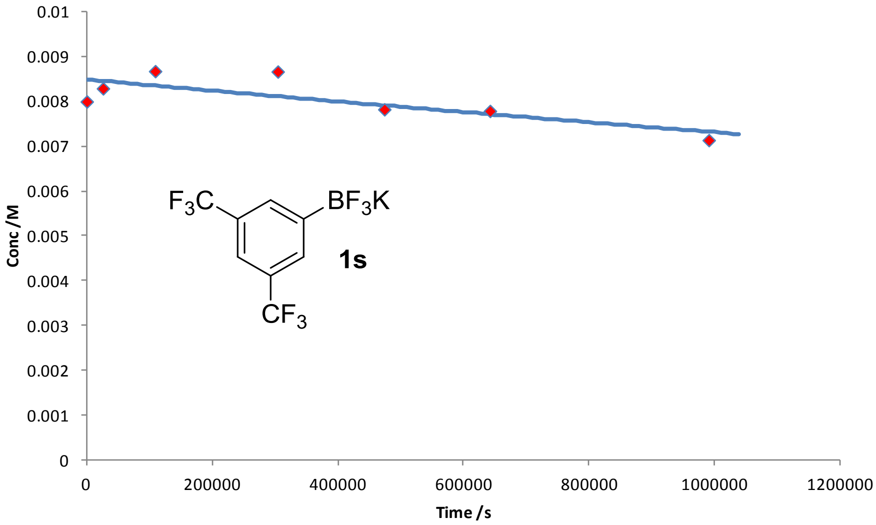

Figure S61. Pseudo first order hydrolysis of potassium 3,5-bistrifluoromethylphenyltrifluoroborate (1s), under basic (Cs_2CO_3) conditions.

Effect of glass powder on hydrolysis rates under basic conditions

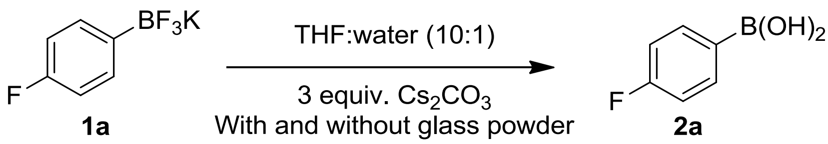

To one Schlenk tube containing potassium 4-fluorophenyltrifluoroborate (**1a**) (5.28 x 10^{-5} mol, 10.6 mg) and cesium carbonate (1.58 x 10^{-4} mol, 51.6 mg) was added THF (6 mL) and water (0.6 mL). To another identically shaped Schlenk tube was added grade 3 glass powder (20 mg) along with potassium 4-fluorophenyltrifluoroborate (**1a**) (5.28 x 10^{-5} mol, 10.6 mg), cesium carbonate (1.58 x 10^{-4} mol, 51.6 mg) and then THF (6 mL) and water (0.6 mL). The two solutions were heated at 55 °C and stirred at 500 rpm. Samples (0.3 mL) were removed at regular time intervals into pre-cooled (0 °C) PTFE lined NMR tubes. Each sample was analysed by ^{19}F NMR spectroscopy and was subjected to 128 scans at 25 °C.

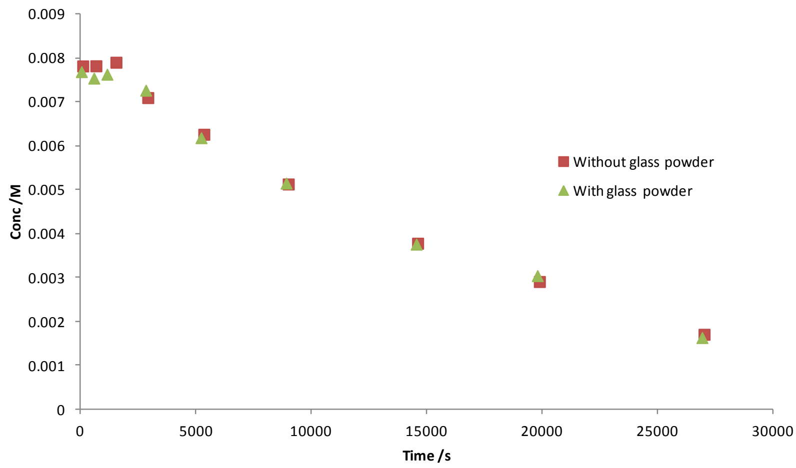

Figure S62. The hydrolysis of 1a to 2a, at 55 °C in basic (3 equiv. Cs_2CO_3) THF:water (10:1) with and without added glass powder, clearly shows the glass has no effect on the rate.

DBU

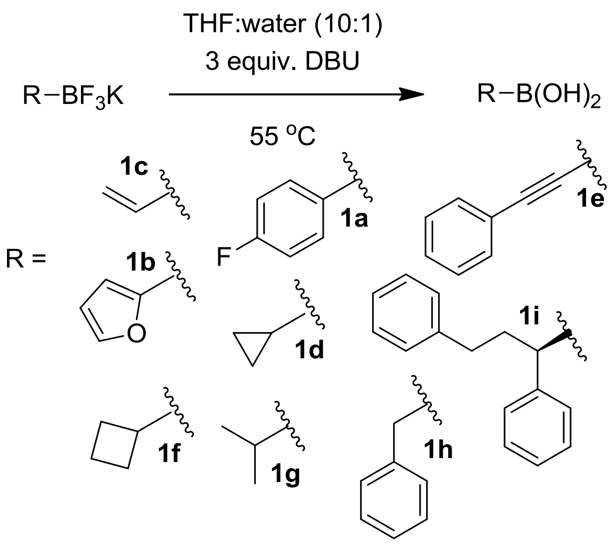

A solution of DBU (1.32 x 10^{-5} mol, 1.968 µL) in THF (0.5 mL) containing benzotrifluoride (1/2 drop) was added to a PTFE lined NMR tube charged with the potassium organotrifluoroborate (4.4 x 10^{-6} mol). After addition of D_2O (0.05 mL) the tube was briefly shaken then immediately placed into the *Varian 500* probe which was preheated to 55 °C. The reaction was monitored by ^{19}F NMR (128 scans, 55 °C) using a time delayed array to separate the acquisitions. The separation time ranged from 0 - 3600 seconds depending on the substrate and extent of reaction

The integration of R-B*F*$_3$K peak was normalised against the standard (benzotrifluoride) and concentrations were calculated by comparison to the first spectrum, assumed to be the known initial concentration.

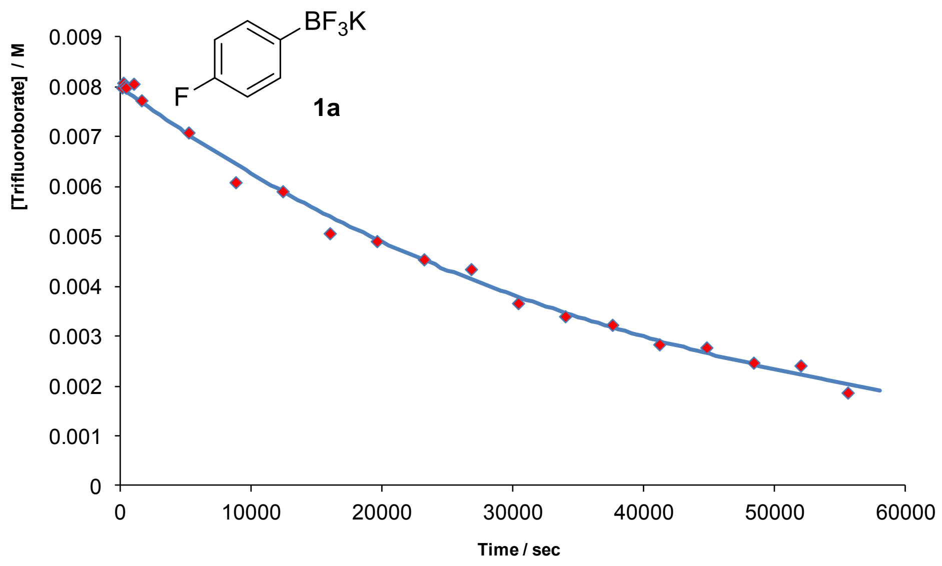

Figure S63 Pseudo first order hydrolysis of potassium 4-fluorophenyltrifluoroborate (1a), under basic (DBU) conditions.

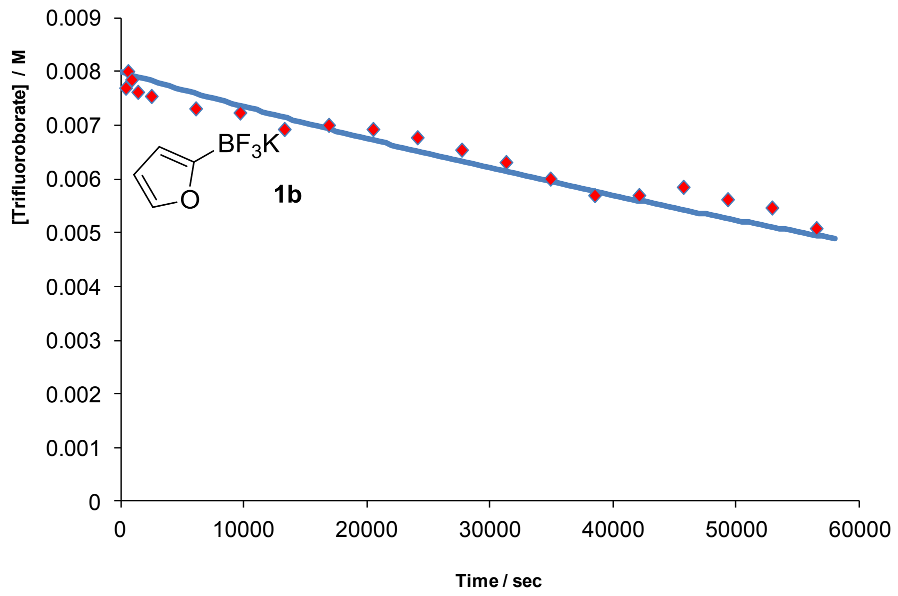

Figure S64 Pseudo first order hydrolysis of potassium 2-furyltrifluoroborate (1b), under basic (DBU) conditions.

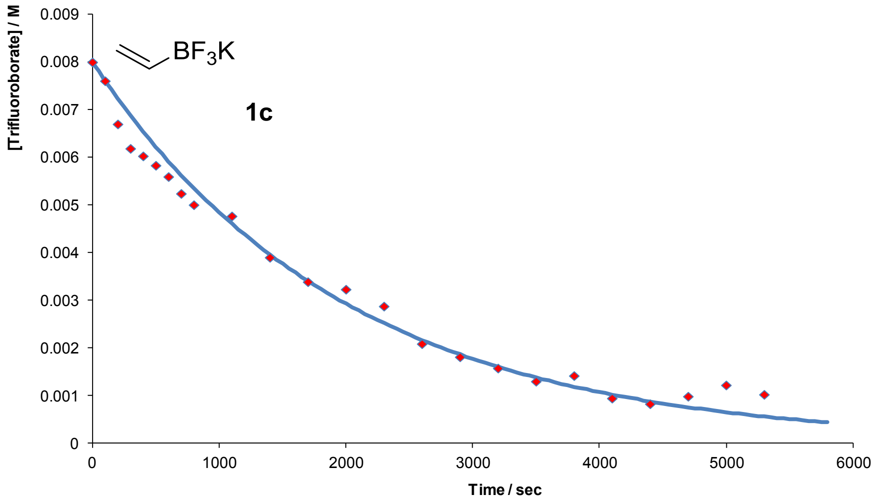

Figure S65 Pseudo first order hydrolysis of potassium vinyltrifluoroborate (1c), under basic (DBU) conditions.

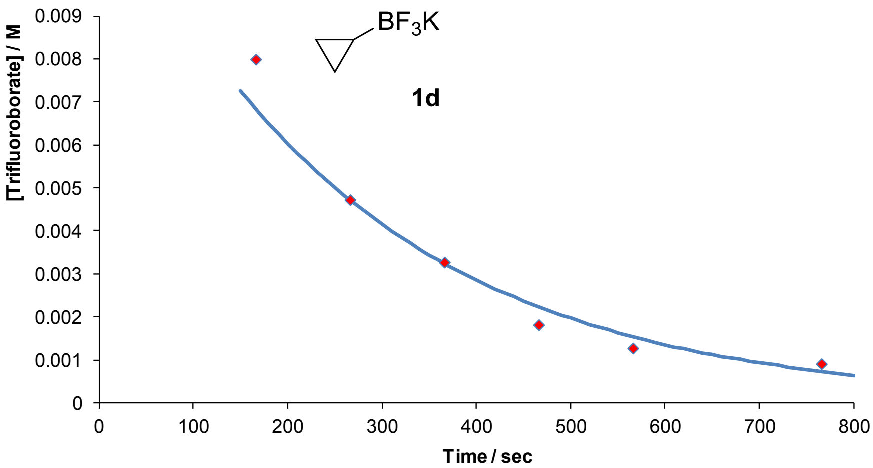

Figure S66 Pseudo first order hydrolysis of potassium cyclopropyltrifluoroborate (1d), under basic (DBU) conditions. The apparent induction period is possibly due to the time taken for 1d to dissolve. Accordingly, the concentration (y-axis) maybe relative rather than absolute. However this should not corrupt the value determined for the pseudo first order rate constant for hydrolysis.

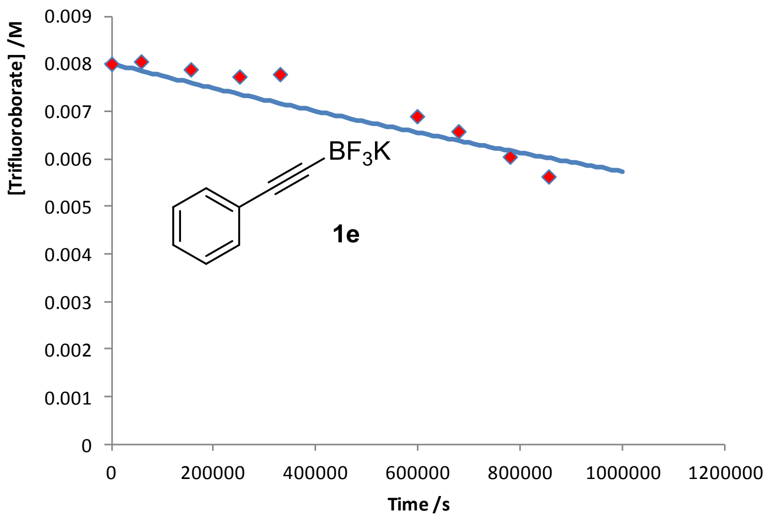

Figure S67 Pseudo first order hydrolysis of potassium phenylethynyltrifluoroborate (1e), under basic (DBU) conditions. We note that there is downward curvature in the hydrolytic decay of 1e. However in contrast to all of the other substrates studied (1a-d, 1f-i) the alkynyl (1e) system does not liberate detectable quantities of the boronic acid (2e). The pseudo first order rate constant may therefore be over estimated.

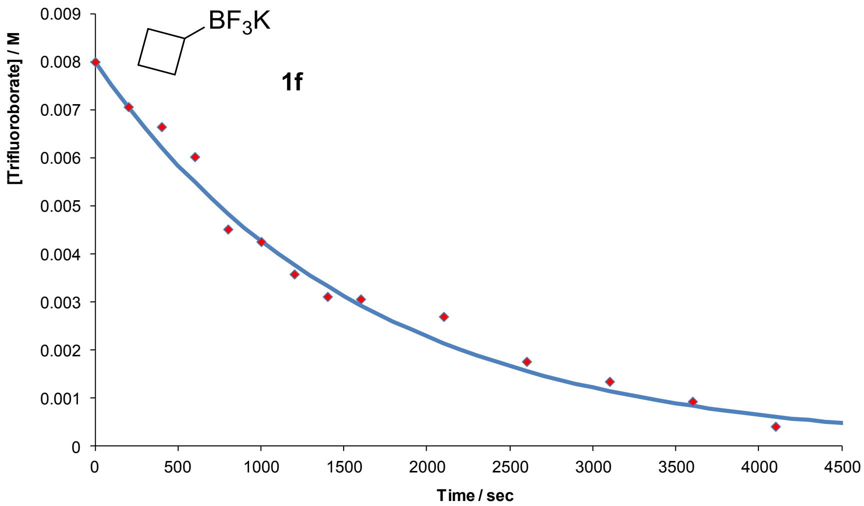

Figure S68 Pseudo first order hydrolysis of potassium cyclobutyltrifluoroborate (1f), under basic (DBU) conditions.

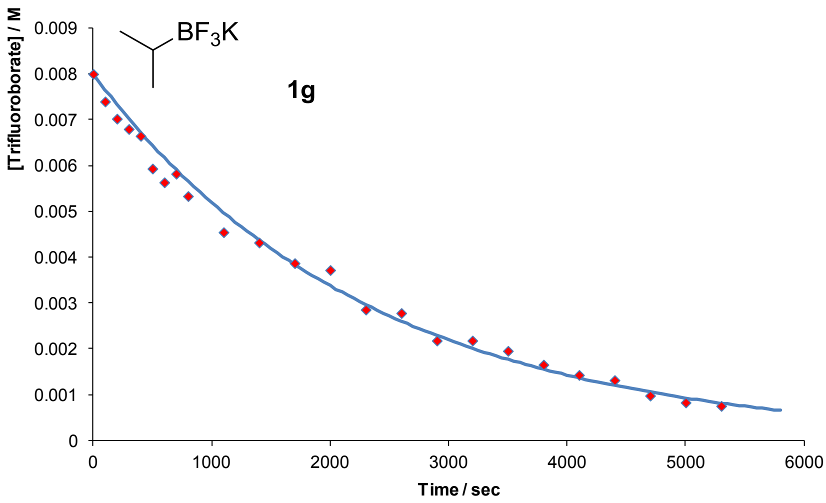

Figure S69 Pseudo first order hydrolysis of potassium isopropyltrifluoroborate (1g), under basic (DBU) conditions.

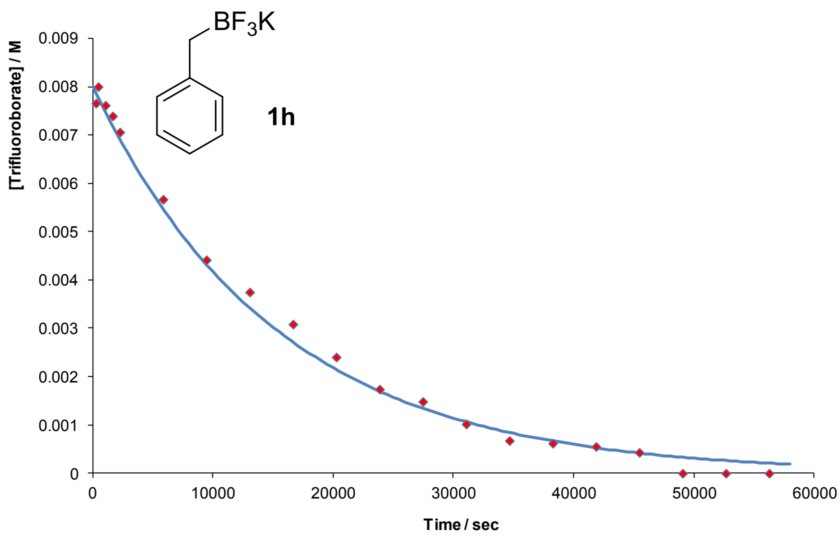

Figure S70 Pseudo first order hydrolysis of potassium benzyltrifluoroborate (1i), under basic (DBU) conditions.

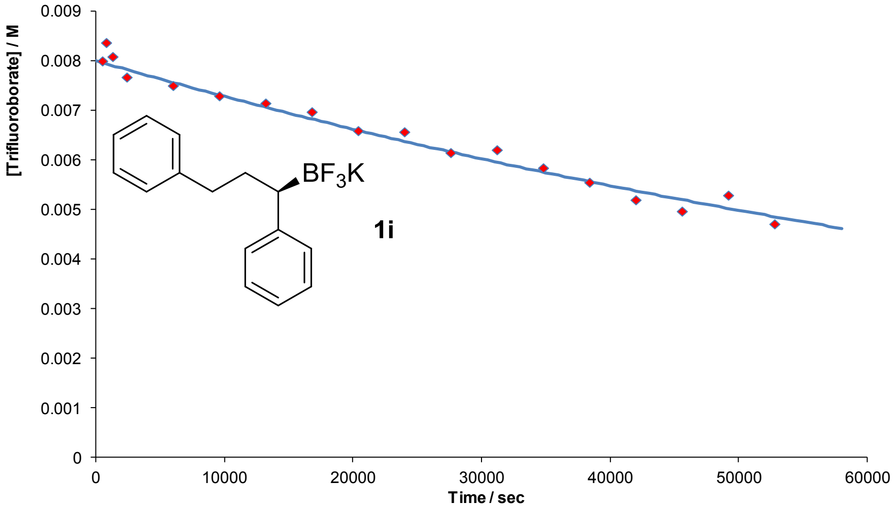

Figure S71 Pseudo first order hydrolysis of potassium 1,3 diphenylpropyltrifluoroborate (1i), under basic (DBU) conditions.

Table S4. Half life of hydrolysis for each substrate

Substrate		$t_{1/2}$ glass	$t_{1/2}$ Cs_2CO_3	$t_{1/2}$ DBU
Aryl	**1a**	28 min	3 hours 20 min	7 hours 50 min
Furanyl	**1b**	33 min	6 hours	26 hours
Vinyl	**1c**	23 min	5 min	23 min
Cyclopropyl	**1d**	7 min	1 min	3 min
Alkynyl	**1e**	12 hours	40 days	27 days
Cyclobutyl	**1f**	18 min	4 min	18 min
Isopropyl	**1g**	25 min	11 min	27 min
Benzyl	**1h**	33 min	3 hours 20 min	3 hours
1,3-Diphenylpropyl	**1i**	39 min	2 hours	18 hours 20 min
Cyclohexyl	**1j**	19 min	9 min	
Phenylethenyl	**1k**	10 min	27 min	
4-Methoxyphenyl	**1l**	10 min	19 min	
4-Methylphenyl	**1m**	16 min	51 min	
Phenyl	**1n**	19 min	1 hour 40 min	
1-Naphthyl	**1o**	25 min	10 hours	
2-Naphthyl	**1p**	22 min	7 hours 10 min	

4-CF_3phenyl	**1q**	1 hour 30 min	2 days 18 hours	
3-Nitrophenyl	**1r**	2 days 13 hours	5 days	
3,5 bisCF_3phenyl	**1s**	3 days	54 days	

Table S5 Pseudo first order rate constant derived from the first order log plot for each substrate

Substrate		k_{obs}^{glass} / s^{-1}	$k_{obs}^{Cs_2CO_3}$/ s^{-1}	k_{obs}^{DBU}/ s^{-1}
Aryl	**1a**	4.2E-04	5.7E-05	2.5E-05
Furanyl	**1b**	3.5E-04	3.2E-05	7.4E-06
Vinyl	**1c**	5.0E-04	2.2E-03	5.0E-04
Cyclopropyl	**1d**	1.7E-03	8.4E-03[a]	4.1E-03[b]
Alkynyl	**1e**	1.6E-05	2.0E-07	3.0E-07
Cyclobutyl	**1f**	6.5E-04	2.8E-03	6.3E-04
Isopropyl	**1g**	4.6E-04	1.0E-03	4.3E-04
Benzyl	**1h**	3.5E-04	5.8E-05	6.5E-05
1,3-Diphenylpropyl	**1i**	3.0E-04	9.3E-05	1.1E-05
Cyclohexyl	**1j**	6.0E-04	1.3E-03	
Phenylethenyl	**1k**	1.1E-03	4.3E-04	
4-Methoxyphenyl	**1l**	1.2E-03	6.0E-04	
4-Methylphenyl	**1m**	7.2E-04	2.3E-04	
Phenyl	**1n**	6.0E-04	1.1E-04	
1-Naphthyl	**1o**	4.6E-04	1.9E-05	
2-Naphthyl	**1p**	5.3E-04	2.7E-05	
4-CF_3phenyl	**1q**	1.2E-04	2.9E-06	
3-Nitrophenyl	**1r**	5.2E-06	1.6E-06	
3,5 bisCF_3phenyl	**1s**	2.7E-06	1.5E-07	

[a] THF:water (20:1) $k_{obs}^{Cs_2CO_3}$ = 7.88E-03 s^{-1}
[b] Double the concentration of DBU k_{obs}^{DBU} = 4.00E-03 s^{-1}

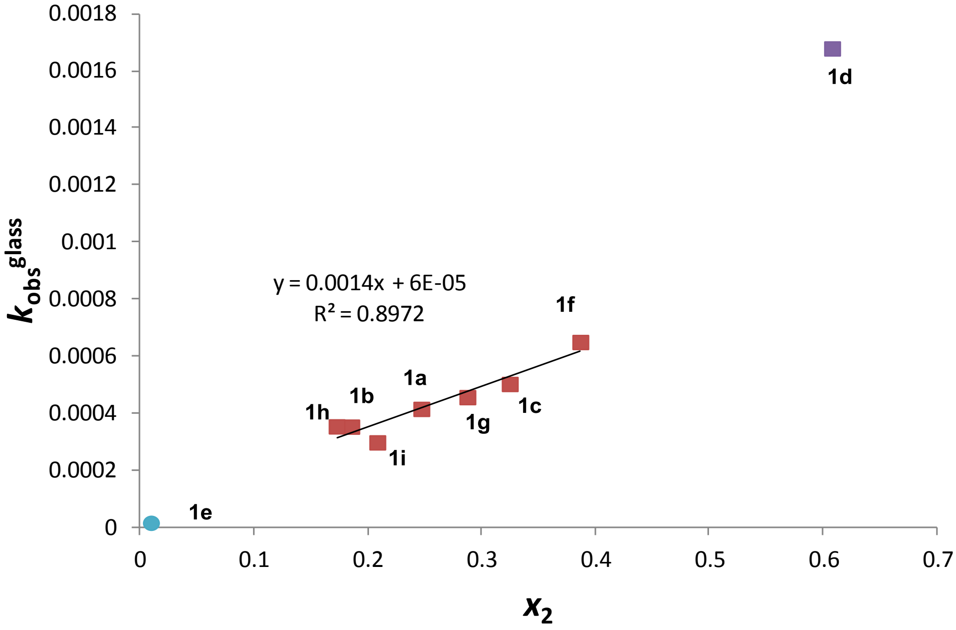

Figure S72. **k_{obs}^{glass} as function of the experimentally determined mole fraction of boronic acid (2a-2i) at hydrolytic equilibrium. Note x_2 of 1e has not been determined due to its hydrolytic unreactivity and instability of 2e.**

Survey of B-F bond lengths from single crystal X-ray diffraction

The following structures were found from a substructure search of C-BF_3 on ConQuest[S11] from The Cambridge Crystallographic Data Centre. Data from structures with a counter cation other than potassium were not included (with one exception – see entry 3).

Table S6. Average B-F bond length from the available crystal structures of various potassium organotrifluoroborates.

Structure	r(B-F)$_{av.}$ / pm	Reference	CCDC number
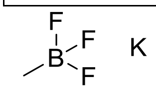	142.4	S12	-
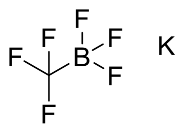	139.1	S13	-
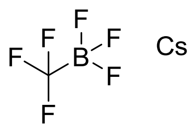	139.1	S12	-

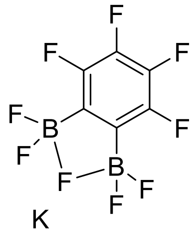	143.9	S14	278389
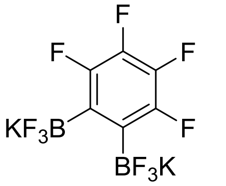	141.5	S14	278193
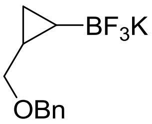	142.4	S15	717834
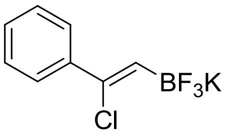	141.9	S16	715783
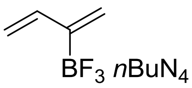	142.2	S17	655091
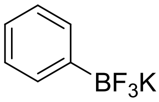	141.7	S18	IUCr NA1133
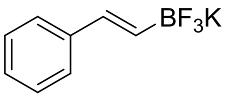	142.5	S19	170861
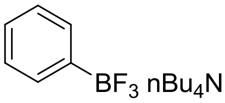	141.8	S20	170890
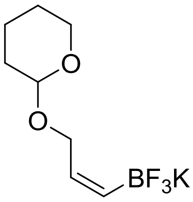	141.9	S21	717377
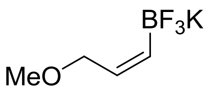	142.5	S22	712290
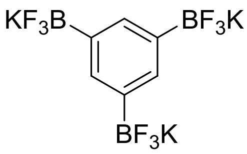	142.7	S23	782522

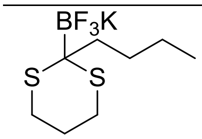	140.1	S24	686771
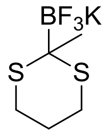	140.5	S25	670905
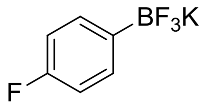 **1a**	142.4	S26	859285
 **1c**	142.6	S26	859286
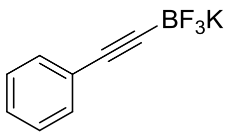 **1e**	140.8	S26	859288
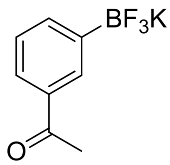	141.9	S26	859287

DFT calculations and Swain Lupton (ℜ) analysis

Geometry optimization in Gaussian 09[S27] was carried out for species **1a-1s** at the B3LYP level of theory, using the standard 6-31+G(d) basis set for all atoms. The calculations were carried out using a continuum solvent model, the IEF-PCM model in Gaussian, with parameters for tetrahydrofuran as solvent.

Normalization

Normalization of the B-F bond lengths was conducted by taking the difference between the $r(\text{B-F})_{\text{av.}}$ in the difluoroborane (**3**) and r(B-F) in BF_3 (132.213 pm) to give Δr(B-F). Normalization of the C-B bond was conducted by taking the difference between r(C-B) in the difluoroborane and r(C-B) in HC≡C-BF_2 to give Δr(C-B). Provided that BF_3 and HC≡C-BF_2 are calculated in conjunction with the substrate in question, this approach should ensure that slightly different basis sets can be used to accurately compare to the rate data reported herein.

Table S7 Geometry optimisations of substrates **3a**-**3s** by DFT

Substrate		***r*(B-F)$_1$ /pm**	***r*(B-F)$_2$ /pm**	***r*(B-F)$_{av}$ /pm**	**Δ*r*(B-F) /pm**
4-Fluorophenyl	**3a**	133.926	133.923	133.925	1.712
2-Furanyl	**3b**	133.868	133.647	133.758	1.545
Vinyl	**3c**	133.978	133.932	133.955	1.742
Cyclopropyl	**3d**	134.657	134.671	134.664	2.451
Alkynyl	**3e**	133.454	133.454	133.454	1.241
Cyclobutyl	**3f**	134.146	134.121	134.134	1.920
Isopropyl	**3g**	134.074	133.976	134.025	1.812
Benzyl	**3h**	133.745	133.757	133.751	1.672
1,3-Diphenylpropyl	**3i**	133.750	133.870	133.810	1.597
Cyclohexyl	**3j**	134.065	134.064	134.065	1.851
Phenylethenyl	**3k**	134.313	134.364	134.339	2.126
4-Methoxyphenyl	**3l**	134.292	134.252	134.272	2.059
4-Methylphenyl	**3m**	134.115	134.110	134.113	1.899
Phenyl	**3n**	133.981	133.976	133.979	1.766
1-Naphthyl	**3o**	134.300	134.022	134.161	1.948
2-Naphthyl	**3p**	134.004	134.025	134.015	1.801
4-CF_3phenyl	**3q**	133.637	133.636	133.637	1.424
3-Nitrophenyl	**3r**	133.474	133.516	133.495	1.282
3,5 bisCF_3phenyl	**3s**	133.366	133.389	133.378	1.165

Table S8 Geometry optimisations of substrates **3a-3s** by DFT

Substrate		***r*(C-B) /pm**	**Δ*r*(C-B) /pm**	**Energy / a.u.**
4-Fluorophenyl	**3a**	154.099	2.399	555.592564
2-Furanyl	**3b**	152.456	0.756	454.127964
Vinyl	**3c**	154.216	2.516	302.683084
Cyclopropyl	**3d**	153.877	2.177	341.987314
Alkynyl	**3e**	151.039	-0.661	532.509487
Cyclobutyl	**3f**	155.553	3.853	381.299782
Isopropyl	**3g**	156.726	5.026	343.225837
Benzyl	**3h**	156.869	5.169	-495.6588
1,3-Diphenylpropyl	**3i**	157.317	5.617	805.345403
Cyclohexyl	**3j**	156.876	5.176	533.756690
Phenylethenyl	**3k**	153.091	1.391	570.880765
4-Methoxyphenyl	**3l**	153.357	1.657	495.669190
4-Methylphenyl	**3m**	153.884	2.184	456.349602
Phenyl	**3n**	154.199	2.499	609.995016
1-Naphthyl	**3o**	154.586	2.886	609.998863
2-Naphthyl	**3p**	154.094	2.394	793.408595
4-CF_3phenyl	**3q**	154.851	3.151	660.862105
3-Nitrophenyl	**3r**	154.934	3.234	1130.46592
3,5 bisCF_3phenyl	**3s**	155.121	3.421	533.756690

Table S9 Geometry optimization of the following difluoroboranes

Entry	Substrate	r(B-F)$_1$ /pm	r(B-F)$_2$/pm	r(B-F)$_{av}$/pm	Δr(B-F)
1	3-pyridyl	133.665	133.710	133.688	1.475
2	4-pyridyl	133.210	133.211	133.211	0.997
3	2-pyrimidyl	132.887	132.896	132.892	0.678
4	4-pyrimidyl	133.247	132.634	132.941	0.727
5	5-pyrimidyl	133.363	133.378	133.371	1.158
6	3-pyridazyl	133.429	132.701	133.065	0.852
7	pyrrole	134.609	134.181	134.395	2.182
8	2-pyridyl	133.109	133.771	133.440	1.227
9	2-thienyl	134.040	133.971	134.006	1.793
10	ethyl	134.029	134.028	134.029	1.815
11	$CH_2CH_2C_6H_4$	133.811	133.959	133.885	1.672
12	cyclopentyl	134.158	134.095	134.127	1.913
13	$C(CF_3)_3$	131.546	131.494	131.520	-0.693
14	3-BrC_6H_4	133.749	133.731	133.740	1.527
15	4-BrC_6H_4	133.847	133.841	133.844	1.631
16	3-ClC_6H_4	133.743	133.724	133.734	1.520
17	4-ClC_6H_4	133.850	133.856	133.853	1.640
18	3-FC_6H_4	133.745	133.744	133.745	1.532
19	3-IC_6H_4[a]	133.970	133.951	133.961	1.747
20	4-$NO_2C_6H_4$	133.248	133.248	133.248	1.035
21	4-EtC_6H_4	134.109	134.109	134.109	1.896
22	4-IC_6H_4 [a]	134.035	134.035	134.035	1.822
23	C_6Cl_5	132.716	132.717	132.717	0.503
24	3-acetylC_6H_4	133.708	133.817	133.763	1.550
25	4-$CH_2OHC_6H_4$	133.960	133.953	133.957	1.743
26	4-CNC_6H_4	133.565	133.565	133.565	1.352
27	4-acetylC_6H_4	133.696	133.735	133.716	1.503
28	C_6F_5	132.889	132.889	132.889	0.676
29	mesityl	134.321	134.318	134.320	2.107
30	CC	133.136	133.136	133.136	0.923
31	$CCCF_3$	132.476	132.476	132.476	0.263
32	$CCCH_3$	133.638	133.637	133.638	1.424

[a] DGDZVP basis set used

Table S10 Geometry optimization of the following difluoroboranes

Entry	**Substrate**	***r*(C-B) /pm**	**Δ*r*(C-B)**
1	3-pyridyl	154.449	2.749
2	4-pyridyl	156.559	4.859
3	2-pyrimidyl	157.340	5.640
4	4-pyrimidyl	156.843	5.143
5	5-pyrimidyl	154.743	3.043
6	3-pyridazyl	156.257	4.557
7	pyrrole	151.542	-0.158
8	2-pyridyl	155.773	4.073
9	2-thienyl	152.641	0.941
10	ethyl	156.229	4.529
11	$CH_2CH_2C_6H_4$	156.288	4.588
12	cyclopentyl	155.963	4.263
13	$C(CF_3)_3$	163.019	11.319
14	$3\text{-}BrC_6H_4$	154.653	2.953
15	$4\text{-}BrC_6H_4$	154.353	2.653
16	$3\text{-}ClC_6H_4$	154.596	2.896
17	$4\text{-}ClC_6H_4$	154.284	2.584
18	$3\text{-}FC_6H_4$	154.567	2.867
19	$3\text{-}IC_6H_4$ [a]	154.432	2.732
20	$4\text{-}NO_2C_6H_4$	156.523	4.823
21	$4\text{-}EtC_6H_4$	153.873	2.173
22	$4\text{-}IC_6H_4$ [a]	154.218	2.518
23	C_6Cl_5	157.686	5.986
24	3-acetylC_6H_4	154.562	2.862
25	$4\text{-}CH_2OHC_6H_4$	154.226	2.526
26	$4\text{-}CNC_6H_4$	154.988	3.288
27	4-acetylC_6H_4	154.757	3.057
28	C_6F_5	155.755	4.055
29	mesityl	154.586	2.886
30	CC	151.700	0.000
31	$CCCF_3$	152.881	1.181
32	$CCCH_3$	150.656	-1.044

Prediction using DFT

In order to predict the hydrolysis rate of a substrate the following steps need to be taken. The two B-F bond lengths (r(B-F)$_1$ and r(B-F)$_2$) are normalized from the DFT derived geometry optimization of the difluoroborane (**3**) of the potassium organotrifluoroborate in question, by comparison to BF_3 and HC≡C-BF_2 for B-F and C-B respectively, see *Normalization* text above. If Δr(B-F)$_1$ and Δr(B-F)$_2$ are ≤ 0.1 ppm different from each other the substrate can be considered to be "normal" and therefore Δr(B-F)$_{av.}$ (Δr(B-F)$_{av.}$ = (r(B-F)$_1$ + r(B-F)$_2$)/2) can be used to read the predicted rate from the Δr(B-F) vs $Log_{10}k_{obs}^{base}$ plot in the main text or Figure S73, Figure S74 or Figure S75.

If however Δr(B-F)$_1$ and Δr(B-F)$_2$ are ≥0.1 ppm different to each other, the substrate can be considered to be "asymmetric", and will therefore sit off the trend as shown in Figure S76. In this case one Δr(B-F)$_{1\ /\ 2}$ may better predict the rate of hydrolysis than the other. The method for determining which Δr(B-F)$_{1\ /\ 2}$ to use comes from comparison to the Δr(B-F) / Δr(C-B) plot, Figure S77, where fits for sp, sp^2 and sp^3 systems are clearly shown and equations tabulated, Table S11. Then to whichever Δr(B-F) (long, short or average) is closest to the line of best fit should be used to read the predicted rate from the Δr(B-F) vs $Log_{10}k_{obs}^{base}$ plot in the main text or Figure S73, Figure S74 or Figure S75. Asymmetric sp^2 examples are shown in Figure S78 where it can be seen that Δr(B-F)$_{av.}$ should be used for substrates ***8***, ***6*** and ***4***; Δr(B-F)$_{long}$ should be used for *7*, ***24*** and **1b;** and finally Δr(B-F)$_{short}$ should be used for substrates **1o**. In this way a more accurate rate prediction can be achieved. It should be noted that the closer to the line of best fit, the better the prediction will thus be. As such, rates predicted from Δr(B-F) values that deviate substantially from the correlation inherently carry greater uncertainty.

There are also a few selected examples (***9***, ***29***, ***5*** and ***28***), where the difference between Δr(B-F)$_1$ and Δr(B-F)$_2$ is ≤ 0.1 ppm but they lie away from the correlation presented in Figure S78. For these examples we estimate their rate of hydrolysis will not easily be predicted by this model, as they may not sit on the Δr(B-F) / $Log_{10}k_{obs}^{base}$ correlation.

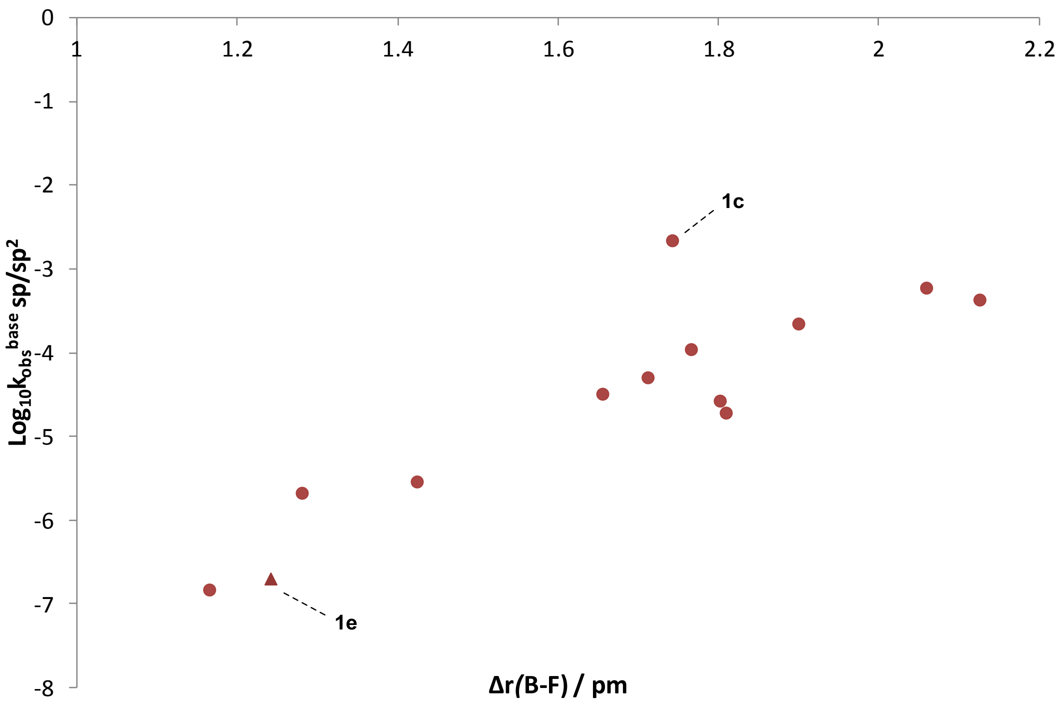

Figure S73. $\mathbf{Log_{10}k_{obs}^{base}}$ **vs Δ*r*(B-F) for all** $\mathbf{sp^2}$ **and sp substrates tested, see Table S5 and Table S7 for values.**

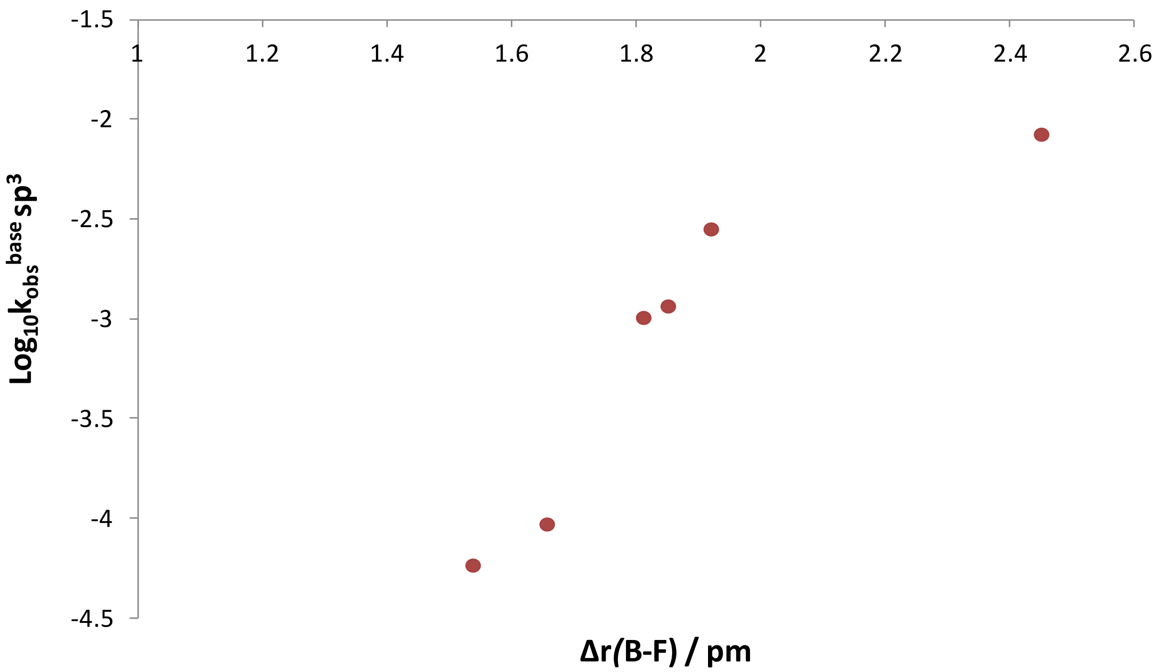

Figure S74 $\mathbf{Log_{10}k_{obs}^{base}}$ **vs Δ*r*(B-F) for all** $\mathbf{sp^3}$ **substrates tested, see Table S5 and Table S7 values.**

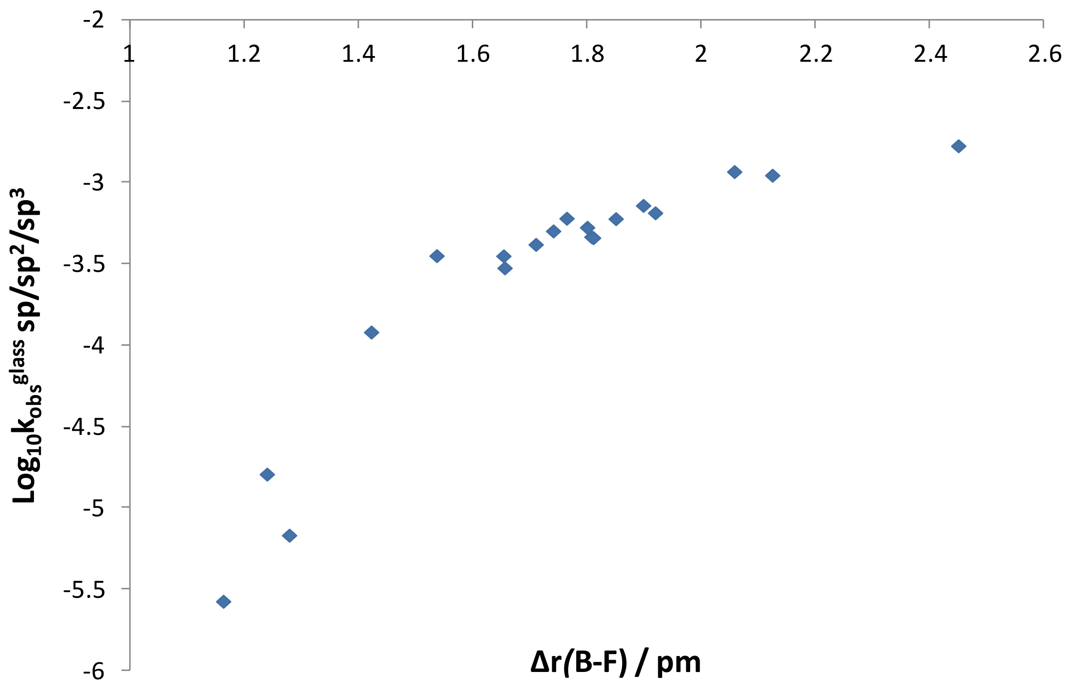

Figure S75 $Log_{10}k_{obs}^{glass}$ vs Δ*r(*B-F) for all sp^2 and sp substrates tested, see Table S5 and Table S7 for values.

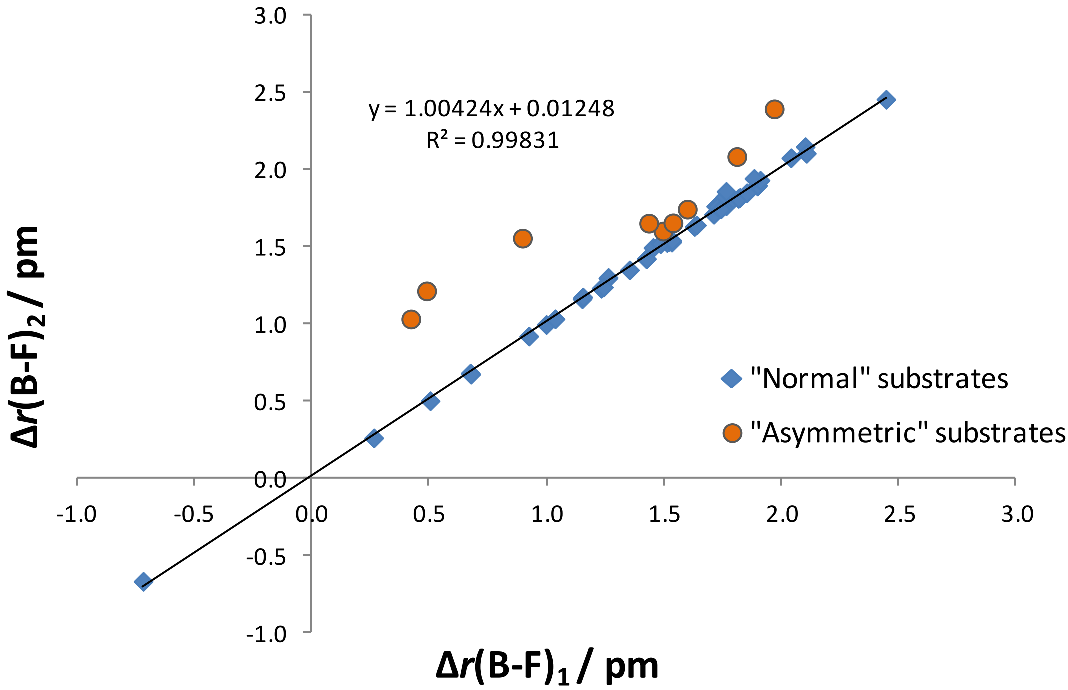

Figure S76 *r*$(B\text{-}F)_1$ vs *r*$(B\text{-}F)_2$ schematically indicating the distinction between "normal" and "asymmetric" substrates from the DFT derived geometry optimisation of the 51 examples calculated.

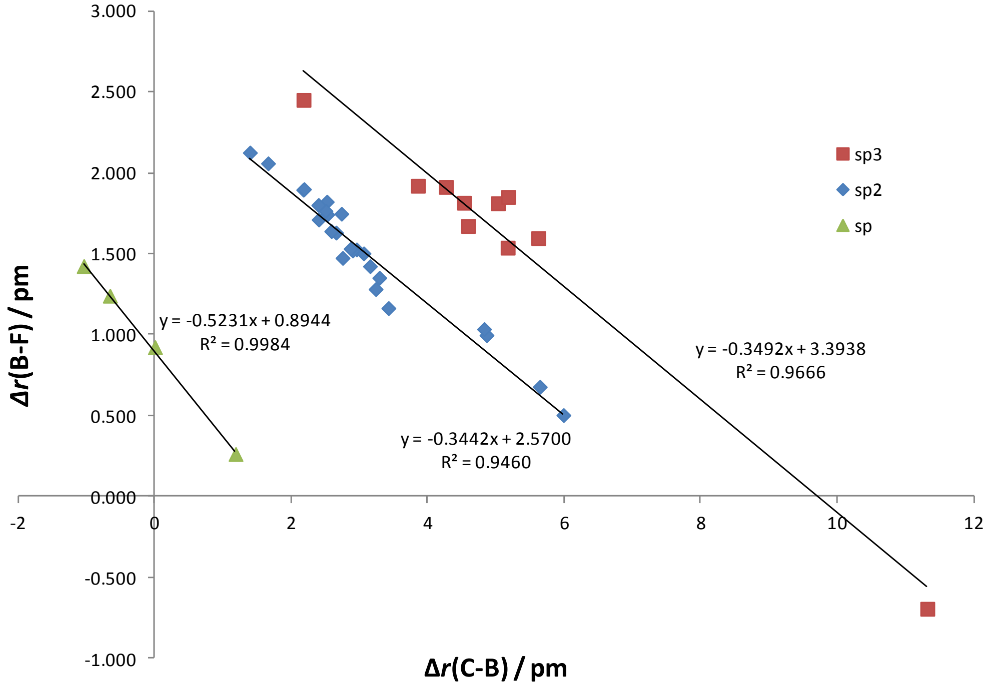

Figure S77 Δ*r*(B-F) vsΔ*r*(C-B) for all "normal" substrates

Table S11. "Normal" Δ*r*(B-F) vs Δ*r*(C-B) correlations

	Correlation fit
sp	Δ*r*(B-F) = -0.5231 Δ*r*(C-B) + 0.8944
sp^2	Δ*r*(B-F) = -0.3442 Δ*r*(C-B) + 2.5700
sp^3	Δ*r*(B-F) = -0.3492 Δ*r*(C-B) +3.3938

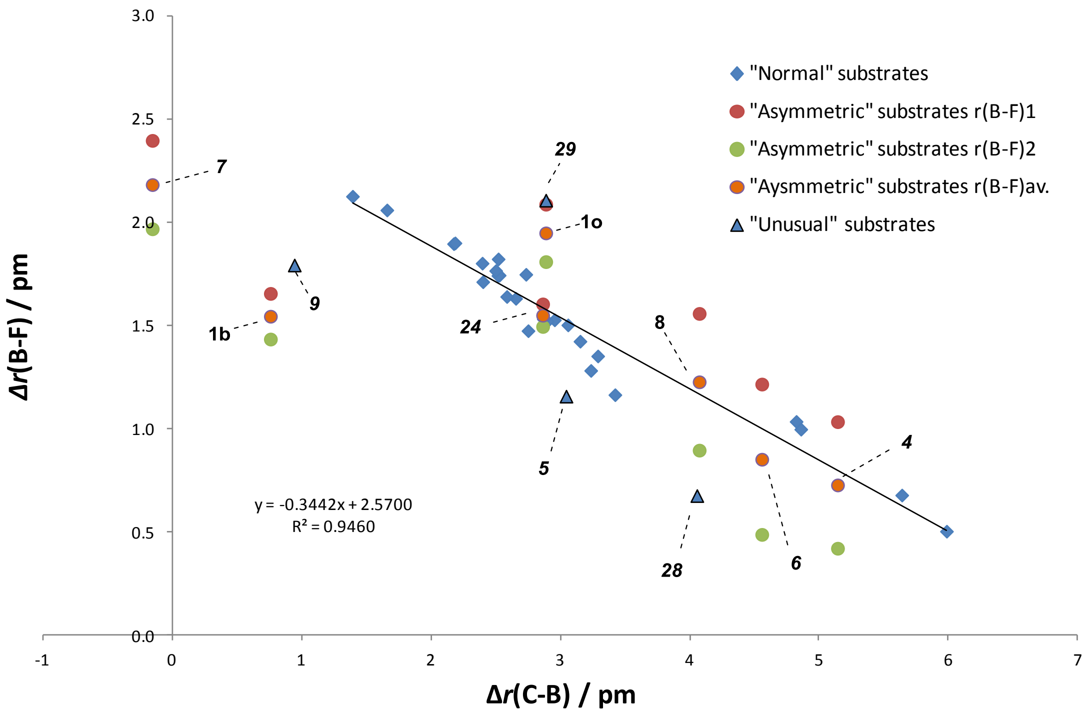

Figure S78 Δ*r*(B-F) vs Δ*r*(C-B) for sp^2 systems only, with Δ*r*$(B\text{-}F)_{1,2\ \text{and av.}}$ for "asymmetric" substrates along with Δ*r*$(B\text{-}F)_{\text{av.}}$ for the "unusual" substrates coploted.

Prediction using Swain Lupton $\Re_{SL}$

Modified Swain-Lupton parameters, $\Re_{MOD,}$ can be easily sourced from the literature[S28] where the authors, Hansch, Leo and Taft, recalculated $\Re_{SL}$ as $\Re_{MOD} = 1.385\sigma_p - 1.297\sigma_m - 0.033$. This value ($\Re_{MOD}$) was found to correlate generally well ($R^2 = 0.9418$) with rates of hydrolysis of substrates **1a**-**1s** (where $\Re_{MOD}$ values exist, and without **1c** (hydrophilic hydrolysis pathway iii (see main text for details) and **1f** (due to major doubts about the reported σ_p and σ_m values)).

We found this correlation could be improved ($R^2 = 0.9558$) by applying the original Swain Lupton calculation of $\Re_{SL} = 1.355\sigma_p - 1.19\sigma_m - 0.03$, which essentially includes the α (0.921) term, Figure S79. We encourage use of this parameter, which gives a very good rate prediction and is simple to calculate from σ_p and σ_m.

However sp^3 systems are observed to hydrolyse at a slightly greater rate than their $\Re_{SL}$ predicts. This is likely due to a steric decompression effect, destabilising the tetrahedral "ate" species, which is not taken into account by the resonance, $\Re_{SL,}$ parameter. By incorporation of the Charton steric parameter (υ)[S29] the correlation could be significantly improved ($R^2 = 0.9801$) and as such gives again a more reliable prediction model, Figure S80 and Figure 10 in main text. The best correlation found was when $\Re_{SL} - 0.09\upsilon$ is plotted against $\log_{10}k_{obs}^{base}$. The main drawback of this approach comes from the scarcity of υ values, of which no sp examples exist, hence its exclusion from the plot. However approximations can be made from substrates of a similar structure which in our experience had no detrimental effect on the fit. As such υ for phenyl (0.57) was used for 2-furyl (**1b**), phenylethenyl (**1k**) and all other aryl (**1a**, **1l**, **1m** and **1r**) substrates. See Table S12 for the prediction equations.

Finally, other than a few exceptions, $\Re_{SL}$ was found to correlate with $\Delta r(\text{B-F})_{av.}$ for each substrate class, thus providing further support to the connection between the two parameters and thus onto the hydrolysis data, Figure S82.

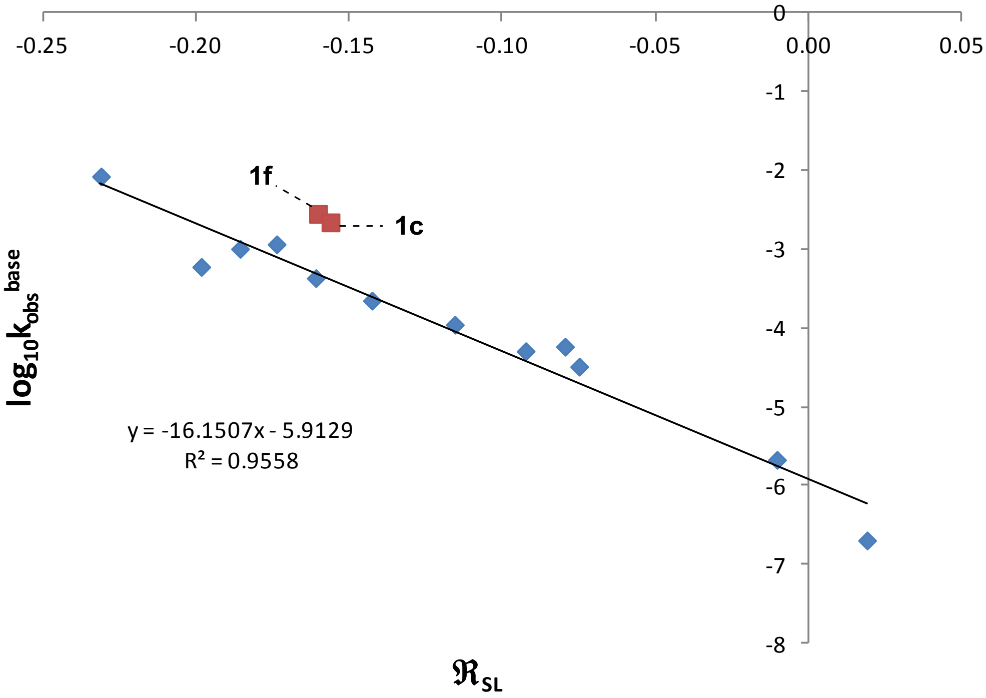

Figure S79 $\text{Log}_{10}k_{obs}{}^{base}$ **vs** $\Re_{SL}$ **for substrates 1a-1s where** $\Re_{SL}$ **values are available**

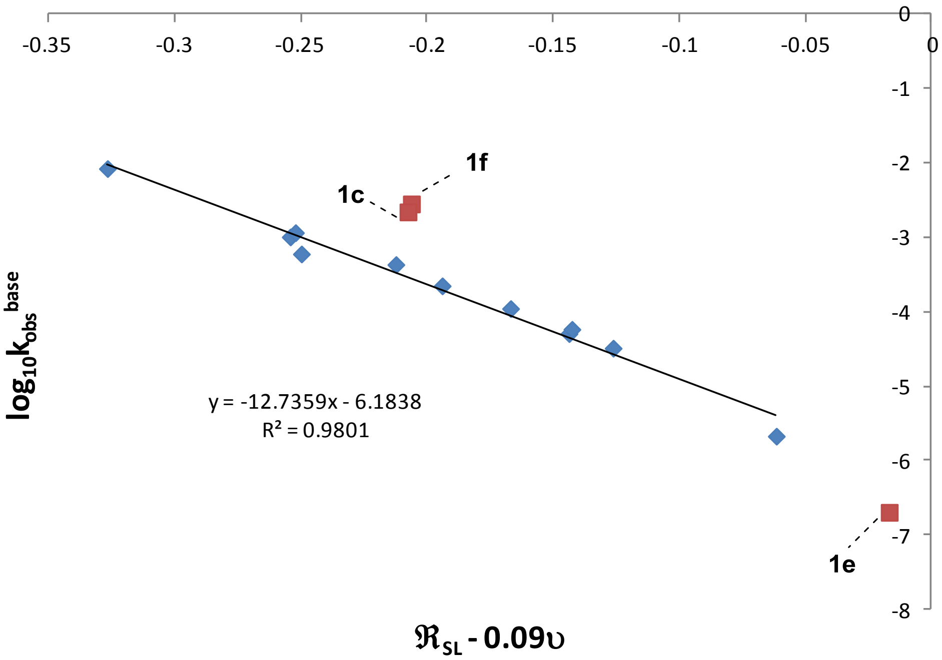

Figure S80 $\text{Log}_{10}k_{obs}{}^{base}$ **vs the steric adjusted** $\Re_{SL} - 0.09\upsilon$ **for substrates 1a-1s where** $\Re_{SL}$ **and** υ **values or approximations are available**

Table S12. Prediction equations from $\Re_{SL}$ or $\Re_{SL} – 0.09\upsilon$ to k_{obs}^{base}

	Equation	R^2
$\Re_{SL}$	$\log_{10}k_{obs}^{base} = -16.1507\Re_{SL} - 5.9129$	0.9558
$\Re_{SL} – 0.09\upsilon$	$\log_{10}k_{obs}^{base} = -12.7359(\Re_{SL} – 0.09\upsilon) - 6.1838$	0.9801

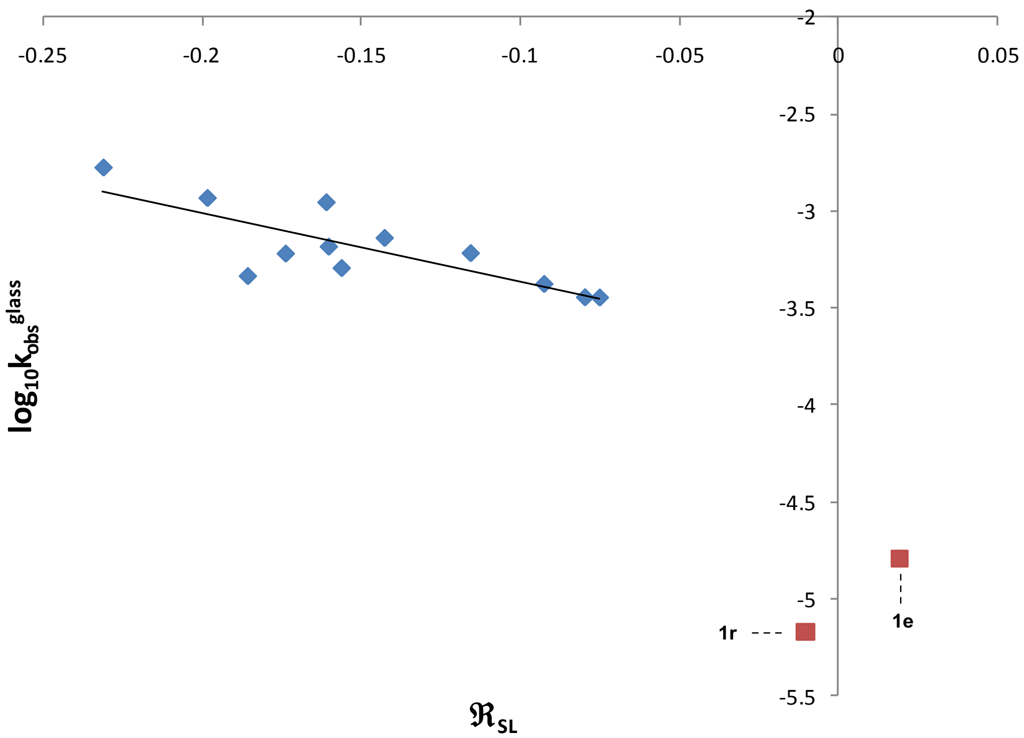

Figure S81. A plot to show the correlation between $Log_{10}k_{obs}^{glass}$ and $\Re_{SL}$, for substrates 1a-1s where $\Re_{SL}$ values are available, under neutral conditions with glass. Substrates 1r and 1e do not correlate well under these glass-mediated conditions due to the rapid drop-off in hydrolysis rate at $\Delta r(B\text{-}F)_{av.}$ values below ca. 1.5 pm; see Figure S75.

Table S13. σ_m and σ_p for substrates **1a-1r** where available and calculation of $\Re_{MOD}$ and $\Re_{SL}$

Substrate		σ_m	σ_p	$\Re_{MOD}$	$\Re_{SL}$
4-Fluorophenyl	**1a**	0.12	0.06	-0.11	-0.09
2-Furanyl	**1b**	0.06	0.02	-0.08	-0.07
Vinyl	**1c**	0.06	-0.04	-0.17	-0.16
Cyclopropyl	**1d**	-0.07	-0.21	-0.23	-0.23
Alkynyl	**1e**	0.14	0.16	0.01	0.02
Cyclobutyl	**1f**	-0.05	-0.14	-0.16	-0.16
Isopropyl	**1g**	-0.04	-0.15	-0.19	-0.19
Benzyl	**1h**	-0.079	-0.106	-0.08	-0.08
1,3-Diphenylpropyl	**1i**				
Cyclohexyl	**1j**	-0.05	-0.15	-0.18	-0.17
Phenylethenyl	**1k**	0.03	-0.07	-0.17	-0.16
4-Methoxyphenyl	**1l**	0.05	-0.08	-0.21	-0.20
4-Methylphenyl	**1m**	0.06	-0.03	-0.15	-0.14
Phenyl	**1n**	0.06	-0.01	-0.12	-0.12
1-Naphthyl	**1o**				
2-Naphthyl	**1p**				
4-CF_3phenyl	**1q**				
3-Nitrophenyl	**1r**	0.21	0.2	-0.03	-0.01
3,5 bisCF_3phenyl	**1s**				

Table S14. Charton[S29] modification of $\Re_{SL}$ to improve fit to rate data

Substrate		**Charton υ**	$\Re_{SL} - 0.09\upsilon$
Cyclopropyl	**1d**	1.06	-0.33
Cyclobutyl	**1f**	0.51	-0.21
Isopropyl	**1g**	0.76	-0.25
Benzyl	**1h**	0.70	-0.14
Phenyl	**1n**	0.57	-0.17
cyclopentyl	***12***	0.72	-0.23
cyclohexyl	**1j**	0.87	-0.25

Table S15. σ_m and σ_p for substrates ***1-32*** where available and calculation of $\Re_{MOD}$ and $\Re_{SL}$

Entry	**Substrate**	σ_m	σ_p	$\Re_{MOD}$	$\Re_{SL}$
1	3-pyridyl	0.23	0.25	0.01	0.03
2	4-pyridyl	0.27	0.44	0.23	0.24
3	2-pyrimidyl	0.23	0.53	0.40	0.41
4	4-pyrimidyl	0.30	0.63	0.45	0.46
5	5-pyrimidyl	0.28	0.39	0.14	0.16
6	3-pyridazyl	0.28	0.48	0.27	0.29
7	pyrrole	0.47	0.37	-0.13	-0.09
8	2-pyridyl	0.33	0.17	-0.23	-0.19
9	2-thienyl	0.09	0.05	-0.08	-0.07
10	ethyl	-0.07	-0.15	-0.15	-0.15
11	$CH_2CH_2C_6H_4$	-0.07	-0.12	-0.11	-0.11
12	cyclopentyl	-0.05	-0.14	-0.16	-0.16
13	$C(CF_3)_3$	0.55	0.55	0.02	0.06
14	3-BrC_6H_4	0.09	0.08	-0.04	-0.03
15	4-BrC_6H_4	0.15	0.12	-0.06	-0.05
16	3-ClC_6H_4	0.15	0.10	-0.09	-0.07
17	4-ClC_6H_4	0.15	0.12	-0.06	-0.05
18	3-FC_6H_4	0.15	0.10	-0.09	-0.07
19	3-IC_6H_4[a]	0.13	0.06	-0.12	-0.10
20	4-$NO_2C_6H_4$	0.25	0.26	0.00	0.02
21	4-EtC_6H_4	0.07	-0.02	-0.15	-0.14
22	4-IC_6H_4 [a]	0.14	0.10	-0.08	-0.06
23	C_6Cl_5	0.25	0.24	-0.03	0.00
24	3-acetylC_6H_4				
25	4-$CH_2OHC_6H_4$				
26	4-CNC_6H_4				
27	4-acetylC_6H_4				
28	C_6F_5	0.26	0.27	0.00	0.02
29	mesityl				
30	CC	0.21	0.23	0.01	0.03
31	$CCCF_3$	0.41	0.51	0.14	0.17
32	$CCCH_3$	0.21	0.03	-0.26	-0.24

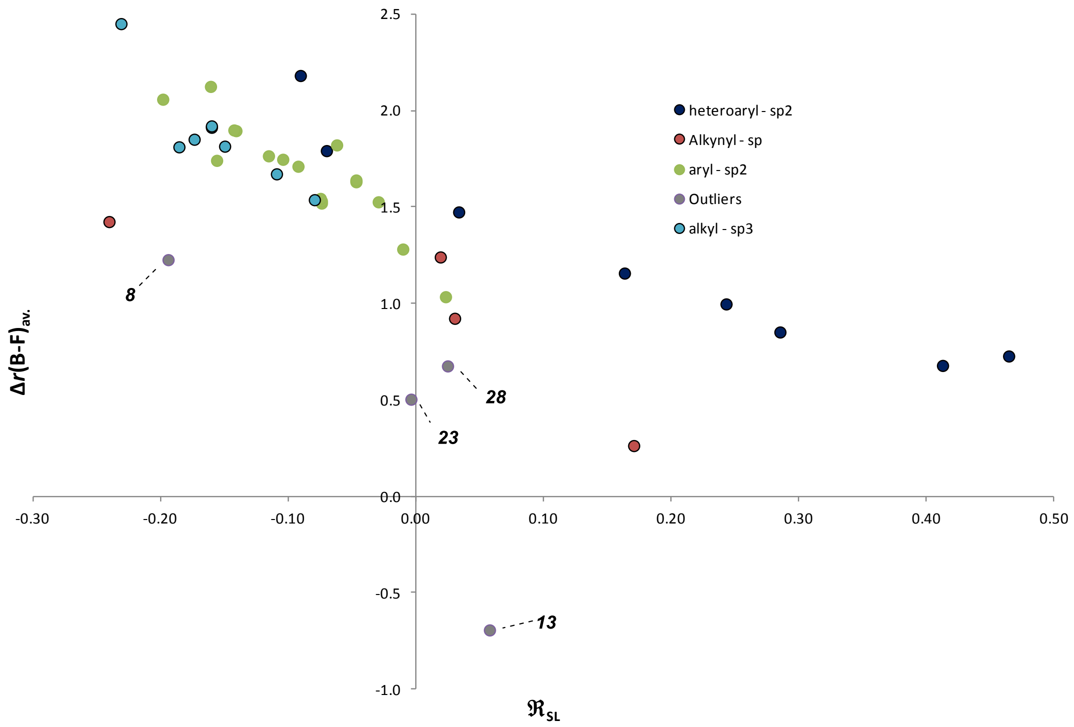

Figure S82. Swain Lupton $\mathscr{R}_{SL}$ parameter vs Δ*r*(B-F)$_{av.}$ for all substrates calculated. Labels of outliers refer to entry numbers in Table S15

Table S16. Correlations between $\mathscr{R}_{SL}$ and Δ*r*(B-F)$_{av.}$

Substrate class	**Equation**	R^2
Heteroaryl – sp^2	Δ*r*(B-F)$_{av.}$ = -2.4651 $\mathscr{R}_{SL}$ + 1.6771	0.9165
Alkynyl – sp	Δ*r*(B-F)$_{av.}$ = -2.567 $\mathscr{R}_{SL}$ + 0.9497	0.7434
Aryl – sp^2	Δ*r*(B-F)$_{av.}$ = -4.0287 $\mathscr{R}_{SL}$ + 1.3179	0.7886
Alkyl – sp^3	Δ*r*(B-F)$_{av.}$ = -5.1482 $\mathscr{R}_{SL}$ + 1.0671	0.7957

Partitioning study

THF (2 mL) was added to a test tube containing the potassium organotrifluoroborate **1c** / **1o** / **1g** and **1f** (1.1×10^{-4} mol). To this was added cesium carbonate (3.3×10^{-4} mol) in water (0.2 mL) and stirred for one minute at room temperature. A sample (50 μL) was removed from the minor biphase and the major bulk phase and added directly to an NMR tube containing KBF_4 (1.1×10^{-5} mol, 1.4 mg) and then diluted with water (0.5 mL). Each sample was analyzed by ^{11}B NMR for 500 scans at 25 °C.

A control experiment showed that a proportion of KBF_4 hydrolyzed under the strongly basic conditions of the minor biphase, giving rise to an extra peak (δ = 1.92 - 1.14) in the ^{11}B NMR spectrum.

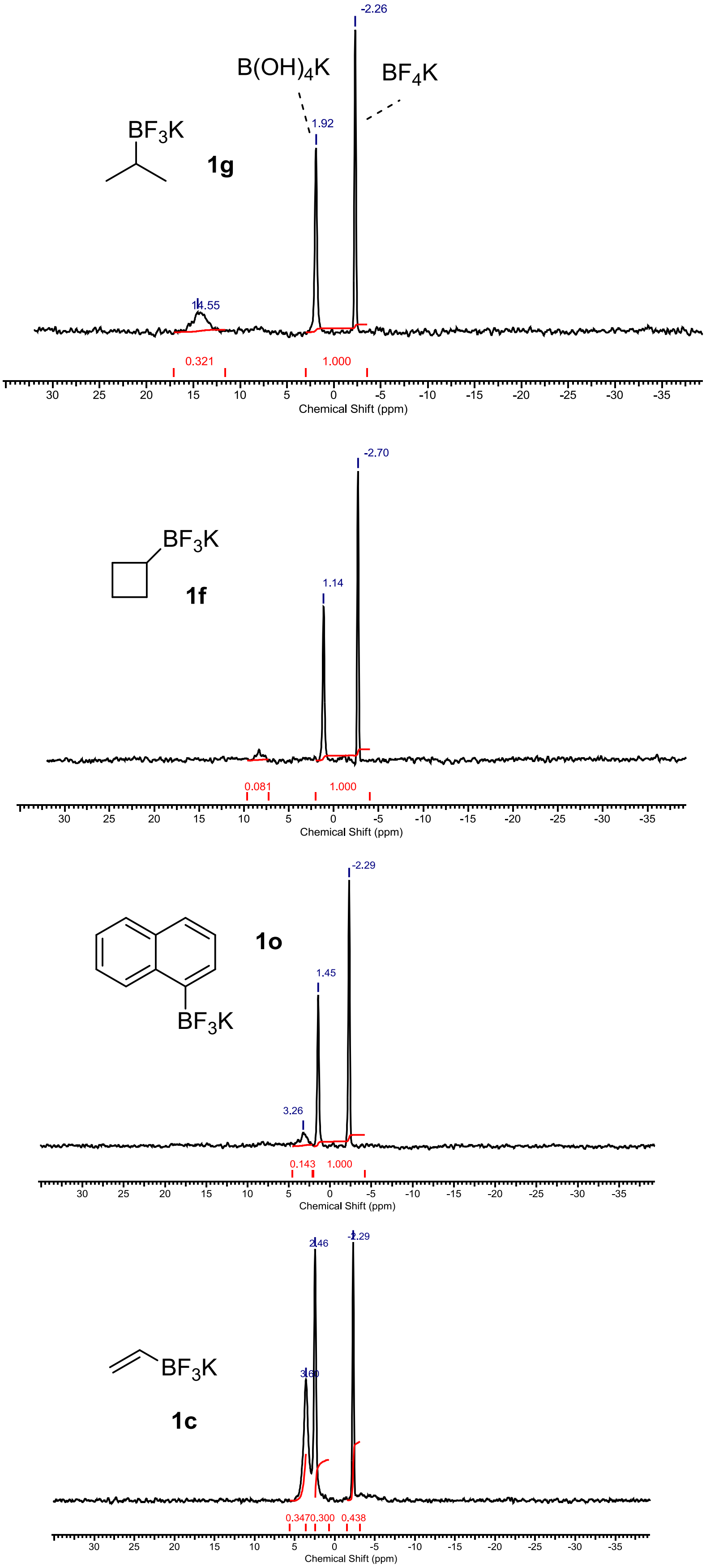

Figure S83. ^{11}**B NMR of the minor basic biphase, containing the product of the hydrolysis** $RB(OH)_3^-$ **(note half integration due to peak overlap in 1c).**

Suzuki vs Sonogashira in potassium alkynyltrifluoroborate couplings

Synthesis of [$^2H_5$]-phenylacetylene

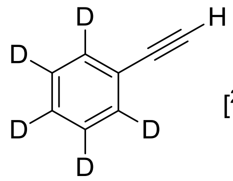

[$^2H_5$]-**6**

Synthesis of TMS protected phenylacetylene

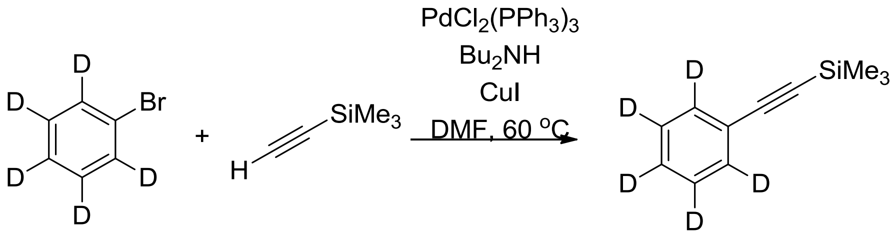

DMF was distilled from 4 Å molecular sieves and left to dry overnight before being degassed by three vacuum/N_2 cycles. Di-*n*-butylamine was distilled from calcium hydride under an atmosphere of dry N_2 prior to use.

To an oven-dried, N_2 purged Schlenk tube, was added firstly di-*n*-butylamine (1.6 mL) and DMF (11 mL), followed by [$^2H_5$]-bromobenzene (9.5×10^{-3} mol, 1 mL) and TMS acetylene (9.64×10^{-3} mol, 1.36 mL). Over a flow of nitrogen was then added copper iodide (2.38×10^{-4} mol, 45 mg) and $PdCl_2(PPh_3)_2$ (2.49×10^{-4} mol, 175 mg). The stirring solution was heated at 60 °C for 16 hours before the mixture was poured onto $HCl_{(aq)}$ (0.1 N, 10 mL). The aqueous phase was extracted with diethylether (3 x 20 mL), the combined organics were washed with water (2 x 10 mL), sat. aqueous sodium bicarbonate (10 mL) and again with water (10 mL). The combined aqueous layers were extracted with diethylether (20 mL) which was added to the other organics, dried over $MgSO_4$, filtered and concentrated before being purified by column chromatography (100 % pentane, Rf = 0.4) to give a clear oil (4.6×10^{-3} mol, 824 mg, 48 %, (99% ^{2}H)). **^{1}H NMR** (300 MHz, $CDCl_3$): δ = 0.26 (s, 9H); **^{13}C{^{1}H} NMR** (125.71 MHz, $CDCl_3$): δ = 131.54 (t ^1J(C,D) = 24.45 Hz, 2C), 127.94 (t ^1J(C,D) = 25.43 Hz, 1C), 127.66 (t ^1J(C,D) = 24.45 Hz, 2C), 122.91 (s), 105.07 (s), 94.09 (s), 0.01 (s).

Data is in accordance with that previously published[S30]

Deprotection to give D₅ phenylacetylene [S31]

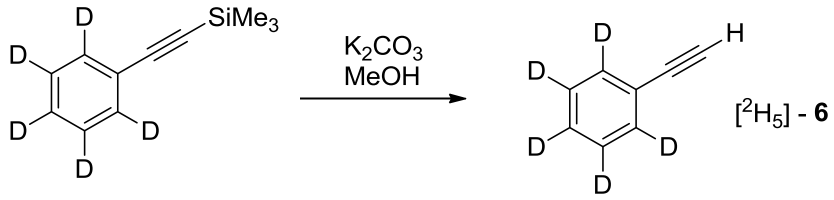

Anhydrous methanol was distilled from calcium hydride onto 4 Å molecular sieves prior to use. D_5 – TMSphenylacetylene (700 mg, 3.9 x 10^{-3} mol) was added to a mixture of MeOH (11.7 mL) and potassium carbonate (0.35 x 10^{-3} mol, 48 mg) and stirred at room temperature for three hours under an atmosphere of dry N_2. The volatiles were removed under reduced pressure before being immediately purified by Kugelrohr distillation to give a clear and colourless oil (61 mg, 5.7 x 10^{-4} mol, 15 %, (99% ^{2}H)). **^{1}H NMR** (300 MHz, $CDCl_3$): δ = 3.07 (s); **^{13}C{^{1}H} NMR** (75.57 MHz, $CDCl_3$): δ = 131.7 (t ^1J(C,D) = 24.91 Hz, 2C), 128.25 (t ^1J(C,D) = 23.65 Hz, 2C), 127.77 (t ^1J(C,D) = 24.23 Hz, 2C), 121.87 (s), 83.85 (s), 77.11 (s).

Data is in accordance with that previously published[S30]

Cross-coupling competition[S32]

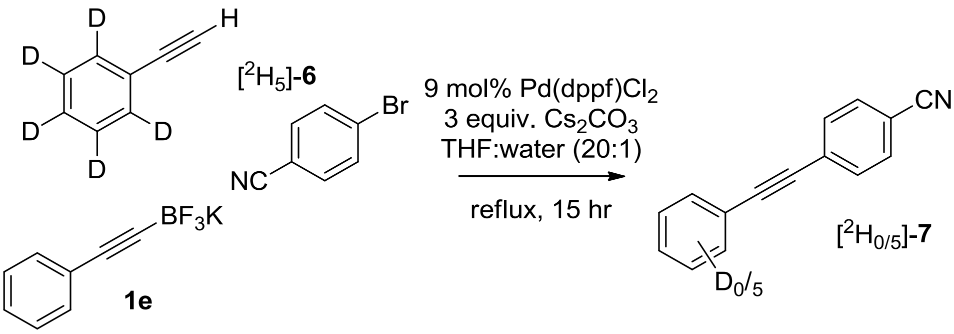

To an oven-dried Schlenk tube was added potassium phenylethynyltrifluoroborate (2.5 x 10^{-4} mol, 26.75 mg), 4-bromobenzonitrile (2.5 x 10^{-4} mol, 45.5 mg), Pd(dppf)Cl_2 (2.25 x 10^{-5} mol, 18 mg) and cesium carbonate (7.5 x 10^{-4} mol, 244 mg). This was then purged with N_2 before a solution of THF:water (20:1, 2.625 mL) and D_5-phenylacetylene were added simultaneously with stirring. The septum was replaced with a condenser over a flow of dry N_2 and the reaction mixture was refluxed at 75 °C for 15 hours. The reaction mixture was then poured onto water (8 mL) and then extracted with diethylether (4 x 10 mL). The organics were combined, washed with $HCl_{(aq)}$ (1N, 6 mL), water (2 x 10 mL) and lastly brine (10 mL) before being dried over Mg_2SO_4, filtered and concentrated. The crude material was purified by column chromatography (10% EtOAc in Hexanes, Rf = 0.27) to give a white solid (2.16×10^{-4} mol, 28 mg, 55%). **^{1}H NMR** (300 MHz, $CDCl_3$): δ = 7.635 (m, 4H), 7.55 (m, 1.7H), 7.39 (m, 2.2H); **MS (EI)** *m/z* (%): 201.1 (18), 202.1 (18), 203.1 (100), 204.1 (32), 205.1 (8), 206.2 (4), 207.2 (7), 208.2 (58), 209.2 (22).

^{1}H NMR shifts are in accordance with that expected based on data published for the unlabelled compound[S33]

References

S1 W. A. Herrmann, A. Salzer, *Synthetic Methods of Organometallic and Inorganic Chemistry*, Vol. 1(Herrmann/Brauer), THIEME, Stuttgart New York, **1996**, p. 160.

S2 Hayashi, T.; Konishi, M.; Kobori, Y.; Kumada, M.; Higuchi, T.; Hirotsu, K. *J. Am. Chem. Soc.*, **1984**, *106*, 158-163.

S3 Molander, G. A.; Gormisky, P. E. *J. Org. Chem.*, **2008**, *73*, 7481-5.

S4 Butters, M.; Harvey, J. N.; Jover, J.; Lennox, A. J. J.; Lloyd-Jones, G. C.; Murray, P. M.; *Angew. Chem. Int. Ed.* **2010**, *49*, 5156-5160

S5 Oliveira, R. A.; Silva, R. O.; Molander, G. A.; Menezes, P. H. *Magn. Reson. Chem.* **2009**, *47*, 873-878

S6 Cole, T. E.; Quintanilla, R.; Rodewald, S. S*ynth. React. Inorg. Met.-Org. Chem.,* **1990**, *20*, 55-63

S7 Genet, J.-P.; Darses, S.; Michaud, G. *Eur. J. Org. Chem.*, **1999**, *1999*, 1875-1883.

S8 The authors are grateful to Paul Cogswell and Nina Ursinyova (University of Bristol) for help with this experiment.

S9 Simulations were conducted using commercially available software (MacKinetics, Leipold Associates, USA) based on published GEAR algorithms: a) Weigert, F. J. *Computers and Chemistry* **1987**, *II*, 273; b) Stabler, R. N.; Cheswick, J. *Int. J. Kinet.* **1978**, *10*, 461; c) McKinney, R. J.; Weigert, F. J. *Quantum Chemistry, Program Exchange, program No. QCMP022* (archived).

S10 Adamo, C.; Amatore, C.; Ciofini, I.; Jutand, A.; Lakmini, H. *J. Am. Chem. Soc.*, **2006**, *128*, 6829-6836.

S11 Bruno, I. J.; Cole, J. C.; Edgington, P. R.; Kessler, M.; Macrae, C. F.; McCabe, P.; Pearson, J.; Taylor, R. *Acta Cryst., B58* **2002**, 389-397

S12 Brauer, D.J.; Burger, H.; Pawelke G. *J. Organomet. Chem.* **1982,** *238,* 267-279

S13 Brauer, D.J.; Burger, H.; Pawelke G. *Inorg. Chem.* **1977,** *16*, 2305

S14 Chase, P. A.; Henderson, L. D.; Piers, W. E.; Parvez, M.; Clegg, W.; Elsegood, M. R. J. *Organometallics*, **2006***, 25*, 351

S15 Hohn, E.; Palecek, J.; Pietruszka, J.; Frey, W. *Eur. J. Org. Chem.* **2009**, 3765–3782
S16 Guinchard, X.; Bugaut, X.; Cook, C.; Roulland, E. *Chem. Eur. J.* **2009**, *15,* 5793–5798
S17 De, S; Day, C.; Welker, M. E. *Tetrahedron* **2007***,* 63, 10939-10948
S18 Conole, G.; Clough, A.; Whiting, A. *Acta Crystallogr. C* **1995,** C51, 1056-1059
S19 Thadani, A. N.; Batey, R. A.; Smil, D. V. Lough, A. J. *Acta Crystallogr. E* **2001**, *57,* m333
S20 Quach, T. D.; Batey, R. A.; Lough, A. J. *Acta Crystallogr E.* **2001**, *57*, o688
S21 Zukerman-Schpector, J.; Guadagnin, R. C.; Stefani, H. A.; Visentin, L. d. C. *Acta Crystallogr. E*. **2009**, *65*, o192
S22 Zukerman-Schpector, J.; Guadagnin, R. C.; Stefani, H. A.; Visentin, L. d. C. *Acta Crystallogr. E.* **2008**, *64*, m1525
S23 Franz, D.; Wagner, M.; Lerner, H.-W.; Bolte, M.; *Acta Crystallogr. C.* **2010**, *66*, m152
S24 Vieira, A. S.; Fiorante, P. F.; Zukerman-Schpector, J.; Alves, D.; Botteselle, G. V.; Stefani, H. A. *Tetrahedron*, **2008,** *64*, 7234
S25 Caracelli, I.; Stefani, H. A.; Vieira, A. S.; Machado, M. M. P.; Zukerman-Schpector, J. *Z. Kristallogr.-New Cryst. St.* **2007**, *222*, 345
S26 CCDC 859285, CCDC 859286, CCDC 859287 and CCDC 859288 contains the supplementary crystallographic data for this paper. These data can be obtained free of charge from The Cambridge Crystallographic Data Centre via www.ccdc.cam.ac.uk/data request/cif
S27 Gaussian 09, Revision **A.1**, Frisch, M. J.; Trucks, G. W.; Schlegel, H. B.; Scuseria, G. E.; Robb, M. A.; Cheeseman, J. R.; Scalmani, G.; Barone, V.; Mennucci, B.; Petersson, G. A.; Nakatsuji, H.; Caricato, M.; Li, X.; Hratchian, H. P.; Izmaylov, A. F.; Bloino, J.; Zheng, G.; Sonnenberg, J. L.; Hada, M.; Ehara, M.; Toyota, K.; Fukuda, R.; Hasegawa, J.; Ishida, M.; Nakajima, T.; Honda, Y.; Kitao, O.; Nakai, H.; Vreven, T.; Montgomery, Jr., J. A.; Peralta, J. E.; Ogliaro, F.; Bearpark, M.; Heyd, J. J.; Brothers, E.; Kudin, K. N.; Staroverov, V. N.; Kobayashi, R.; Normand, J.; Raghavachari, K.; Rendell, A.; Burant, J. C.; Iyengar, S. S.; Tomasi, J.; Cossi, M.; Rega, N.; Millam, N. J.; Klene, M.; Knox, J. E.; Cross, J. B.; Bakken, V.; Adamo, C.; Jaramillo, J.; Gomperts, R.; Stratmann, R. E.; Yazyev, O.; Austin, A. J.; Cammi, R.; Pomelli, C.; Ochterski, J. W.; Martin, R. L.; Morokuma, K.; Zakrzewski, V. G.; Voth, G. A.; Salvador, P.; Dannenberg, J. J.; Dapprich, S.; Daniels, A. D.; Farkas, Ö.; Foresman, J. B.; Ortiz, J. V.; Cioslowski, J.; Fox, D. J. Gaussian, Inc., Wallingford CT, 2009.
S28 Hansch, C.; Leo, A.; Taft, R. W. *Chem. Rev.* **1991**, *91*, 165-195.
S29 a) Charton, M. *J. Org. Chem.* **1976**, *41*, 2217-2220; b) Charton, M. *J. Am. Chem. Soc.* **1975**, *97*, 1552-1556
S30 Dougherty, T. K.; Lau, K. S. Y.; Hedberg, F. L. *J. Org. Chem.*, **1983**, *48*, 5273-5280.
S31 Wang, Y.; Huang, B.; Sheng, S.; Cai, M. *J. Chem. Res.* **2007**, 728-732
S32 Molander, G. A.; Katona, B. W.; Machrouhi, F. *J. Org. Chem.*, **2002**, *67*, 8416-8423.
S33 Wu, X.-F.; Neumann, H.; Beller, M. *Chem. Commun.*, **2011**, *47*, 7959-7961.